IL
NUOVO CIMENTO
ORGANO DELLA SOCIETÀ ITALIANA DI FISICA
SOTTO GLI AUSPICI DEL CONSIGLIO NAZIONALE DELLE RICERCHE

VOL. XVII, N. 2 *Serie decima* 16 Luglio 1960

On the Momentum Spectrum of Particles in Cosmic Ray Jets.

J. PERNEGR, V. ŠIMÁK and M. VOTRUBA
Institute of Physics of the Czechoslovak Academy of Sciences - Prague

(ricevuto l'8 Gennaio 1960)

Summary. — It is shown that the form of momentum spectrum of jet particles is essentially dependent on the degree of anisotropy of the angular distribution, and that *e.g.* the form dp/p^2 corresponds to a definite « medium » anisotropy. Integral spectra of directly measured values of p indicate a systematic decrease of transversal momenta in the vicinity of the axis and of the $\pi/2$-plane in C.M. system.

The momentum spectrum of particles emitted in nuclear interactions with primary energies above $5 \cdot 10^{11}$ eV has been investigated in nuclear emulsions by direct measurements of the momenta p in individual events (*e.g.* [1-3]) as well as indirectly using the angular distribution of large collections of jets [4]. As a generally accepted result the differential momentum spectrum in C.M. system is of the Heisenberg form dp/p^2.

[1] A. DEBENEDETTI, C. M. GARELLI, L. TALLONE and M. VIGONE: *Nuovo Cimento* **4**, 1142 (1956).

[2] E. G. BOOS, A. KH. VINETSKY, J. S. TAKIBAYEV and I. YA. CHASNIKOV: *Žurn. Éksp. Teor. Fiz.*, **34**, 622 (1958).

[3] E. FENYVES, E. GOMBOSI and P. SURÁNYI: *High Energy Physics Conference at Geneva* (1958); *Nuovo Cimento*, **11**, 21 (1959).

[4] B. EDWARDS, J. LOSTY, D. H. PERKINS, K. PINKAU and J. REYNOLDS: *Phil. Mag.*, **3**, 327 (1958); S. HASEGAWA, J. NISHIMURA and Y. NISHIMURA: *Nuovo Cimento*, **6**, 979 (1957).

We should like to point out that the form of the momentum spectrum depends strongly on the degree of anisotropy of the angular distribution and we shall try to show that the above result does not hold generally.

At first, let us suppose that the transversal component of the momentum p_T is constant and independent on the primary energy as well as on the angle of emission θ. Then it follows from the definition $p = p_T \operatorname{cosec} \theta$ that any form of the momentum spectrum is connected with one definite type of the angular distribution; *e.g.* for the Heisenberg type spectrum we have in the C.M. system the angular distribution $\operatorname{cotg} \theta \, \mathrm{d}(\cos \theta)$ representing a « medium » anisotropy.

$$\mathrm{d}n \sim \frac{\mathrm{d}p}{p^2} \sim \frac{\mathrm{d}(\operatorname{cosec} \theta)}{\operatorname{cosec}^2 \theta} = \operatorname{cotg} \theta \, \mathrm{d}(\cos \theta) \,. \tag{1}$$

Expressing the angular anisotropy in the more usual way as $\cos^m \theta \, \mathrm{d}(\cos\theta)$ we have a spectrum

$$\mathrm{d}n \sim \cos^m \theta \, \mathrm{d}(\cos \theta) \sim \left(1 - \frac{p_T^2}{p^2}\right)^{(m-1)/2} \cdot \frac{1}{p^3} \, \mathrm{d}p \tag{2}$$

going over to $\mathrm{d}n \sim \mathrm{d}p/p^3$ for large values of p. For a « medium » anisotropy about $m = 4$ the distribution eq. (2) is similar to that of the formula (1).

To investigate the influence of the angular distribution on the form of the momentum spectrum we divided 21 jets with primary energy above $5 \cdot 10^{11}$ eV from our laboratory and several others from the literature [4,5] into three groups according to their anisotropy expressed by the value of $\gamma \equiv \langle \operatorname{cosec} \theta \rangle_{\mathrm{av}} \doteq$ $\doteq 1.25 \sqrt{m}$ (for large values of m) acc. to [4] and [6]:

(I)	$\bar{\gamma} < 1.4$	isotropy	$\langle \bar{\gamma} \rangle_{\mathrm{av}} = 1.3$	122 tracks
(II)	$1.6 < \bar{\gamma} < 3$	medium anisotropy	$\langle \bar{\gamma} \rangle_{\mathrm{av}} = 2.3$	116 tracks
(III)	$4 < \bar{\gamma} < 16$	strong anisotropy	$\langle \bar{\gamma} \rangle_{\mathrm{av}} = 5.5$	40 tracks .

In Fig. 1 we plotted the integral spectra of the values (in the C.M. system) of $\operatorname{cosec} \theta = \text{const.}$ p for individual groups. The group I of isotropic jets follows fairly well the curve corresponding to $m = 0$ in eq. (2), the spectrum of the medium anisotropic events (group II) is very near to the form $\mathrm{d}p/p^2$, while the sequence of points related to the strongly anisotropic group III decreases much more slowly. The hard tails of all the spectra seem to have a parallel slope approximately as $\mathrm{d}p/p^{3.5}$.

---

[5] M. SCHEIN, R. G. GLASSER and D. M. HASKIN: *Nuovo Cimento*, **1**, 647 (1955).

[6] P. CIOK, T. COGHEN, J. GIERULA, R. HOŁYNSKI, A. JURAK, M. MIĘSOWICZ T. SANIEWSKA, O. STANISZ and J. PERNEGR: *Nuovo Cimento*, **8**, 166 (1958); **10**, 741 (1958)

2378

In Fig. 2 we collected together the data of all events from group I, II and III. The average value of $\bar{\gamma}$ of all these jets is $\langle\gamma\rangle_{av} = 2.0$ corresponding to a « medium » anisotropy (roughly $m = 4$ in eq. (2)); we were therefore not surprised that we obtained a rather good agreement with the line dp/p^2 [4].

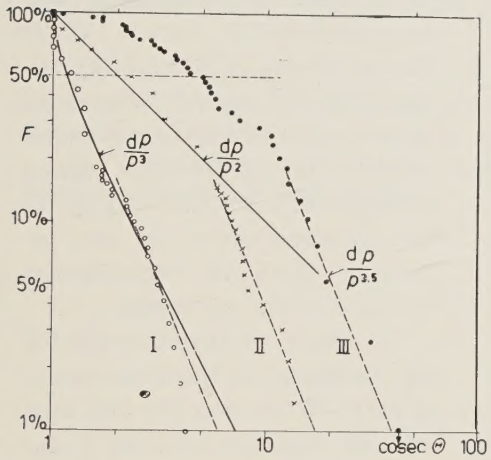

Fig. 1. – Integral momentum spectra of three groups of jets with different anisotropy.

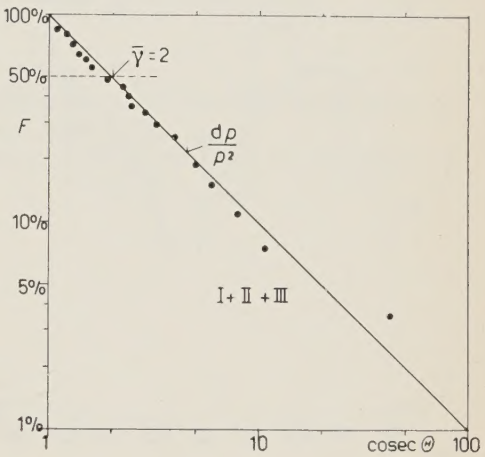

Fig. 2. – Integral momentum spectrum of all jets from Fig. 1 together.

It is shown on Figs. 1 and 2 that the dashed line drawn for the fraction $F = 0.5$ crosses the spectrum of any group of jets in the point $\operatorname{cosec}\theta = \langle\operatorname{cosec}\theta\rangle_{av} = \bar{\gamma}$. Consequently the spectra of isotropic events lie to the left of the line dp/p^2 while the strong anisotropic jets have the momentum spectrum shifted towards higher values of p.

Similar argumentation holds also for the directly measured spectra. *E.g.* the Torino jet [1] with the experimental momentum spectrum dp/p^2 has a medium anisotropy $\bar{\gamma} = 1.8$ which is very near to our group II or to the collection of our Fig. 2. An eventual difference between the integral spectra

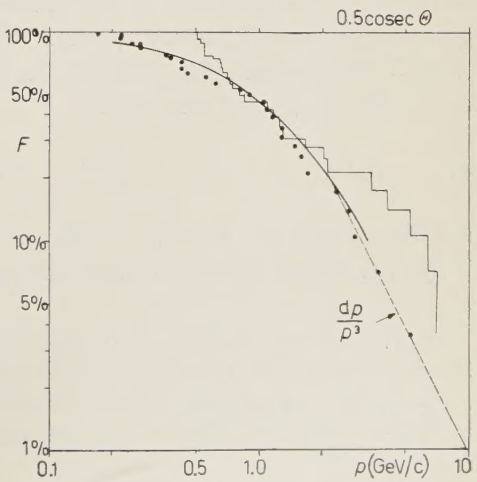

Fig. 3. – Integral spectrum of directly measured values of p (points) and of momenta defined as $p = 0.5 \operatorname{cosec}\theta$ (histogram); average anisotropy $\gamma = 2$.

of cosec θ and of the measured p values might come from some kind of deviation from our assumption $p_T = \text{const}$ ([7-9]). In Fig. 3 we compared the sequence of points related to the experimental values of p of four jets measured in this laboratory (the mean $\bar{\gamma} = 2$) with the histogram of their 0.5 cosec θ GeV/c values. While the agreement is satisfactory between $F = 0.7$ and 0.3 there seems to be a shift of the experimental points to the left in the regions corresponding to the vicinity of the $\pi/2$-plane and of the axis, indicating there an experimental decrease of the p_T values.

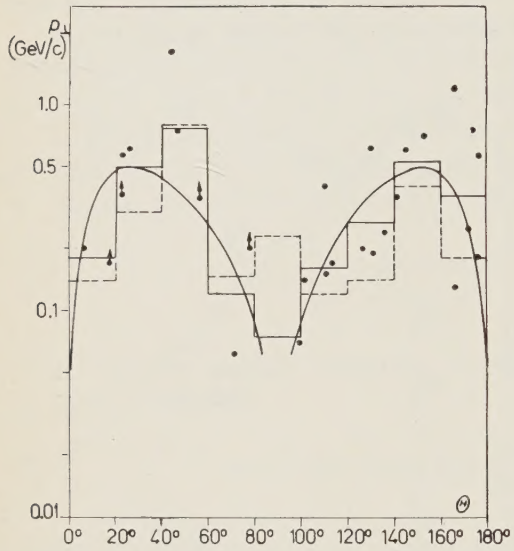

Fig. 4. – Angular dependence of transversal momentum of a group of jets from Fig. 3; points: individual values; full lines: mean values; dashed lines: mean values of lg p_T together with jets ([1]) and ([5]).

In Fig. 4 we therefore plotted the histogram of the mean values of log p_T of the same jets (full line) and also together with the S-star and the Torino jet (dashed line). There appears to be a decrease of p_T values in the neighbourhood of the axis and of the $\pi/2$-plane as it was already indicated on the integral momentum spectrum (Fig. 3).

The full curves in Figs. 3 and 4 are drawn as predictions ([7]) of the two-centres model ([6]) of particle emission. Adhering tentatively to this model we tried to guess the form of the energy spectrum in the rest-system of the emitting centres C^*. The hard tails of the momentum spectra are nearly insensitive to transformation into another system; we may deduce from their parallel slopes in the C.M. system (Fig. 1) that in the C^*-system the momentum spectrum near to the axis is also of the form

$$\frac{\mathrm{d}p}{p^{1+\alpha}} \qquad \text{with } \alpha \geqslant 2 \tag{3}$$

(see Figs. 1 and 3). Because of the isotropy of the angular distribution in the C^* system ([6]) and having in mind the approximate $\mathrm{d}p/p^3$ law for the isotropic

([7]) J. PERNEGR: *Conference on High Energy Physics* (Prague, June 1958), II-55; *Moscow Conference of Cosmic Rays* (July 1959).

([8]) E. M. FRIEDLÄNDER: *Nuovo Cimento*, **12**, 483 (1959).

([9]) J. G. MCEVEN: preprint (we are greatful to prof. GIERULA for kindly sending us the preprint).

group I (Fig. 1) we may deduce that a similar spectrum as (3), is valid in the whole space of the C^*-system and that the interaction (proportional to α) among created particles is very strong in this emitting centre. The resemblance of eq. (3) with the laboratory spectrum of photon-electron cascades with primary energy above 10^{12} eV ([10-11]) seems to be interesting.

([10]) J. G. DUTHIE, C. M. FISHER, P. H. FOWLER, A. KADDOURA, D. H. PERKINS and K. PINKAU: *Moscow Conference on Cosmic Rays* (1959).

([11]) Y. FUDJIMOTO, S. HASEGAWA, M. KAZUNO, J. NISHIMURA and K. NIU: *Moscow Conference on Cosmic Rays* (1959).

RIASSUNTO (*)

Si mostra che la forma dello spettro della quantità di moto dei getti è essenzialmente dipendente dal grado di anisotropia delle distribuzioni angolari, e che, p. es., la forma $\mathrm{d}p/p^2$ corrisponde ad una definita anisotropia del mezzo. Spettri integrali di valori di p misurati direttamente indicano una diminuizione sistematica dei momenti trasversali nella vicinanza dell'asse e del piano $\pi/2$ nel sistema del c.m.

(*) *Traduzione a cura della Redazione.*

IL NUOVO CIMENTO Vol. XVII, N. 2 16 Luglio 1960

An Experiment on Nuclear Interactions of High Energy ((10 ÷ 100) GeV).

E. R. T. Awunor-Renner, L. Blaskovitch, B. R. French, C. Ghesquière I. B. de Minvielle-Devaux, W. W. Neale, C. Pelletier, P. Rivet, A. B. Sahiar and I. O. Skillicorn

Imperial College - London
Ecole Polytechnique - Paris

(ricevuto il 29 Febbraio 1960)

Summary. — 117 interactions of cosmic ray particles with aluminium nuclei have been studied. 101 showers containing no apparent unstable particles yielded the following multiplicities:

$$\langle n_s \rangle = 7.3; \qquad \langle n_s^+ \rangle = 3.9; \qquad \langle n_s^- \rangle = 2.7; \qquad \langle n_s^\pm \rangle = 0.6 .$$

The momentum and angular distributions of the secondary particles were examined, and an attempt was made to study the momentum-angle correlation. The mean transverse momentum was 0.31 GeV/c, the RMS deviation about this mean being 0.23 GeV/c. A quantity related to the $(U - p_L)$ of the recoil nucleon was also investigated. 12 showers containing one V^0 each and 1 shower containing two V^0 particles were studied; this showed that the 117 showers contained: $29.5^{+14.0}_{-11.0}$ Λ^0 and $18.0^{+15.0}_{-10.0}$ θ^0 particles. 3 showers containing $V^\pm$ particles were also studied; one of them was probably a Ξ^- particle.

1. – Introduction.

Two groups of physicists from the Imperial College (London) and the Ecole Polytechnique (Paris) took part in this experiment. It was carried out with the equipment of the Ecole Polytechnique at the Pic du Midi de Bigorre (alt. 2 860 m). This equipment, originally used for work on V^0 particles, has a maximum detectable momentum of about 30 GeV/c, and is therefore not unsuited to the study of nuclear interactions with primary momenta around 40 GeV/c.

2842

An aluminium producer was chosen, as it satisfied the following conditions:

a) its low atomic weight favoured the occurrence of a high proportion of nucleon-nucleon interactions;

b) at the altitude of operation the producer could be made thin enough (4 cm) for the loss of wide-angle particles to be small, the detection efficiency of unstable particles to be relatively high, and yet the frequency of occurrence of well measurable interactions to be sufficient for a statistical study.

2. – Experimental procedure.

2·1. *Apparatus.* – The installation at the Pic du Midi was described in detail in a previous article, ref. (1). We mention here its essential characteristics and any modifications made during the present experiment.

Two Wilson cloud chambers were situated one above the other as illustrated in Fig. 1. The upper chamber, of useful volume ($68 \times 68 \times 30$) cm^3, was situated in a magnetic field of about 5000 gauss whilst the lower chamber, of similar useful volume, contained 13 copper plates each 1 cm thick. A lead slab 22 cm in thickness separated the two chambers. The aluminium producer, 4 cm thick, formed the roof of the magnet chamber. The expansion of the chambers was initiated by a coincidence pulse from the counter trays *B*, *C*, *D* and *E*. Two combinations $BCD_2E_2 - B_2$ and $BCD_2E_2 - B_3$ where used.

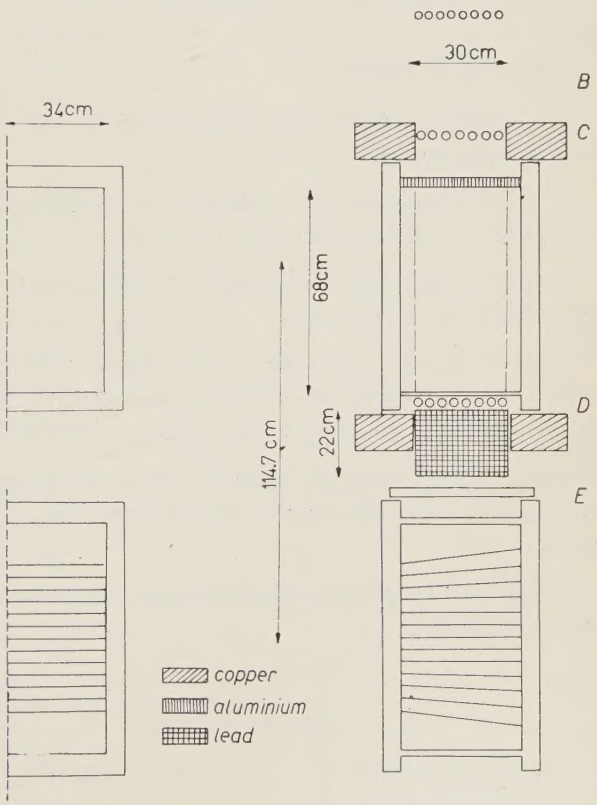

Fig. 1.

(1) B. P. Grégory, A. Lagarrigue, L. Leprince-Ringuet, F. Muller and C. Peyrou: *Nuovo Cimento*, **11**, 292 (1954).

Each chamber was photographed by 3 cameras, and a supplementary camera placed on a level with the underside of the producer improved visibility in the important region near the origin of the interaction.

2·2. *Measurement.* – The three magnet chamber photographs of each event were projected in turn at unit magnification and the curvature of each track measured by comparison with standard curves.

The maximum detectable momentum (M.D.M.) of the chamber was determined by measuring 145 no field μ-meson tracks which passed through the lead slab and the multiplate chamber. From the distribution of the measured sagittae of these μ-mesons tracks we have obtained a value of M.D.M. of 30 GeV/c for a track length of 40 cm.

The reconstruction of the tracks in space was obtained from full scale drawings of the three projections. The relevant calculations using these measurements were then undertaken with the aid of an electronic computer.

3. – Selection of events.

The events analysed were selected from the non-electronic showers using the following criteria:

i) *Multiplicity*: the number of minimum ionizing tracks with momentum > 110 MeV/c, n_s, must be $\geqslant 3$.

ii) *Energy*: the total resultant momentum of the charged secondaries, $\sum p_L$, must be $\geqslant 10$ GeV/c.

iii) *Geometry*: the events must have good geometry, that is:
— be visible on all three photographs, and
— have $> 60\%$ of all tracks measurable over 25 cm of track length.

iv) *Origin*: we have rejected all events which had two or more particles incompatible with the origin defined from the drawings of the three photographs.

In 9 600 photographs, we found 142 showers satisfying the first three criteria, as follows:

142 $\sum p_L \geqslant 10$ GeV, $n_s \geqslant 3$, good geometry

- 96 unique origin
  - 84 without V^0
  - 8 with V^0
  - 1 with 2 V^0
  - 3 with $V^{\pm}$
- 21 one incompatible
  - 17 without V^0
  - 4 with V^0
- 25 $n > 1$ incompatible
  - 16 shower origins detectable
  - 9 multiple origin

2344

We have therefore chosen for study 101 showers apparently unaccompanied by unstable particles, and 16 showers with unstable particles.

In addition we have three showers of energies certainly greater than 100 GeV, which we have been unable to study because of superposition of the tracks.

4. – Showers with no apparent unstable particle.

4·1. *Introduction.* – Among the 117 showers selected as described in Section 3 there were 101 without apparent unstable particles.

In this Section, we shall study the properties of the 101 showers under the following headings:

— the primary particles and the nature of the interaction;

— the secondary particles: nature, multiplicity, distributions of momenta, angles and transverse momenta;

— the quantity $1.5 \sum (U - p_L)$.

4·2. *Primary particles.*

4·2.1. Mean momentum. – The primary momentum was defined from the vector sum of the momenta of the charged secondary particles ($\sum p_L$). Fig. 2 shows the distribution of $\sum p_L$ for the 101 showers. The mean and median values are about 28 and 27 GeV/c, respectively.

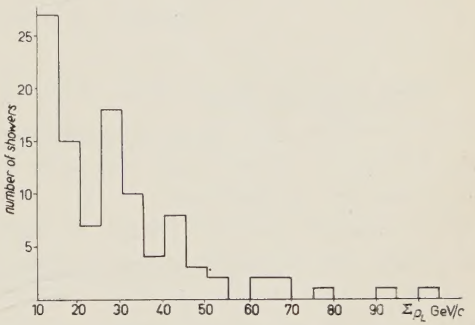

Fig. 2. – Total visible momenta of the showers.

Assuming that there is charge independence in the production of secondary particles, and that in each shower the primary particle becomes the most energetic of the visible particles, we can write:

$$\overline{p} = \overline{\sum p_L} + \tfrac{1}{2}\,\overline{\sum (p_L - p'_L)}\,,$$

where $\overline{p}$ is the mean primary momentum,

$\overline{\sum p_L}$ is the mean value of the vector sum of all the charged secondaries,

$\overline{\sum (p_L - p'_L)}$ is the mean difference between $\overline{\sum p_L}$ and the momentum of the most energetic visible particle.

Among our showers,

$$\overline{\sum p_L} = 28 \text{ GeV/c} ,$$

$$\overline{\sum (p_L - p'_L)} = 16 \text{ GeV/c} ,$$

$$\therefore \overline{p} = 36 \text{ GeV/c} .$$

This is compatible with the mean energy of primary protons between 10 and 100 GeV, obtained from ref. [2].

4·2.2. Nature of the interaction. – For our experiment we adopted a triggering system designed to eliminate neutral primary particles (cf. Section 2·1). At the altitude of the Pic du Midi, the interacting charged component of cosmic rays contains protons, $\pi^{\pm}$-mesons, α-particles. The proportion of α-particles at our altitude is negligible (ref. [2,3]).

From ref. [4], the ratio

$$\frac{\text{number of charged } \pi\text{-mesons}}{\text{number of protons}} \sim 0.4 \pm 0.1 .$$

From the ratio given above, we have calculated the numbers of our primary particles which may have been protons and $\pi^{\pm}$-mesons. Assuming that these two types of particles have the same interaction cross-section, we have found the following proportions:

70% of interactions were caused by protons,

and

30% by charged π-mesons.

We have attempted to use the distribution of the mean excesses of positive particles among our showers (Fig. 3*a*) in order to obtain some information about the nature of the interaction of the primaries with the nucleus of aluminium. For each shower, the positive excess is the number of positive particles minus the number of negative particles. Electrons identified as in Section 4·3 (below) are ignored.

---

[2] S. F. Singer: *Progr. Cosmic Ray Phys.*, **4**, 282 (1958).
[3] H. V. Neher: *Ann. Rev. Nucl. Sci.*, **8**, 225 (1958).
[4] K. Greisen: *Progr. Cosmic Ray Phys.*, **3**, 108 (1956).

2346

The mean positive excess is 1.7, after account has been taken of the particles of unknown sign. The mean positive excess depends not only on the mean positive excess in the primaries but also on the mean number of target

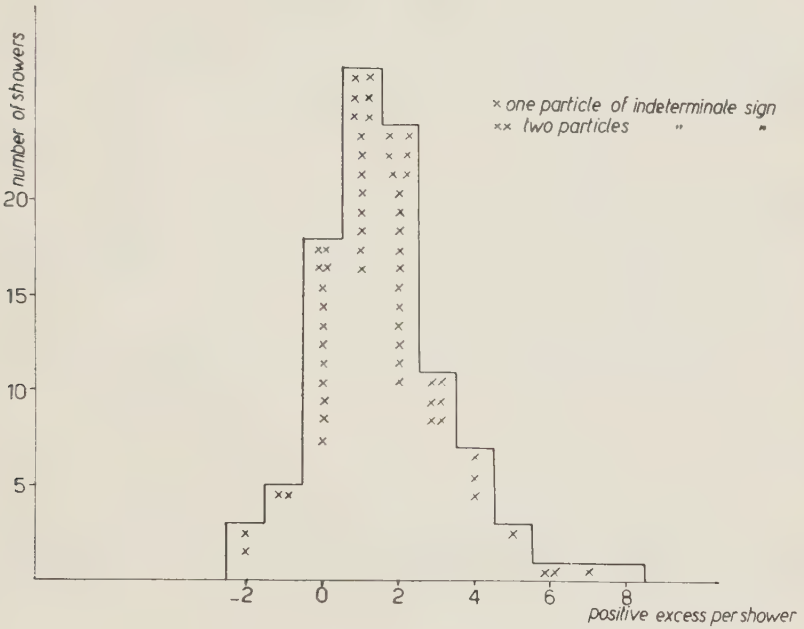

Fig. 3*a*. – Excess of positive particles.

nucleons involved in the collision. If there are equal numbers of positive and negative π-meson primaries then the mean positive excess in the primaries for the quoted ratio of $\pi^{\pm}$-mesons to protons (~ 0.4), is 0.7. Since there are 14 neutrons and 13 protons in the aluminium nucleus we should therefore have an average of two nucleons involved in the collision in order that the struck protons may yield the residual positive excess of unity. If the nuclear radius is given by

$$R_n = r_0 A^{\frac{1}{3}},$$

where

$$r_0 = 1.3 \cdot 10^{-13} \text{ cm}$$

and

$$A = \text{atomic weight},$$

a calculation based on a simple model of the nucleus (ref. [5]) shows that a single particle travelling through the nucleus of aluminium will make an aver-

[5] B. Rossi: *High Energy Particles* (1952), p. 360.

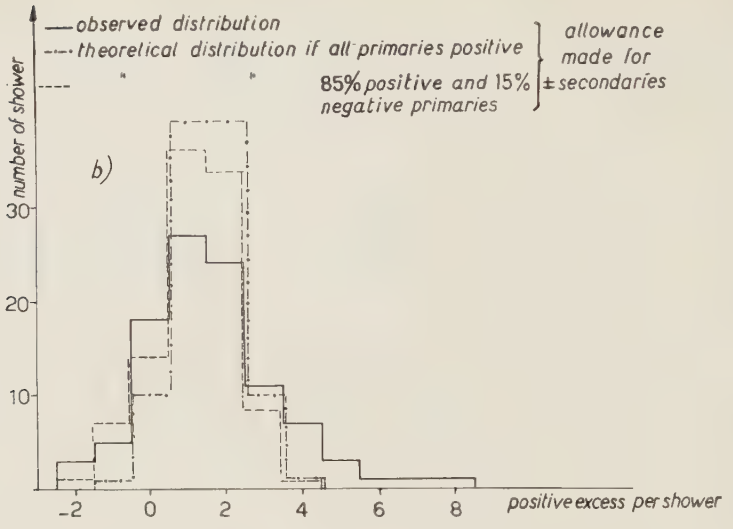

Fig. 3*b*. – Excess of positive particles: primary-nucleon collisions.

age of 1.8 collisions, provided the nucleon-nucleon cross-section is taken as 20 mb. Since this is close to the experimental values of the nucleon-nucleon cross-section at 10 GeV, ref. ([6]), we have calculated the expected distribution

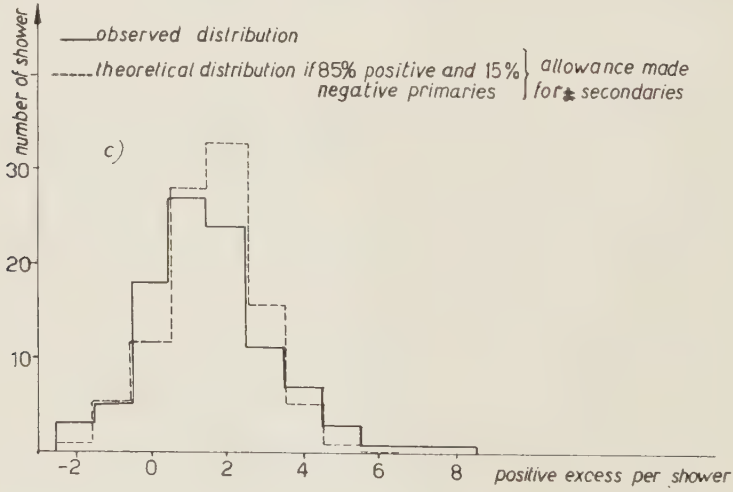

Fig. 3*c*. – Excess of positive particles: primary-Al nucleus collisions.

([6]) V. S. Barashenkov, V. A. Belyakov, E. G. Bubelev, Wang Shou Feng, W. M. Maltsev, Ten Gyn and K. D. Tolstov: *Nucl. Phys.*, **9**, 74 (1958).

2348

of the positive excess for the simple case of a single particle traversing an aluminium nucleus. The broadening effect due to the particles of unknown sign was taken into account and the nucleus was assumed of uniform density. Fig. 3*b* and 3*c* show the results.

Fig. 3*b* demonstrates the expected distribution if the primaries consisted of 30% $\pi^{\pm}$-mesons and 70% protons and collided with a single nucleon in the aluminium nucleus (dashed curve). For comparison we have shown the distribution we would have expected if the primaries had consisted solely of protons (dot-dash curve).

Fig. 3*c* then gives the expected distribution when the probabilities of colliding with several nucleons in the aluminium nucleus is taken into account. The disagreement between the expected distribution and the observed distribution is not large. This may indicate that there is a mechanism which prevents the π-meson secondaries produced in the collision from interacting again in their parent nucleus, for otherwise we might expect a considerably larger positive excess than observed.

4·3. *Nature of the secondary particles.* – These may consist of protons, charged hyperons and K-mesons, charged π-mesons, and electrons.

At momenta below a few GeV/c, the ionizing effect of the particles increases as the momentum falls. The ratio of track ionization to minimum ionization is > 2 for protons and hyperons of momenta < 750 MeV/c, K-mesons < 350 MeV/c, and $\pi^{\pm}$-mesons < 110 MeV/c. We therefore estimated that we could identify baryons, K-mesons, and $\pi^{\pm}$-mesons, below the corresponding momenta given above. All particles below 110 MeV/c with minimum ionization have been considered electrons.

In addition we have thought it possible to identify among the minimum ionizing particles with momenta over 110 MeV/c a number of electron pairs from considerations of geometry and scattering.

This method yielded 45 pairs of electrons. Assuming that the momentum spectra of the negative shower particles and the π^0-mesons were similar, we estimated that in addition to these 45 pairs with both electrons over 110 MeV/c, there were about 20 electron pairs with one electron below and one electron above 110 MeV/c. This means that about 20 single electrons are probably included in our shower particles, since we have found it impossible to associate them with their low-energy partners because of the large angle through which the latter were scattered.

In our study of the secondary particles in the paragraphs which follow, we have used all particles which appear to come from the shower origins, less the identified electrons and heavily ionizing particles with momenta >110 MeV/c. Separate histograms will be drawn for these latter particles.

Hence the particles we have studied and which are shown in our various histograms are $\pi^{\pm}$-mesons, possibly contaminated with:

— charged nucleons and hyperons, of momenta > 750 MeV/c;
— charged K-mesons, of momenta > 350 MeV/c;
— electrons which may have escaped detection, of momenta > 110 MeV/c

According to various observers, the proportion of heavy particles (nucleons, K-mesons, hyperons) among charged shower particles may be of the order of 20% (ref. [7-9]).

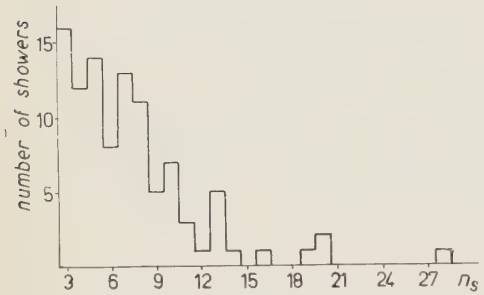

Fig. 4. – Particle multiplicities of the showers.

4·4. *Multiplicity.* – In Fig. 4 we have plotted the distribution of the multiplicity of our showers. This multiplicity, n_s, was defined as the number of particles described at the end of Section 4·3. The mean and median multiplicities are 7.3 and 7.0 per shower.

The mean multiplicities are given in the following table:

mean n_s	$= \langle n_s \rangle$	$= 7.28$ particles per shower
mean multiplicity of positives	$= \langle n_s^+ \rangle$	$= 3.93$
mean multiplicity of negatives	$= \langle n_s^- \rangle$	$= 2.70$
mean multiplicity of particles of indeterminate sign	$= \langle n_s^{\pm} \rangle$	$= 0.64$
mean multiplicity (including heavily ionizing particles)	$= \langle n_s + n_h \rangle$	$= 7.63$
mean multiplicity of positives (including heavily ionizing particles)	$= \langle n_s^+ + n_h \rangle$	$= 4.28$

If we distribute the $n_s^{\pm}$ between n_s^+ and n_s^- in the proportion $n_s^+ : n_s^-$, *i.e.* 1.44:1, we shall have:

$$\langle n_s^+ + n_h \rangle' = 4.66 , \qquad \langle n_s^- \rangle' = 2.96 .$$

In order to estimate the number of particles produced in a collision of a primary with an aluminium nucleus in our energy region we have proceeded as follows.

(7) B. Edwards, J. Losty, D. H. Perkins, K. Pinkau and J. Reynolds: *Phil. Mag.*, **3**, 237 (1958).

(8) L. F. Hansen and W. B. Fretter: preprint.

(9) A. I. Alikhanov, G. P. Eliseev, V. Š. Kamaljan, B. A. Liubimov, B. I. Moiseev i A. B. Khrimjan: *Žurn. Eksp. Teor. Fiz.*, **36**, 404 (1959).

2050

Since $\pi^{\pm}$-mesons and protons formed the major fraction of incident primaries and on the average a neutron and a proton in the aluminium nucleus were probably involved in the collision (see Section 4·2) we have assumed that the following reactions took place:

$$\pi^{\pm} + (p + n) \rightarrow 0.33\,\pi^{\pm} + 0.33\,\pi^{\mp} + 0.33\,\pi^{0} + (p + n) + \text{produced particles}$$

$$p + (p + n) \rightarrow 0.5\ p + 0.5\ n + (p + n) + \text{produced particles},$$

where the first two occurred 30 % of the time, the third 70 % of the time, and it is assumed that charge independence holds. Hence the charge remaining on the degraded primary and the target particles after collision was 1.45 positive and 0.10 negative per interaction. Since 4.46 positive and 2.96 negative secondaries were observed per interaction then 3.21 positive and 2.86 negative were really produced.

The distribution of n_s as a function of $\sum p_L$ is shown in Fig. 5. There is a tendency for high energy events to have a larger number of secondary particles than low energy events.

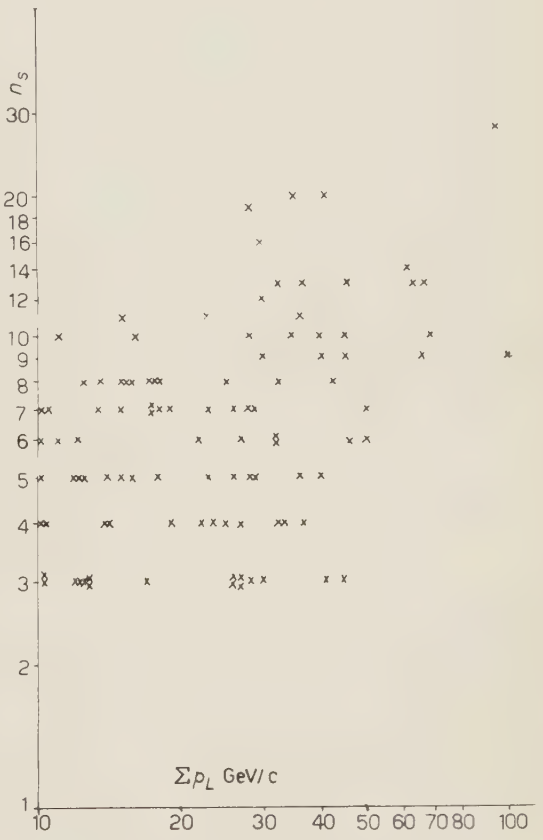

Fig. 5. – Momentum-multiplicity correlation of the showers.

4·5. *The momenta of the secondary particles.* – Fig. 6 shows the distribution of the momenta (p) of all shower particles (as defined at the end of Section 4·3) and Fig. 7*a* those of the positive and negative particles. There are also 32 M.D.M. particles with $p > 20$ GeV/c which are not shown in these histograms. For the calculation of primary momenta (Section 4·2.1) and axis directions (Section 4·6) we have assigned a value of 20 GeV/c to these particles. (Ideally, all particles with measured momenta approaching the M.D.M. should

be corrected for the effect of simulation which, because of the rapidly falling secondary momentum spectrum, makes it possible for a given particle to simulate one of higher or lower momentum depending on whether the differential secondary momentum spectrum has a slope greater ot less than -2. But in our case the slope is too badly defined in the required momentum region.)

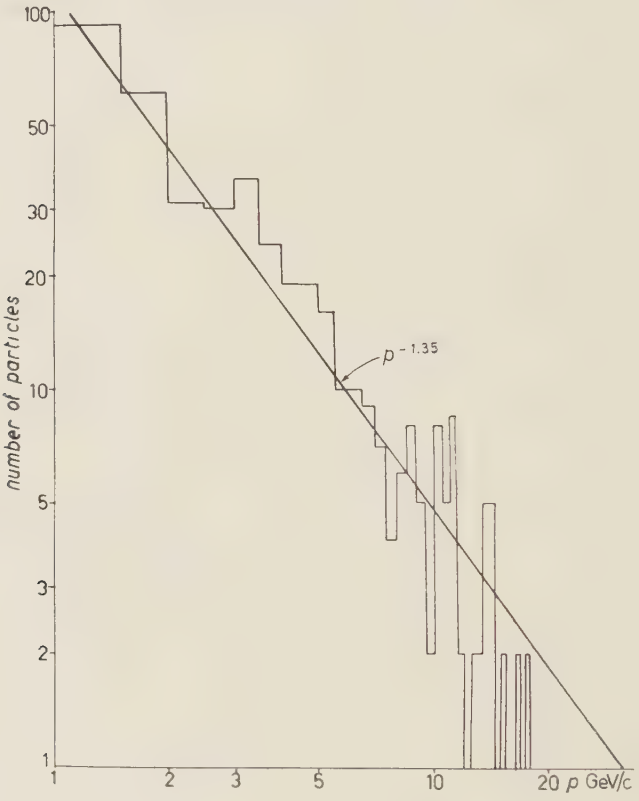

Fig. 6. – Particle momenta.

For $1 < p < 15$ GeV/c, the distribution in Fig. 6 is given by

$$\frac{1}{N_s}\frac{\mathrm{d}n_s}{\mathrm{d}p} \sim 0.3p^{-q}, \qquad \text{with } 1 < q < 1.6,$$

where $N_s = \sum n_s$. The positive and negative particles, taken separately, also seem to be distributed according to the same law.

There is some difference between our results and those of ref. (6): this may be due to the different range of primary energies in our case.

2352

The ratio of the numbers of positive and negative particles (n_s^+/n_s^-) as a function of momentum is given in Fig. 7*b*. This diagram has a maximum at $0.5 < p < 1.0$ GeV/c, which is probably due to recoil protons with $0.75 < p <$

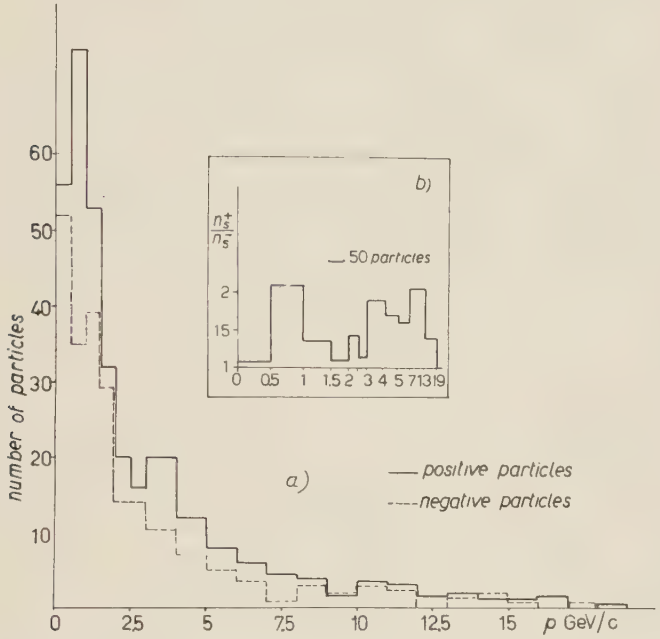

Figs. 7*a*, *b*. – Distribution of particle momenta.

< 1.0 GeV/c. (Recoil protons with $p < 0.75$ GeV/c, identified by the ionization of their tracks, are not shown in the figure.) There appears to be another increase in the positive excess at about 3 GeV/c.

4·6. *Angular distribution of secondary particles.* – In the absence of more precise information, we have taken the direction of the resultant momentum of all the secondary particles as an estimate of the primary direction. The error due to fluctuation in the number of π^0-mesons is negligible, while that due to fluctuation in their angular distribution is (cf. Appendix I):

$$\Delta\varphi = \frac{0.4\sqrt{2}}{\beta_c \gamma_c \sqrt{n_s}} \text{ rad} .$$

For example, the axis of a shower of 7 charged particles with $\sum p_L$ of 28 GeV/c, is defined with an error, $\Delta\varphi$, of about 2° (assuming a nucleon-nucleon interaction.)

We have studied the detection efficiency in the illuminated region of the chamber for all the showers. We found that:

all particles with $\theta < 40°$
two-thirds of particles with $40° < \theta < 60°$
one-third of particles with $60° < \theta < 90°$

would be detected. θ is the angle at the origin between the shower axis and the particle's track.

Fig. 8*a* shows the angular distribution of positive and negative particles. The median angle is 8°. There is a noticeable positive excess below 5°. Angular distributions of particles of indeterminate sign (including M.D.M. particles) and of heavily ionising particles are given in Fig. 8*b* and 8*c*.

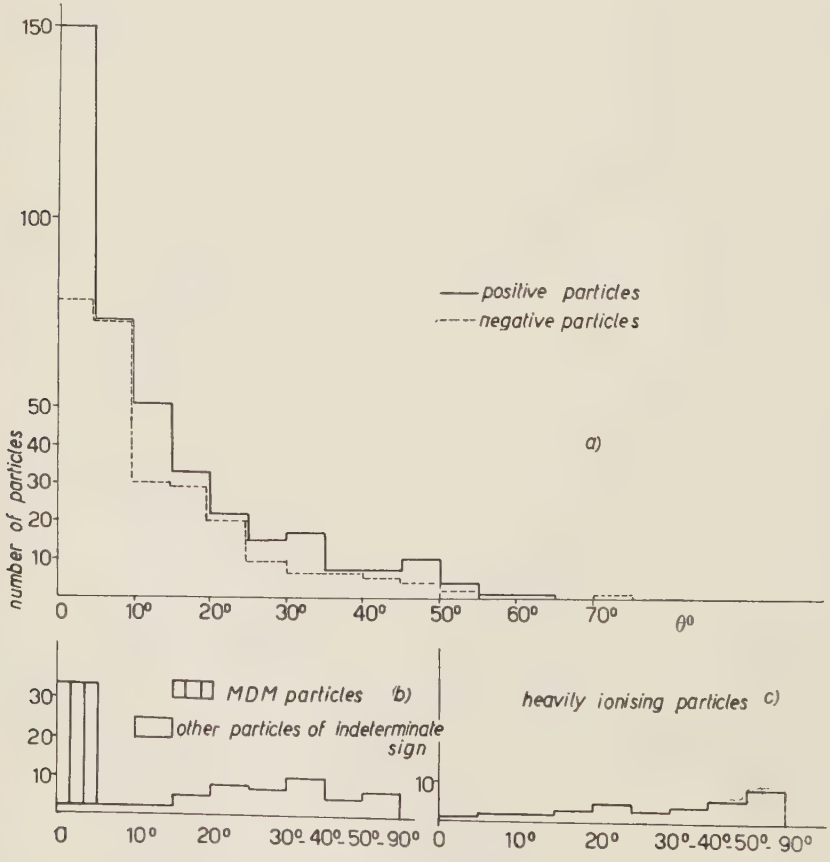

Fig. 8*a*, *b*, *c*. – Angular distribution of particles.

The angular distribution of all our minimum ionizing particles is similar to that in ref. (6).

2354

4·7. *Momentum-angle correlation.* – We examined our showers in an attempt to discover whether there was any correlation between the angles of emission and the momenta of the particles. Fig. 9 shows the results.

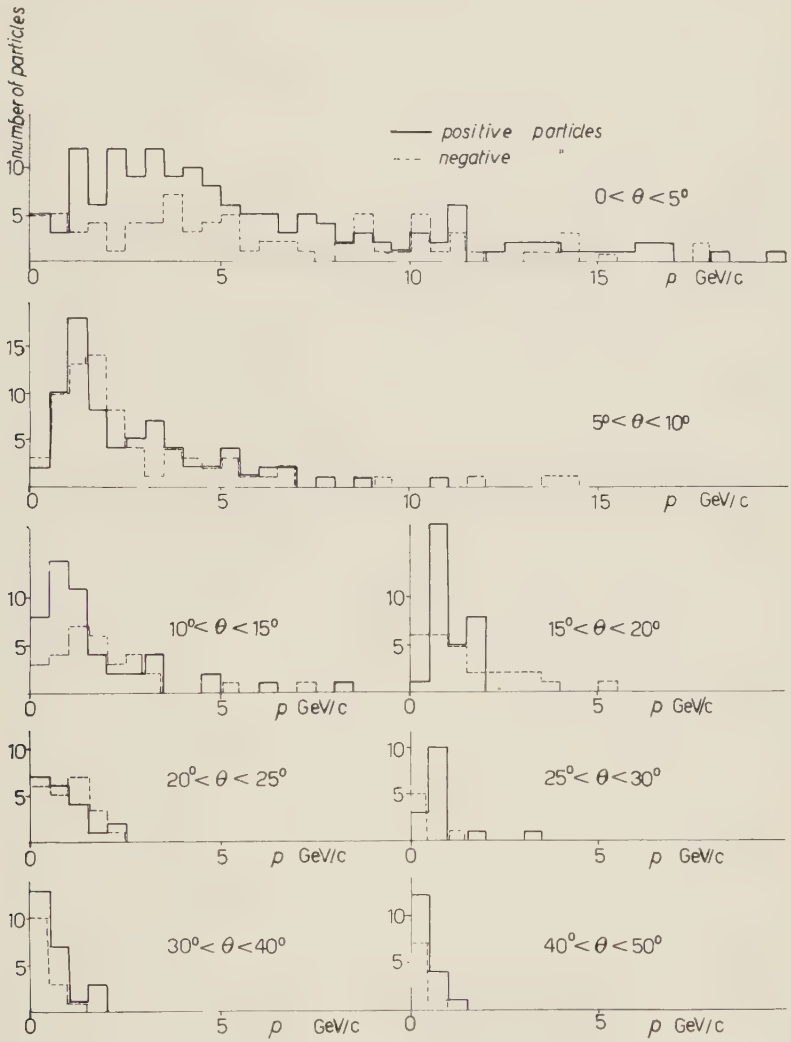

Fig. 9. – Momentum-angle correlation.

As one would expect, the mean momentum of the particles decreases as the angle of emission increases. There is an excess of positive particles at most angles as we saw in Section 4·6, but this excess is unusually great between 0° and 5°. It is difficult to explain this observation in terms of either

a) recoil protons which are unlikely to be found preferentially at $\theta < 5°$ or

b) a simple mechanism in which the primary particles (mainly protons) lose only a small fraction of their energy, since the ratio n_s^+/n_s^- is greatest at low particle momenta.

Particle momenta = (0 ÷ 5) GeV/c	$n_s^+/n_s^- = 2.2$
— (5 ÷ 10)	= 1.6
= (10 ÷ 15)	= 1.3

4·8. *Transverse momenta of secondary particles.* – The transverse momentum (p_t) of a secondary particle produced in a high energy interaction is an important experimental quantity since it is invariant under a transformation from the laboratory to the centre of mass system of the interaction. The distribution of p_t observed in the laboratory system should therefore represent the true distribution in the C.M.S. and as such may be readily compared with theory.

Since in the laboratory system the particles emitted in the C.M.S. backward hemisphere make relatively larger angles with the primary direction than do the particles emitted in the C.M.S. forward hemisphere, one might expect the p_t values of the former to be biased to slightly higher values than those of the latter. In order to test this hypothesis, each interaction was transformed to an effective C.M.S. in which the resultant momentum of the charged particles was zero. The p_t distributions of forward and backward particles were found to be similar. We surmise that the error in the primary direction (cf. Section 4·6) has little effect on the distribution of p_t.

The p_t distributions of positive and negative secondaries (defined at the end of Section 4·3) have been normalized and superposed in Fig. 10, which

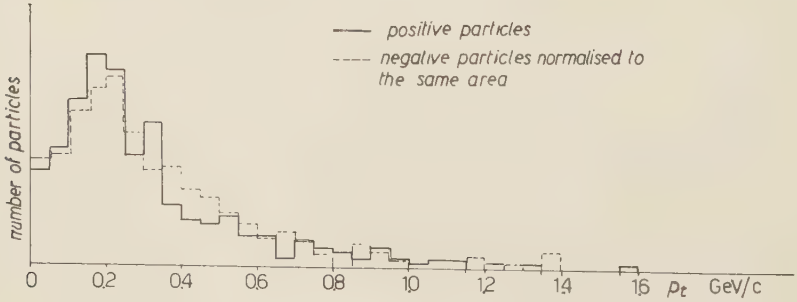

Fig. 10. – Transverse momenta.

indicates that there is no significant difference between them. The mean value of p_t is 0.31 GeV/c, and the R.M.S. deviation is 0.23 GeV/c. From the simi-

21156

larity of the two distributions we infer that since particles of nucleonic mass must be present in reasonable number they must either

i) have a p_t distribution not very different from that of the π^+-meson secondaries (if they are present predominantly as particles of the same sign, *e.g.* protons); or

ii) exist in approximately equal numbers with positive and negative charges (if their p_t distribution is appreciably different from that of the $\pi^{\pm}$-mesons).

As shown in Section 4·4, it seems that there were very few charged hyperons among our showers. This indicates that the particles of nucleonic mass were in a large majority protons. The similarity of the positive and negative p_t distributions is therefore good evidence that the p_t distribution of the protons is not markedly different from that of the π^+-mesons. We note in passing that the p_t of the heavily ionizing particles has a mean value of 0.21 GeV/c, with a R.M.S. deviation of 0.12 GeV/c.

Fig. 11 is a histogram of the p_t values of shower particles of both signs. Two curves have been superposed on it for purposes of comparison. The dotted curve is a theoretical p_t distribution taken from ref. ([10]), for a final thermal

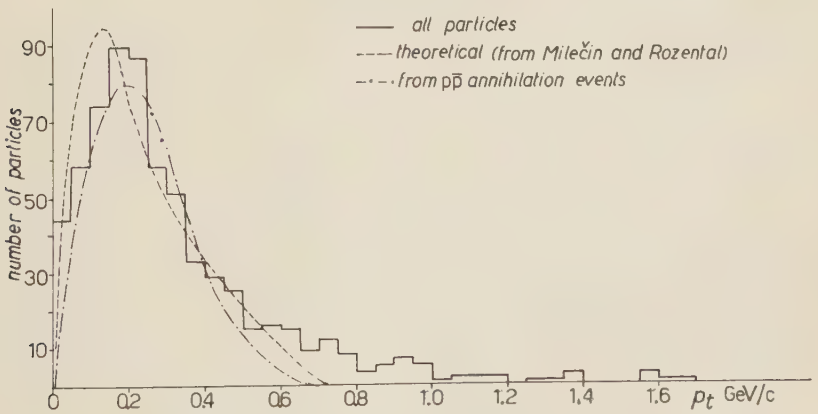

Fig. 11. – Transverse momenta.

equilibrium temperature of $T_f = m_\pi c^2/2k$. The other curve is derived from the experimental momentum distribution of the π^+-mesons created in antiproton annihilation events, ref. ([11]).

([10]) G. A. Milečin and I. L. Rozental: *Suppl. Nuovo Cimento*, **8**, 770 (1958).
([11]) E. Segrè: *Report of Kiev Conference*, (1959).

22357

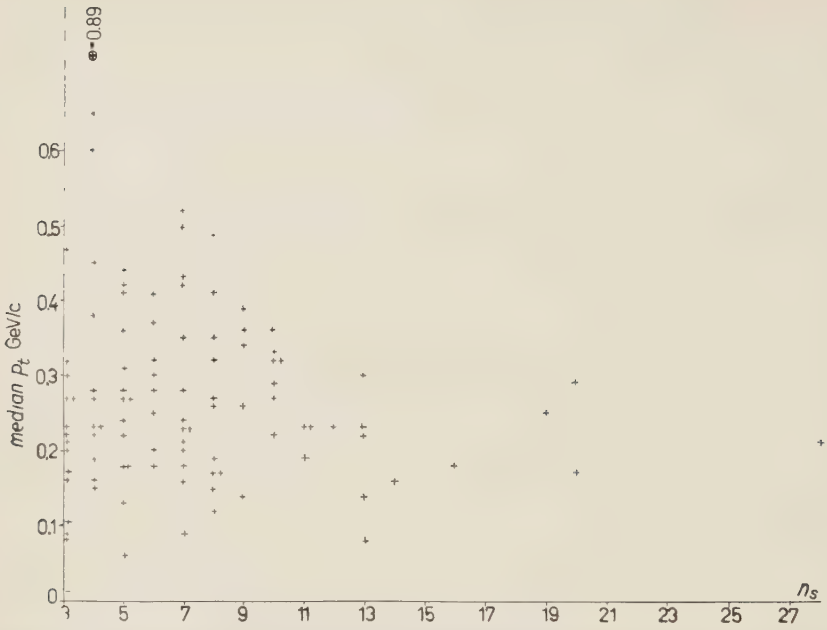

Fig. 12*a*. – The correlation of the median transverse momentum of the showers and their multiplicity.

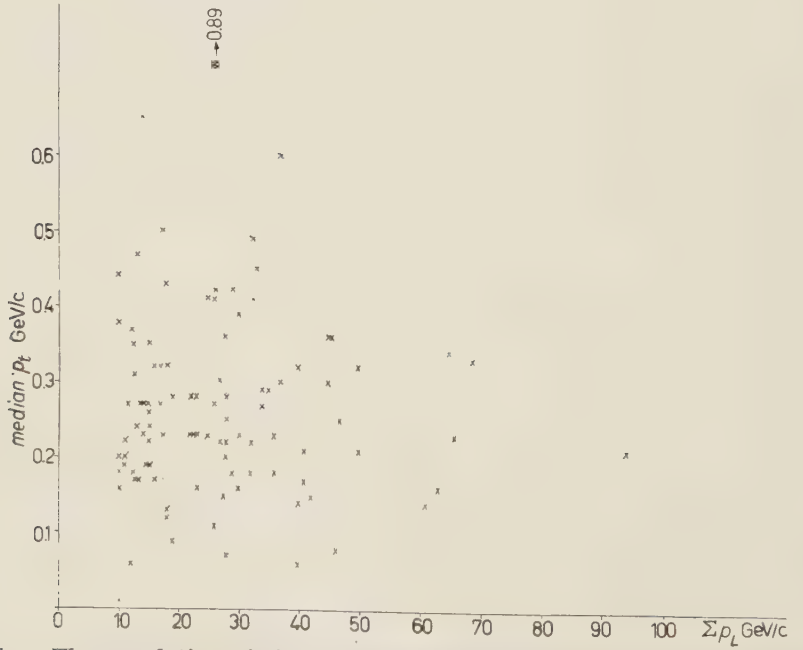

Fig. 12*b*. – The correlation of the median transverse momentum of the showers and their total visible momentum.

2358

The fact that we were able to measure the momenta of most particles of each shower allows us to consider each interaction separately. Fig. 12*a* shows the median p_t value of each shower as a function of its multiplicity. These quantities are independent. For each value of n_s the values of median p_t are widely dispersed. This diagram may be of theoretical interest if p_t really reflects the C.M.S. momentum of the particle. This would be true if the $\pi^{\pm}$-mesons were emitted isotropically from their centre of production. We also found that the median p_t is independent of the total visible momentum, $\sum p_L$ (Fig. 12*b*).

4·9. *The quantity* $1.5 \sum (U - p_L)$. – We have thought it if interest to construct the distribution of the quantity $1.5 \sum (U - p_L)$ for the minimum ionizing particles of each shower (Fig. 13), where U is the laboratory energy of

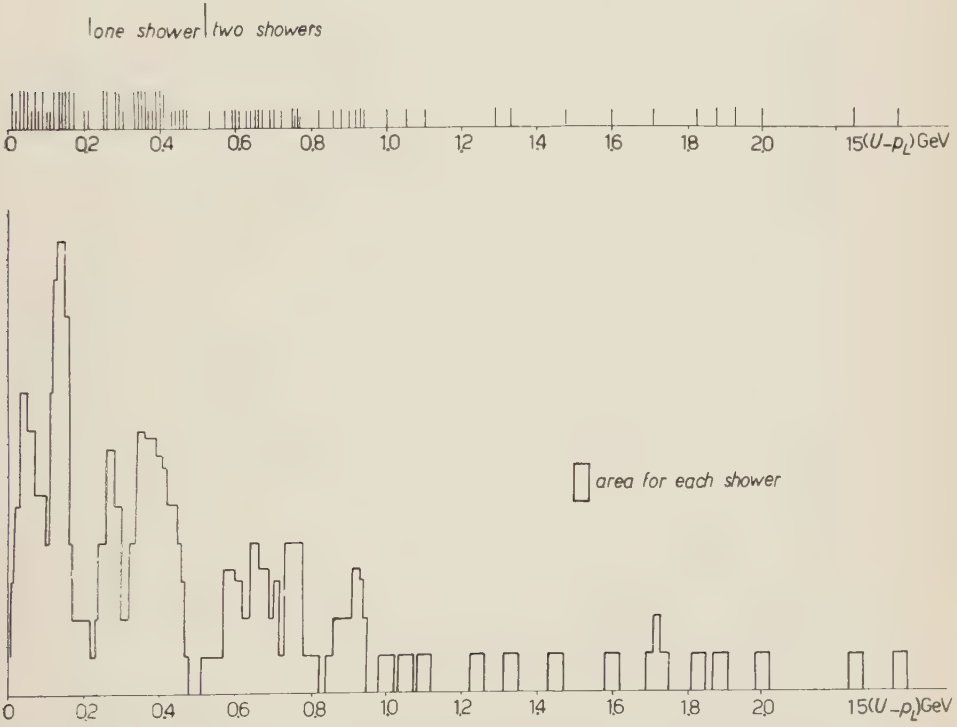

Fig. 13. – $1.5(U - p_L)$ for all minimum ionizing particles; all particles taken as π-mesons.

each shower particle, assumed of pion rest mass, and p_L the longitudinal component of particle momentum along the primary direction. The factor 1.5 is introduced to take account of the unseen π^0-mesons. In Fig. 14 the same

quantity has been plotted except for those events where the most energetic particle had a momentum greater than twice that of any other particle in the shower. In these cases the fastest particle was assigned the mass of the nucleon and its $(U - p_L)$ was not multiplied by the factor 1.5. This procedure was followed since it was thought not unlikely that this particle was the degraded primary nucleon.

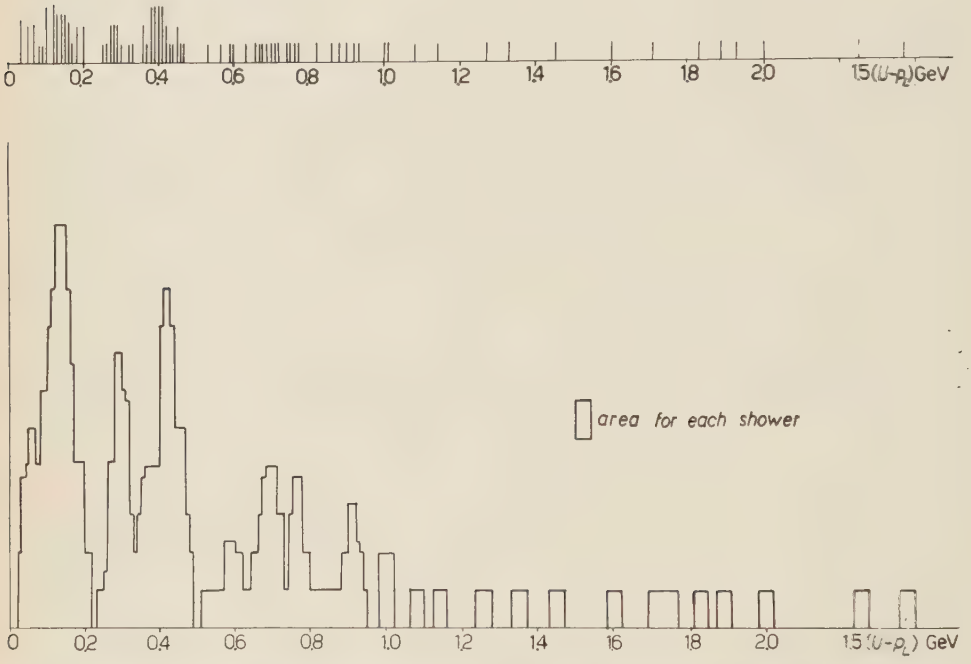

Fig. 14. – $1.5\,(U - p_L)$ for all minimum ionizing particles; all particles taken as π-mesons (except that any particle with momentum at least twice that of any other in its shower, is taken as nucleon).

In these figures the upper diagram represents the distribution of $1.5\,\sum(U - p_L)$ where each event is indicated by a vertical line. In order to bring out the concentration of these events along the $(U - p_L)$ axis each event has been assigned the same area and the lower diagram has been constructed. Both figures show evidence of structure rather than a continuous distribution. We note that the first three maxima of Fig. 14 are situated at approximately m_-, $2m_\pi$ and $3m_\pi$. The distribution of $1.5\,\sum(U - p_L)$ below 0.42 GeV ($\sim 3\,m_\pi$) is of special interest since any recoil proton associated with these events is likely to be identified by its ionization and therefore not included in the summation $1.5.\ \sum(U - p_L)$. The reason for this is that there exists, for nucleon-

2360

nucleon or π-nucleon collisions, a direct correspondence between the quantity $1.5 \sum (U - p_L)$ and the $(U - p_L)$ of the recoil nucleon given by the equation (cf. Appendix II):

$$1.5 \sum (U - p_L) + (U - p_L)_{\text{recoil}} = M_N = \text{Nucleon mass}.$$

Thus for events with $1.5 \sum (U - p_L) < 0.42$ the $(U - p_L)_{\text{recoil}}$ is greater than 0.52 GeV. Reference to Fig. 15, which shows the relation between the momentum and angle of the recoil proton for various values of its $(U - p_L)$, then indicates that recoil protons with $(U - p_L) > 0.52$ GeV and transverse momenta in the region below 0.3 GeV/c will have momenta < 750 MeV/c and therefore be detected by ionization.

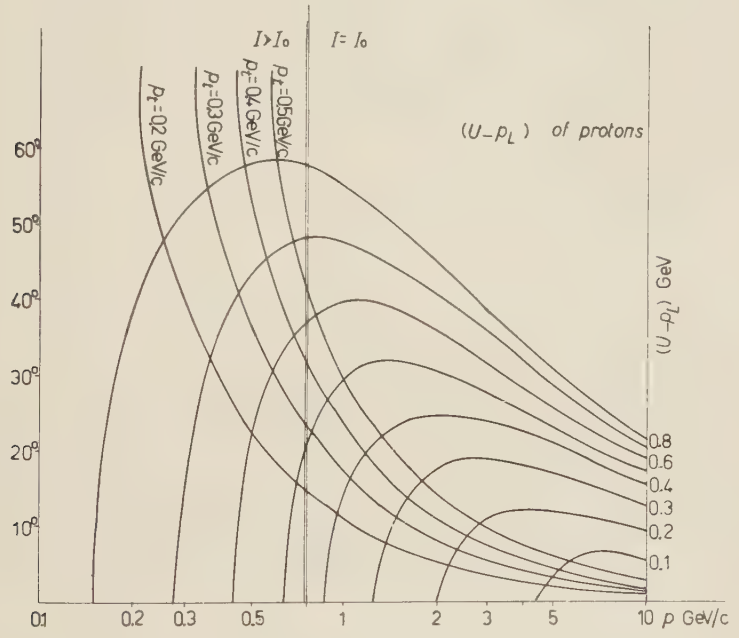

Fig. 15.

The apparent structure in the distribution of $1.5 \sum (U - p_L)$ may thus reflect the fact that the $(U - p_L)$ of the recoil nucleon is restricted to certain values.

In Fig. 16 a plot of the multiplicity of each event against its $1.5 \sum (U - p_L)$ shows that a correlation exists between these two quantities.

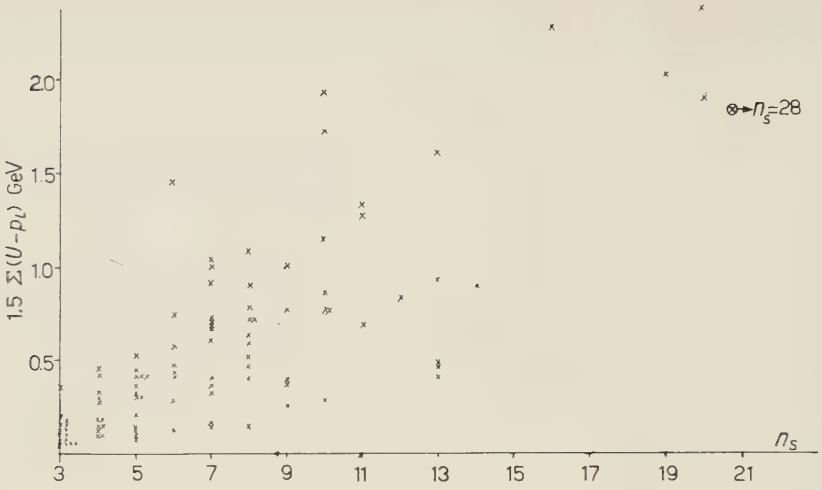

Fig. 16. – The correlation of $1.5 \sum (U - p_L)$ and multiplicity.

5. – Showers with unstable particles.

5·1. *Introduction.* – Among the 117 showers selected as described in Section 3, we observed:

12 showers each associated with the production of one neutral unstable particle;
1 shower associated with two neutral unstable particles;
3 showers each associated with a charged unstable particle.

Of our neutral unstable particles 12 had both decay products with measurable momenta.

In the remainder of this Section we shall refer to neutral unstable particles as V^0 particles, and to charged unstable as $V^{\pm}$ particles.

In this Section, we shall study:

— the V^0 particle alone;
— the showers with V^0 particles, after the V^0 particles have been incorportated into their respective showers;
— three showers and their associated $V^{\pm}$ particles.

5·2. *The* V^0 *particles.*

5·2.1. Compatibility of the V^0 particle with the shower origin. – We tested the vector sum of the two decay products of each V^0 to see

whether the vector direction passed through the shower origin. By taking into account the errors in

— the position of the shower origin,
— the position of the decay point of the V^0,
— the direction of the decay products, we found that the measured deviations were always smaller than the calculated values. This means that all our V^0 particles can be considered as:

i) originating at the shower origin,

ii) decaying into two particles only.

5·2.2. Efficiency of detection of V^0 particles. – An attempt was made to estimate the number of V^0 particles which escaped detection. For this purpose we defined a « visible region » in the chamber, believing that any V^0 particle decaying in this region was bound to be observed.

For each of our observed V^0 particles we measured the distance it would have travelled inside the visible region if it had not decayed on the way. We called this distance L. We then calculated the probability that it should have decayed within the region, *i.e.*

$$P = \exp\left[-\frac{l'}{\lambda}\right] - \exp\left[-\frac{l}{\lambda}\right],$$

where: λ is the mean distance travelled before decay by a V^0 of the same energy,

l' is the distance between the shower origin and the V^0 particles entry into the visible region, and

l is $(l' + L)$.

For each V^0 particle we have calculated P on both θ_1^0 and Λ^0 hypotheses, assuming that the mean lifetimes of θ_1^0 and Λ^0 particles are 10^{-10} s and $3 \cdot 10^{-10}$ s, respectively; ref. ([12]). This yielded:

$$\Lambda^0 \text{ hypothesis} \qquad \langle 1/P \rangle = 2.0$$

$$\theta_1^0 \text{ hypothesis} \qquad \langle 1/P \rangle = 1.9$$

The R.M.S. deviations of the distributions of $1/P$ are 0.5 and 0.7, respectively.

Our detection efficiencies were therefore similar for Λ^0 and for θ_1^0 particles, if we suppose that both particles are created with the same momentum and angular distributions.

([12]) C. Franzinetti and G. Morpurgo: *Suppl. Nuovo Cimento*, **6**, 469 (1957).

2363

5·2.3. *Momenta of the* V^0 *particles.* – The distribution of the momenta of the V^0 particles is given in Fig. 17*a*, which shows that 8 out of the 12 V^0 particles have momenta greater than 3 GeV/c. In addition to the 12 V^0 particles included in the figure, there were two whose decay products were visible along 10 cm only and whose momenta could not be measured.

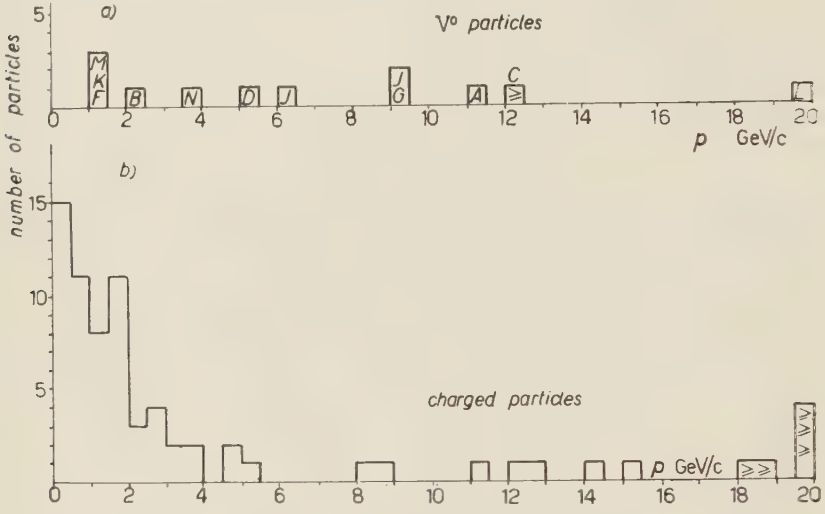

Fig. 17. – *a*) Momenta of particles from showers with V^0 particles.

5·2.4. *Armenteros-Podolanski diagram.* – If a V^0 particle decays to give two charged secondaries, it may be represented by a point on this diagram, ref. [13]. The position of the point is defined by the transverse momentum (p_t) of the secondaries, and by the α-value of the V^0, where

$$\alpha = \frac{p_+^2 - p_-^2}{p_0^2},$$

p_0, p_+, p_- are the momenta of the V^0 and its positive and negative secondary particles, respectively. The points representing different V^0 particles lie on families of ellipses. There is one family for each decay scheme of the V^0, and one member ellipse of each family for each value of p_0. If p_0 is greater than about 2 GeV/c, then for each decay scheme the ellipses become indistinguishable.

Hence, for $p_0 > 2$ GeV/c, we can draw a single ellipse (shown on the dia-

[13] J. Podolanski and R. Armenteros: *Phil. Mag.*, **45**, 13 (1954).

2364

gram, Fig. 18) for V^0 particles (Λ^0 particles) with the decay scheme:

$$\Lambda^0 \to p + \pi^- + 37.9 \text{ MeV}, \qquad \text{Ref. } (^{14}).$$

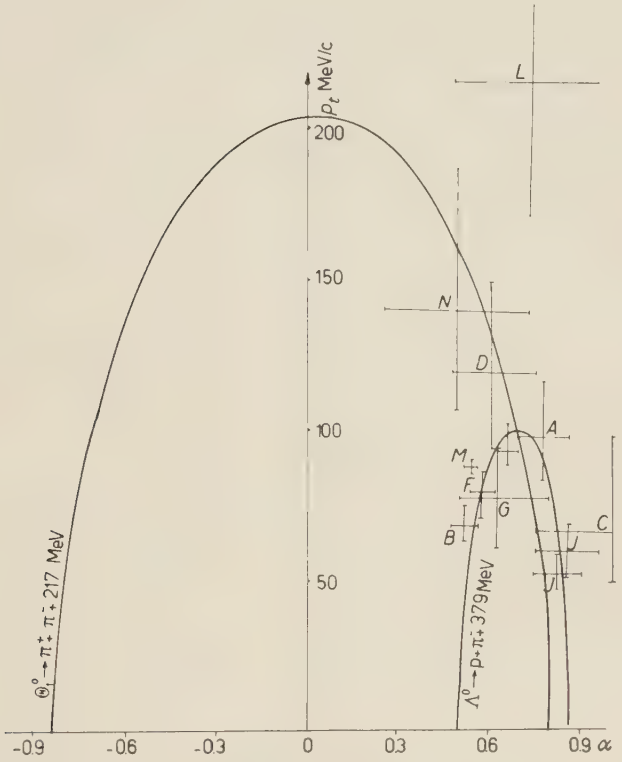

Fig. 18. – Armenteros-Podolanski diagram.

All Λ^0 particles have a positive value of α. For $p_0 > 2$ GeV/c, we can also draw a single ellipse (Fig. 18) for V^0 particles (θ_1^0 particles) with the decay scheme

$$\theta_1^0 \to \pi^+ + \pi^- + 217 \text{ MeV}, \qquad \text{Ref. } (^{14}).$$

The values of α of θ_1^0 particles have equal *a priori* probabilities of being either positive or negative.

The values of α and p_t are plotted in Fig. 18. The errors given are calculated from the extreme values of the angle between the secondaries, and of their momenta. This figure shows that all 12 V^0 particles have positive values

---

(14) C. D'ANDLAU, R. ARMENTEROS, A. ASTIER, H. C. DESTAEBLER, B. P. GREGORY, C. LEPRINCE-RINGUET, F. MULLER, C. PEYROU and J. H. TINLOT: *Nuovo Cimento*, **6**, 1135 (1957).

2365

of α. Since the α-values of θ_1^0 particles are equally likely to be positive or negative, this result inclines us to suppose that a high proportion of our observed V^0 particles are Λ^0.

This conclusion is borne out by the distribution of θ^* for Λ^0 and θ_1^0 hypotheses, shown in Fig. 19. θ^* is the angle in the rest mass system of the V^0 particle between the positive decay product's direction and the line of flight of the V^0.

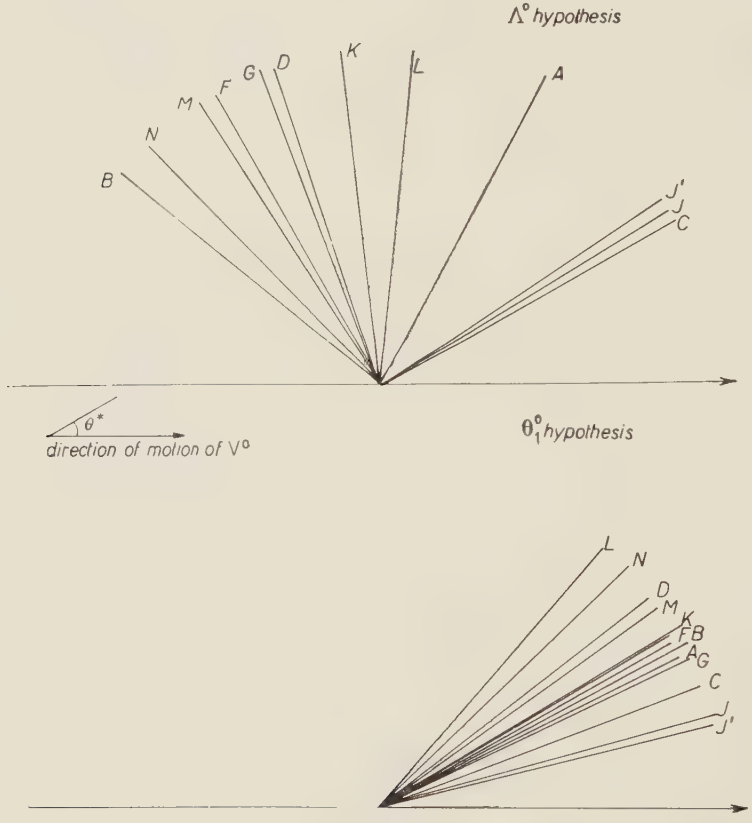

Fig. 19. – Distribution of θ^*.

We may note that of the 5 V^0 particles with showers of $\sum p_L$ below 10 GeV/c which occur among our 9600 photographs, three have α positive and two have α negative.

5.2.5. *Number of Λ^0 and θ^0 actually produced.* – In order to calculate these numbers we had to know two things: the numbers of Λ^0 and of θ_1^0 particles among our 14 V^0 particles, and the proportions of the total numbers produced

2366

(allowing for the undetected V^0 particles) which these numbers represented.

Of the 12 V^0 particles on the Armenteros-Podolanski diagram, 3 are compatible with θ_1^0 and lie in a region where the probability of finding a Λ^0 is nil. The other 9 are in a region of $p_t = 50$ to 100 MeV/c and $\alpha > 0$. If we suppose that decay products of a V^0 particle are on the average emitted isotropically in the rest mass system of the V^0, a given Λ^0 has a probability of 86 %, of lying here, and a given θ_1^0 has a probability of 8 %. Hence in a given batch of V^0 particles we would have expected about 10.5 times as many Λ^0 as θ_1^0 particles in this region. This would indicate that there were about 8 Λ^0 and 4 θ_1^0 among these 12 V^0 particles. Each of the 2 unmeasurable V^0 particles was thus twice as likely to be a Λ^0 than a θ_1^0 particle.

We therefore supposed that 10 ± 1 of our V^0 particles were Λ^0 and 4 ∓ 1 were θ_1^0.

Using the detection efficiency determined in Section 5·2.2 and the following branching ratios, ref. [12]:

$$\Lambda^0 \begin{cases} \nearrow p + \pi^- & (68 \pm 5)\,\% \\ \searrow n + \pi^0 & (32 \pm 5)\,\% \end{cases}$$

$$\theta^0 \begin{cases} \nearrow \theta_1^0 & (50\,\%) \\ \searrow \theta_2^0 & (50\,\%) \end{cases} \qquad \theta_1^0 \begin{cases} \nearrow \pi^+ + \pi^- & (85 \pm 6)\,\% \\ \searrow \pi^0 + \pi^0 & (15 \pm 6)\,\% \end{cases}$$

we estimated the total numbers of Λ^0 and θ^0 particles produced in our 117 showers. We found:

$$29.5^{+14.0}_{-11.0}\ \Lambda^0 \text{ particles},$$

$$9.0^{+7.5}_{-5.0}\ \theta_1^0 \text{ particles}, \quad \text{or} \quad 18^{+15.0}_{-10.0}\ \theta^0 \text{ particles}.$$

The branching ratios quoted in ref. [15] are slightly different and would have given us mean numbers of particles produced of 31.5 for Λ^0 and 19.0 for θ^0.

It is interesting to note that if the 4 V^0 particles interpreted as θ_1^0 were indeed θ_1^0 particles, then the probability of observing and $\alpha - p_t$ distribution similar to theirs was only 6 %.

5·3. *Showers with* V^0 *particles incorporated.*

5·3.1. Momenta of the primary particles. – The total visible momenta ($\sum p_L$) of our 11 showers with measurable V^0 particles are shown in

[15] *Report of Annual International Conference on High Energy Physics* (CERN, 1958).

Fig. 20*a* and 20*b*. The median value is 24 GeV/c. The presence of the neutral particle has a notable effect on the distribution of $\sum p_L$.

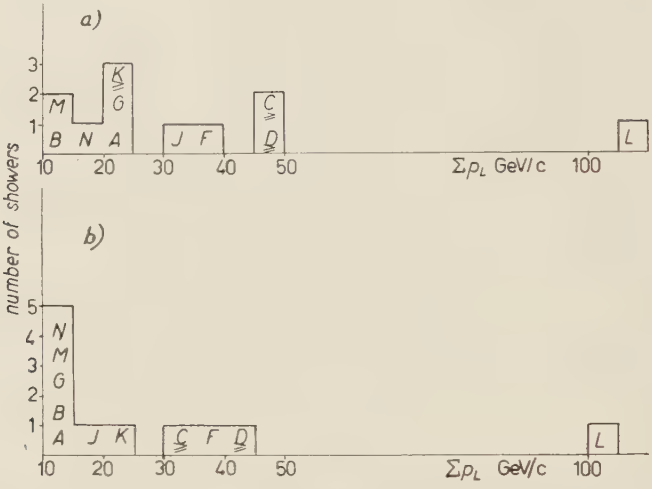

Fig. 20. – Total visible momenta of showers with V^0 particles. *a*) Including V^0 particles. *b*) Excluding V^0 particles.

5·3.2. Multiplicity, momenta, angular distribution and transverse momenta of the particles. –

a) The mean multiplicity of charged particles (other than heavily ionizing particles and identified electrons) is 6.9 particles per shower. This is similar to the value obtained for the showers without apparent unstable particles (cf. Section 4·4).

b) The momenta of all the measurable particles are shown in Fig. 17*b*. It will be seen that below 10 GeV/c the charged shower particles are distributed roughly according to the formula given in Section 4·5. The momenta of the V^0 particles show no such distribution.

The relatively small number of secondary charged particles with sufficient momentum to produce V^0's of the observed momenta indicates that, unless their cross-section for producing V^0 particles on their way out of the aluminium nucleus was high, then the V^0 particles must have been produced directly in the collision of the primary particle with a target nucleon.

c) We have defined the primary directions by the vector sum of the momenta of all particles, including the V^0 particles. The angular distribution of V^0 particles is shown in Fig. 21; all are emitted with an angle $< 20°$ with

2368

the direction defined above. The angular distribution of charged particles is compatible with that of the particles from showers without V^0 (cf. Section 4·8).

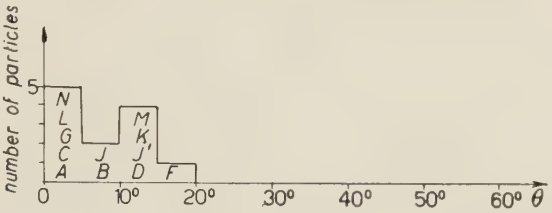

Fig. 21. – Angular distribution of V^0 particles.

d) The mean transverse momentum of the V^0 particles (Fig. 22*a*) is 0.59 GeV/c with an R.M.S. deviation of 0.15 GeV/c, and of the other particles 0.31 GeV/c with an R.M.S. deviation of 0.16 GeV/c. There is no apparent

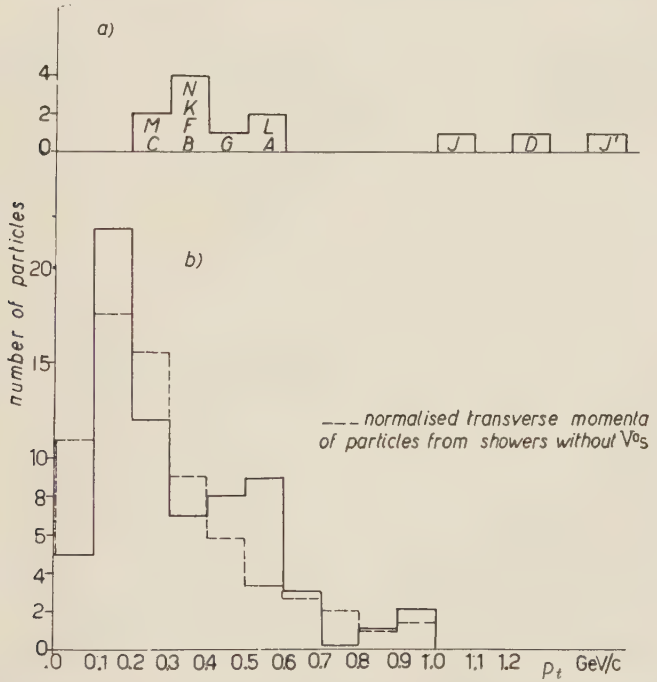

Fig. 22. – *a*) Transverse momenta of V^0 particles. *b*) Transverse momenta of charged particles from showers with V^0 particles.

difference between the transverse momenta of positive and negative particles. In Fig. 22*b*, the transverse momentum distribution of the charged particles from the V^0 showers is superposed on the normalized distribution for the non-

V^0 showers. The χ^2 test indicated that the two distributions are significantly different. The main contribution to χ^2 comes from the excess of particles with p_t values in the region of 0.5 GeV/c in the case of the V^0 showers.

5·3.3. Positive excess. – The mean positive excess of the 11 showers with V^0 particles of measurable momenta is 2.5 particles per shower. If we add the two V^0 showers with unmeasurable V^0's the mean excess does not change. This is significantly greater than the mean positive excess of the 101 showers without apparent V^0 particles (cf. Section 5·2.2), and may indicate that on the average more nucleons of the aluminium nucleus are involved in interactions in which V^0's are produced than in others.

5·4. *Charged unstable particles* ($V^\pm$).

5·4.1. Experimental data. – We observed three showers with charged unstable particles among our 117 showers. Their chief characteristics are given in the Table:

Nature	Momentum of $V^\pm$	Momentum of charged secondary (GeV/c)	Momentum of neutral secondary	Angle of decay of $V^\pm$
$V^\pm$	$p >$ MDM along 25 cm	too short	?	$\sim 1°$
V^-	too short	0.61 ± 0.02	?	6.1°
V^-	too short	0.2 ± 0.01	2.78 ± 0.3	25.3°

As the mean lifetimes of $K^\pm$ and charged hyperons are of the order of 10^{-8} and 10^{-10} s, respectively, the $V^\pm$ particles may be considered hyperons under our experimental conditions.

The third particle (V^-) is accompanied by a V^0 particle which decays in the chamber about 1 cm from the point of decay of the V^-. The vector sum of the momenta of the charged secondaries of the V^0 coincides with the line passing through the point of decay of the V^- and the shower origin. On the Armenteros-Podolanski diagram, this V^0 seems compatible with both Λ^0 and θ_1^0. It lies, however, in a part of the diagram where a Λ^0 has a higher probability of occurring than a θ_1^0. The best explanation of this event seems to be:

$$\Xi^- \rightarrow \Lambda^0 + \pi^- .$$

5·4.2. Number of charged hyperons. – It is difficult to calculate the detection efficiency for charged hyperons as it is difficult to detect small angles of decay, especially

i) if the particle decayed near the top or bottom of the visible region of the chamber;

ii) if the angle of decay were in the plane perpendicular to the front glass of the chamber.

(However, one of our three charged hyperons was detected with a decay angle of about 1°.) Consideration of the data from V^0's suggests that the mean decay angle of $\Sigma^{\pm}$ particles is of the order of 10°. Taken in conjunction with what is known of the lifetimes of charged hyperons, ref. ([15]) and ([16]), this makes it reasonable to suppose that our detection efficiency for charged hyperons was not very different from that for Λ^0's of similar energy. It therefore seems that in our interactions charged hyperons were produced in significantly smaller numbers than Λ^0 particles.

* * *

We would like to thank Dr. J. Rösch, director of the Observatoire du Pic du Midi, and his staff, who made this experiment possible; Dr. R. de Possel, director of the Institut Blaise Pascal, who kindly placed a Bull electronic computer at our disposal; and Dr. B. W. Powell.

Appendix I

The error in the estimated primary direction due to non-observation of π^0-meson secondaries.

The variance in p_t for isotropic emission is given by

$$\overline{p_t^2} = \frac{1}{2}\int p^{*2} \sin^2\theta^* \, \mathrm{d}(\cos\theta^*) = \frac{2}{3} p^{*2} \therefore \sqrt{\overline{p_t^2}} = 0.82 \sqrt{p^{*2}} .$$

p^* = C.M.S. momentum, θ^* = angle in C.M.S. with primary direction.

The projected value of p_t is given by $0.82\sqrt{p^{*2}}/2$. If then n_s charged mesons are produced the deviation of the resultant transverse momentum from the true value due to the unseen π^0-mesons is $0.41\sqrt{n_s p^{*2}}$. The corre-

([16]) P. H. Fowler *et al.*: quoted by A. Alvarez in *Report of Kiev Conference* (1959).

sponding angular deviation of the estimated primary direction from the true primary direction, in one plane, is then given by

$$\operatorname{tg} \Delta\varphi = \frac{0.41\sqrt{n_s \overline{p^{*2}}}}{\sum_{n_s} p_L \cos\theta} = \frac{0.41\sqrt{n_s \overline{p^{*2}}}}{\beta_c \gamma_c \sum_{n_s} E^*} .$$

Putting $\beta_c = 1$ and $\overline{p^{*2}} = \overline{E^{*2}}$ we have the total error in the primary direction:

$$\operatorname{tg} \Delta\varphi = \frac{0.41\sqrt{2}}{\beta_c \gamma_c \sqrt{n_s}} .$$

Appendix II

By energy conservation we have:

$$U_P + U_T = \sum U ,$$

where U_P is the energy of the primary particle,
U_T is the energy of the target particle,
$\sum U$ is the total energy of the secondary particles in the laboratory system after the collision.

By momentum conservation we have:

$$p_P \pm p_F = \sum p \cos\theta = \sum p_L ,$$

where p_P is the primary momentum,
p_F is the Fermi momentum of the target particle,
p_L is the total longitudinal component of momentum of the secondary particles along the primary direction.

$$(U_P - p_P) + U_T \pm p_F =$$
$$= 1.5 \sum_{\pi} (U - p_L) + (U - p_L) \text{ degraded primary} + (U - p_L) \text{ recoil} .$$

If the recoil nucleon is either neutral and unseen or heavily ionizing we have:

$$1.5 \sum (U - p_L) + (U - p_L) \text{ degraded primary} = (U - p_L) \text{ recoil} + M_N .$$

Since for a 30 GeV primary nucleon

$$(U_p - p_P) = 0.01 \text{ GeV} , \qquad p_F = 0 , \qquad U_T = \text{mass of target} = M_n .$$

RIASSUNTO (*)

Si sono studiate 117 interazioni di particelle da raggi cosmici con nuclei di alluminio. 101 sciami non contenenti in apparenza particelle non stabili d'edero le seguenti molteplicità:

$$\langle n_s \rangle = 7.3; \qquad \langle n_s^+ \rangle = 3.9; \qquad \langle n_s^- \rangle = 2.7; \qquad \langle n_s^\pm \rangle = 0.6 .$$

Si sono esaminati gli impulsi e le distribuzioni angolari delle particelle secondarie, e si è fatto un tentativo di studiare la correlazione tra impulso ed angolo. L'impulso trasversale medio è 0.31 GeV/c; la deviazione RMS su questa media è 0.23 GeV/c. Si è anche studiata una quantità riferentesi all'$(U - p_L)$ del nucleone di rinculo. Si sono studiati 12 sciami contenenti un V^0 ciascuno ed uno sciame contenenti due particelle V^0; ciò ha dimostrato che i 117 sciami contenevano: $29.5^{+14.0}_{-11.0}$ particelle Λ^0 e $18.0^{+15.0}_{-10.0}$ particelle θ^0. Si sono studiati anche sciami contenenti particelle $V^\pm$; una di esse era probabilmente una particella Ξ^-.

(*) *Traduzione a cura della Redazione.*

2373

A Cloud Chamber Study of Nuclear Interactions with Energies of about 100 GeV.

L. Montanet, J. A. Newth, G. Petrucci
R. A. Salmeron and A. Zichichi
CERN - Geneva

(ricevuto il 18 Marzo 1960)

Summary. — A cosmic ray experiment to study 100 GeV nuclear interactions with a magnet cloud chamber is reported. The analysis of the interactions is described and the hypotheses necessary for interpreting the measurements are discussed. Results from a first sample of 41 interactions are given. They show that 1) the transverse momenta of the secondary particles are generally low (< 0.5 GeV/c) and 2) in the centre of momentum frame of reference the emitted particles mostly have low momenta and their angular distribution is anisotropic. There is also some evidence that in a nucleon-nuclear interaction at these energies the number of nucleons involved is small. The proportion of strange particles among the secondaries is similar to that found in interactions of much lower energy.

Introduction.

This paper reports the first results of an experimental study of the nuclear interactions of cosmic rays with energies of about 100 GeV. The interactions occurred above the sensitive volume of a magnet cloud chamber situated at an altitude 3 500 m. No direct observations of the primary particles were made.

The experiment to be described was essentially exploratory. The apparatus was not specifically designed for the experiment and was, in some ways, unsuitable. One important aim of the work was to find, from experience, the difficulties that arise in analysing 100 GeV interactions and to see what apparatus would be required if a further experiment were envisaged.

In the following sections we describe the way in which the cloud chamber photographs were selected for analysis, the methods of analysis, and the results obtained from a sample of 41 high energy interactions.

1. – Apparatus, selection of photographs, yield.

The cloud chamber and magnet installed at the Jungfraujoch have been described previously (1). The useful volume of the cloud chamber is $(55 \times 55 \times 16)$ cm^3 and is placed in a magnetic field of 5 000 gauss. The maximum detectable momentum for tracks longer than 30 cm was about 10 GeV/c.

A vertical section through the apparatus is shown in Fig. 1. The wedge-shaped volume at the top of the cloud chamber that is not « seen » by the cameras was filled by a block of paraffin wax of mean thickness 6 cm. This paraffin target was chosen to give a high probability of observing a single nuclear interaction free from complication due to secondary processes (either nuclear interactions or materialisation of high-energy γ-rays from π^0-decay). The « geometrical » interaction length in paraffin is 63 cm and the cascade length is 52 cm. Moreover, one third of the geometrical cross-section is due to simple hydrogen nuclei.

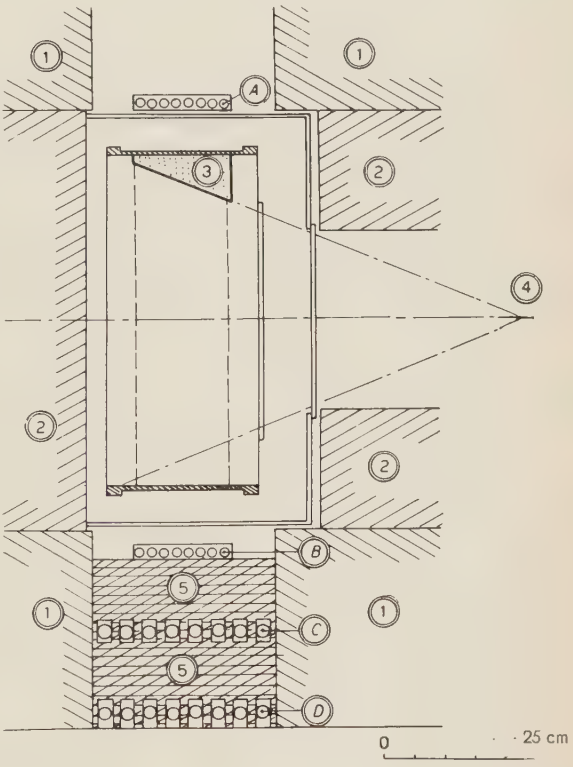

Fig. 1. – Vertical section through the apparatus. 1) Magnet coils. 2) Iron pole pieces. 3) Paraffin target. 4) Stereoscopic camera. 5) Lead. *A*, *B*) Counter trays containing 8 counters 2 cm × 40 cm. *C*, *D*) Counter trays containing 8 counters 3 cm × 60 cm separated by 0.5 cm lead.

The Geiger counters used to control the expansion of the cloud chamber are also shown in Fig. 1. A number of different counter combinations were

(1) J. A. Newth: *Suppl. Nuovo Cimento*, **11**, 297 (1954).

initially tested for rather brief periods and, finally, the simultaneous discharges necessary to expand the chamber were selected to be one or more from tray A and three or more from tray B *and* two or more from each of trays C and D ($A_{\geq 1}+B_{\geq 3}+C_{\geq 2}+D_{\geq 2}$). With this combination, the counting rate of the selection system was 7.6 per hour and, with a dead time of 4 minutes after each photograph, the rate of photography was 4.9 per hour.

The photographs were scanned by projecting to about full size and those showing high-energy nuclear interactions apparently occurring in the paraffin target were selected for careful measurement. The wide-angle photographic system makes it difficult to locate the site of an interaction by simple scanning; after measuring the stereoscopic pair of photographs it was frequently found that the interaction, in fact, occurred in the brass roof of the cloud chamber or even above the roof.

Initially, the criteria used to select interactions for analysis were rather loose but, after some experience the following strict criteria were adopted:

1) The photograph should show at least three copunctual tracks of fast particles (*i.e.* particles with momentum greater than 1 GeV/c) of which one had a momentum greater than 10 GeV/c *or* three had momenta greater than 5 GeV/c *or* five had momenta greater than 1 GeV/c.

2) There should be no evidence for a second nuclear interaction in or near the target.

3) The interaction should not be explicable as pure electron-photon cascade; this meant that the angles between the trajectories should not all be compatible with zero.

4) The majority of the tracks should lie in the well-illuminated volume of the cloud chamber.

5) The photograph should not show evidence for anomalously large distortion of the tracks.

Interactions that satisfied these criteria were termed « class A » interactions and a summary of the yield of such interactions over a period of three months

TABLE I. – *Yield of interesting interactions.*

Duration of experiment	Number of photographs	Number of class « A » interactions	Interactions with $n_T > 15$	Interactions with $n_T < 5$
85 days	9153	188	19	40

The table shows the results of careful scanning, with uniform selection criteria, of the main body of photographs. Class « A » interactions are those with good geometry in the illuminated region of the cloud chamber and where there is no confusion with particles not directly associated with the interaction.

2376

is shown in Table I. The distribution of *total* multiplicity (n_T) for these interactions is shown in Fig. 2.

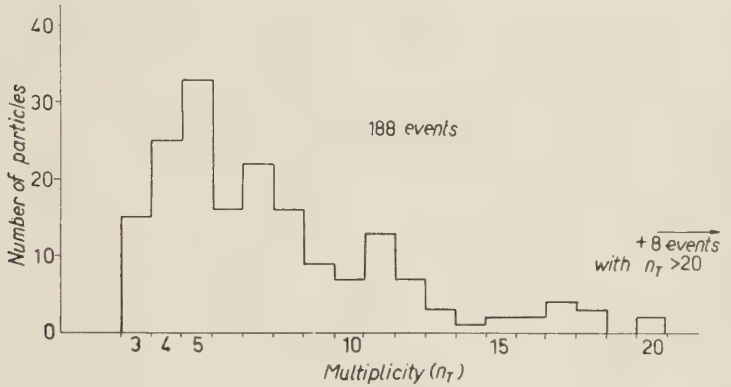

Fig. 2. – The multiplicity distribution for 188 class « A » interactions selected from 9.153 photographs. There is a cut-off imposed by the scanning criteria that eliminates multiplicities below 3. The small numbers of interactions with $n_T=4$ or 3 is probably due to the discrimination of counter tray B against low multiplicities.

When the total multiplicity is greater than about fifteen the measurements on the tracks become inaccurate because of overlapping and confusion. For very low multiplicities ($n_T< 5$) the analysis becomes inaccurate owing to the difficulty of determining the axis of the interaction. In our experiment we concluded that only the interactions with n_T between five and fifteen could profitably be analysed. From Table I it is clear that about 1.5 such interactions are recorded per day. Of these, about one half occur in the paraffin target; the remainder are nuclear interactions in the roof of the cloud chamber or other neighbouring material. This yield of interactions is obtained with an « acceptance » of about 40 cm²·sr for the primary particles.

2. – Measurements and analysis in the laboratory system.

About 50 interactions (*) were selected for measurement. The photographs were projected through a photographic enlarger on to a horizontal table and the curvatures of the tracks were measured by comparison with standard engraved circular arcs. Drawings of the two stereoscopic views were then

(*) Most of these were selected before the criteria given in Section 1 were established. Some of the 50 were later rejected for various reasons. An analysis of the remaining interactions is being made (²).

(²) L. Montanet: to be published.

made and the relevant tracks were extended to find the co-ordinates of the nuclear interaction. The direction cosines of the tangent to each track at the interaction were then calculated.

In order to define an axis for each interaction, the vector sum of the momenta of all the charged particles having momenta above 1 GeV/c was found. (In the case of a particle whose momentum was too high to measure the appropriate maximum detectable momentum was used in the calculation.)

The whole interaction was then referred to a system of spherical co-ordinates with the axis as pole. Every track was specified by its co-latitude (θ) and its longitude (φ). A target diagram of each interaction was then drawn on polar graph paper.

The above operations were all routine in character. Before proceeding with the analysis of the interactions an attempt was made to exclude the tracks due to electron pairs, to knock-on electrons and to evaporation protons. Low-energy electrons were rejected by excluding any particle with minimum ionization and momentum less than 100 MeV/c. Protons that could be identified from ionization and momentum (< 500 MeV/c) were also excluded. Electron pairs were more difficult to recognize and no really satisfactory identification was made. However, on a target diagram an electron pair that is not close to the axis of an interaction stands out as a pair of tracks with opposite curvatures and with a negligible included angle. Ten such pairs were observed and rejected while a rough calculation based on the number of π^0-mesons expected in the interactions predicted that fourteen electron pairs should be produced. It seems clear that the majority of the pairs were identified but, equally, that a small number probably remained among the particles used in the later analysis.

To summarize, at the conclusion of this stage of the analysis each interaction was specified by its origin (P in the paraffin target, M in the doubtful region near the roof of the chamber) and by the multiplicity (n_s) of fast charged secondary particles. Each fast secondary particle had a momentum (p_i) and angular co-ordinates (θ_i, φ_i) referred to the axis of the interaction.

3. – Determination of the C-system.

The next step in the analysis was the determination of a Lorentz transformation along the axis of each interaction such that, after transformation, the interaction possessed some specified forward-backward symmetry. We call the frame of reference in which this symmetry exists the C-system and its velocity relative to the laboratory is β_c, $\{\gamma_c = (1 - \beta_c^2)^{-\frac{1}{2}}\}$. The physical significance of the C-system and of γ_c is clear when the interaction is between like particles as in the collision of an incident proton with a hydrogen nucleus in the paraffin target and, among our interactions, some are probably of this

2378

type. When the interactions are more complex the significance, if any, of γ_c depends upon the phenomenological model that is used to describe the interactions. Here we describe only the procedure for finding γ_c and defer the discussion of its meaning until later (Section 8).

The main problem in determining γ_c is to choose from an infinity of possibilities some criterion of symmetry that must be satisfied in the C-system. If all the momenta in the laboratory system are accurately measured the choice of γ_c can be made so that the total momentum of the charged particles in the C-system is zero or

$$\sum_1^{n_s} p_i^* \cos\theta_i^* = 0\,, \tag{1}$$

where p^* and θ^* are the momentum and co-latitude of a particle after transformation. In our experiment this criterion of symmetry is not usable because there are, in nearly every interaction, one or more particles with momenta to high to measure.

We adopted the criterion

$$\overline{\cos\theta^*} = \frac{1}{n_s}\sum_1^{n_s} \cos\theta_i^* = 0\,, \tag{2}$$

as our condition for symmetry. It has several properties that are worth noting. First, the value of $\overline{\cos\theta^*}$ is a smoothly varying function of γ and the value γ_c that satisfies condition (2) can be found graphically by interpolation after making only two or three trial transformations.

Second, there are circumstances in which the application of criterion (1) would lead to results that are physically quite unreasonable and where criterion (2) would be more satisfactory. For example, if a neutral particle is emitted with a high momentum from an interaction the application of (1) to the charged particles only may lead to an unrealistic value of γ_c. For reasonably high multiplicities condition (2) is less affected by the presence of high-energy neutral secondaries.

Third, condition (2) has the advantage that the statistical error in γ_c may easily be found for any assumed angular distribution of the secondary particles in the C-system. Specifically, if the angular distribution is of the form $N(\theta^*)\,\mathrm{d}\theta^* \propto \cos^m\theta^* \sin\theta^*\,\mathrm{d}\theta^*$ the average value of $\cos\theta^*$ will be zero with an R.M.S. deviation of $\sqrt{(m+1)/(n_s(m+3))}$ so that the condition (2) becomes

$$\overline{\cos\theta^*} = 0 \pm \sqrt{\frac{m+1}{n_s(m+3)}} \tag{2a}$$

or

$$= 0 \pm \sqrt{\frac{1}{3n_s}} \qquad \text{for } m = 0 \text{ (isotropy)} \tag{2b}$$

or

$$= 0 \pm \sqrt{\frac{1}{n_s}} \qquad \text{for large } m \,. \tag{2e}$$

In its practical application, the procedure was as follows. A guess at the value of γ_c was made and the Lorentz transformation was calculated using the measured values of p_i and θ_i and assuming *all* the fast charged particles to be π-mesons. The value of $\overline{\cos\theta^*}$ for the interaction was found. This was repeated for two or three further values of γ and the results were plotted in the form of a graph of $\overline{\cos\theta^*}$ against γ. The intersection of the graph with the axis of γ gave the value γ_c and the values of γ corresponding to $\overline{\cos\theta^*} = \pm\sqrt{1/3n_s}$ gave limits to γ_c at one standard deviation.

Fig. 3, curve 1, shows a typical result for interaction XS 29 (Plate I) where the value of γ_c derived is $9.3^{+3.5}_{-2.2}$ and these numbers give some idea of the

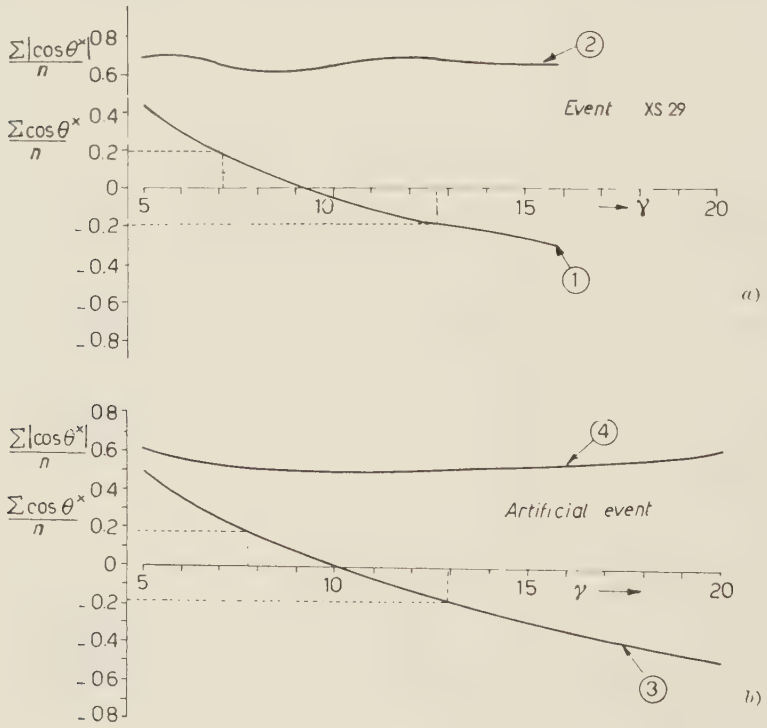

Fig. 3. – Diagram showing the determination of γ_c and of the anisotropy in an interaction. In *a*) are shown the variation of $\cos\theta^*$ and $|\overline{\cos\theta^*}|$ as functions of the γ of the Lorentz transformation for event XS 29 (see Table II and plate 1). In *b*) the same variations are shown for an artificial event with $\gamma_c = 10$, consisting of 10 π-meson isotropically distributed and each having a p^* of 350 MeV/c. The points to notice in these curves are the large errors in γ_c and the slow variation of $|\overline{\cos\theta^*}|$ with γ.

2280

TABLE II. – *Details of* 41 *analysed interactions.*

No.	Origin	n_T	n_H	n_+	n_-	$n_?$	$\gamma_c \pm \Delta\gamma_c$	$A \pm \Delta A$	$\frac{n_s}{\gamma_c - 1}$
XI 826	P	10	0	3	3	4	$5\ ^{+2.5}_{-1.9}$	0.64 ± 0.12	2.50
XO 826	P	7	0	0	0	7	$12\ ^{+4.4}_{-4}$	0.47 ± 0.14	0.64
XO 693	M	9	0	3	3	3	$5.6^{+3.5}_{-2.1}$	0.69 ± 0.13	1.95
XO 857	M	8	0	4	2	2	$4.6^{+1.9}_{-1.6}$	0.55 ± 0.16	2.22
XO 871	M	6	0	1	1	4	$20\ ^{+12}_{-9}$	0.59 ± 0.21	0.32
XO 874	P	6	0	3	2	1	$5.5^{+2.9}_{-2}$	0.57 ± 0.17	1.33
XO 968	M	8	0	2	3	3	$6\ ^{+3.2}_{-2.2}$	0.68 ± 0.12	1.60
XO 1229	M	6	0	2	2	2	$5.9^{+4}_{-1.6}$	0.66 ± 0.18	1.22
XO 1568	M	7	0	2	3	2	$10\ ^{+4}_{-4}$	0.66 ± 0.19	0.79
XO 1696	P	8	0	3	2	3	$8.9^{+9}_{-3.6}$	0.805 ± 0.16	1.01
XO 1928	M	7	0	3	1	3	$10.3^{+4.2}_{-3.3}$	0.56 ± 0.16	0.75
XP 505	P	5	0	1	0	4	$5.6^{+2.7}_{-1.9}$	0.51 ± 0.16	1.09
XP 506	M	6	1	3	0	2	10.7^{+7}_{-7}	0.75 ± 0.38	0.52
XQ 35	P	12	0	5	1	6	$5.8^{+7}_{-3.3}$	0.88 ± 0.14	2.50
XQ 42	P	7	0	5	2	0	$12.2^{+4.6}_{-4.6}$	0.63 ± 0.13	0.62
XQ 185	M	5	0	2	0	3	$34\ ^{+12}_{-8}$	0.33 ± 0.24	0.15
XR 109	P	8	1	3	1	3	$4.5^{+2.7}_{-2.2}$	0.76 ± 0.16	2.00
XR 207	P	9	1	4	2	2	6.2^{+8}_{-4}	0.80 ± 0.14	1.54
XR 311	M	6	0	2	0	4	6.4^{+3}_{-2}	0.40 ± 0.15	1.11
XR 880	P	5	0	2	1	2	$32\ ^{+16}_{-13}$	0.65 ± 0.16	0.16
XR 971	M	7	1	2	2	2	$7.4^{+4.6}_{-3.5}$	0.62 ± 0.33	0.94
XR 1019	M	6	0	1	1	4	17.3^{+7}_{-6}	0.62 ± 0.32	0.37
XS 29	P	9	0	4	1	4	$9.3^{+4}_{-2.5}$	0.65 ± 0.12	1.08
XS 190	P	7	0	3	0	4	17.5^{+13}_{-5}	0.49 ± 0.37	0.42

2381

TABLE II (*continued*).

No.	Origin	n_T	n_H	n_+	n_-	$n_?$	$\gamma_c \pm \Delta\gamma_c$	$A \pm \Delta A$	$\frac{n_s}{\gamma_c - 1}$
XS 250	M	11	0	3	3	5	$5.2^{+2.1}_{-1.5}$	0.65 ± 0.14	2.62
XT 70	M	8	1	3	2	2	$5.5^{+2.9}_{-2.1}$	0.56 ± 0.18	1.55
XT 123	M	11	0	6	2	3	$9.4^{+3.8}_{-3.3}$	0.68 ± 0.13	1.31
XT 280	P	10	1	3	2	4	$12^{+3.5}_{-3.2}$	0.48 ± 0.14	0.82
XT 279	P	18	1	2	5	10	$12.5^{+3.3}_{-3.0}$	0.56 ± 0.09	1.48
XT 466	P	7	1	0	0	6	23^{+17}_{-17}	0.82 ± 0.26	0.27
XT 841	M	11	0	3	2	6	$9.5^{+2.9}_{-2.2}$	0.48 ± 0.12	1.30
XT 1071	M	6	0	3	1	2	$32.5^{+5.5}_{-5.5}$	0.40 ± 0.15	0.19
XT 1186	M	7	0	3	3	1	$15.5^{+5.7}_{-4.0}$	0.5 ± 0.14	0.48
XT 1785	M	17	0	8	2	7	$14.5^{+3.5}_{-3.5}$	0.65 ± 0.12	1.26
XT 2053	M	11	0	2	6	3	$4.0^{+2.1}_{-1.1}$	0.72 ± 0.16	3.66
XT 2156	P	8	1	4	2	1	$5.6^{+3.6}_{-2.1}$	0.64 ± 0.18	1.52
XR 179	M	20	1	9	5	5	<3.5	—	—
XS 119	M	7	1	2	3	1	$2.5^{+1.6}_{-1.6}$	0.70 ± 0.24	—
XS 498	M	20	1	4	6	9	$4.6^{+1.3}_{-1.2}$	0.62 ± 0.09	—
XT 1627	P	10	4	2	1	3	2.7?	—	—
XR 1004	P	20	0	1	2	17	—	—	—

This table lists the details of 41 interactions that had $n_s \geqslant 5$ and could be analysed by the method of Fig. 3 to give a value of γ_c. The origin P is in the paraffin target, M is doubtful-copper, aluminium or paraffin. A is the mean value of $|\cos\theta^*|$ for the tracks from each interaction after applying the Lorentz transformation γ_c.

The errors in γ_c and A were calculated assuming that the angular distribution in the C.M.S. was anisotropic with a value 0.65 for A. The mean value of A found, in fact is 0.615 ± 0.025. This means that the errors have been over-estimated. Moreover, the error in A due to the error in γ_c has been taken as symmetrical whereas, in fact, there is a slight bias that tends to underestimate the value of A (see Fig. 3). Therefore the ΔA are generally rather larger than they should be and the overall mean value ($A = 0.61$) is probably slightly too low.

The five interactions below the interrupted line are excluded from the later analysis because, for the first four there are very good reasons to think that they are very complex interactions and for event XR 1004 the resolution of the separate tracks on the photographs does not allow accurate measurement.

2382

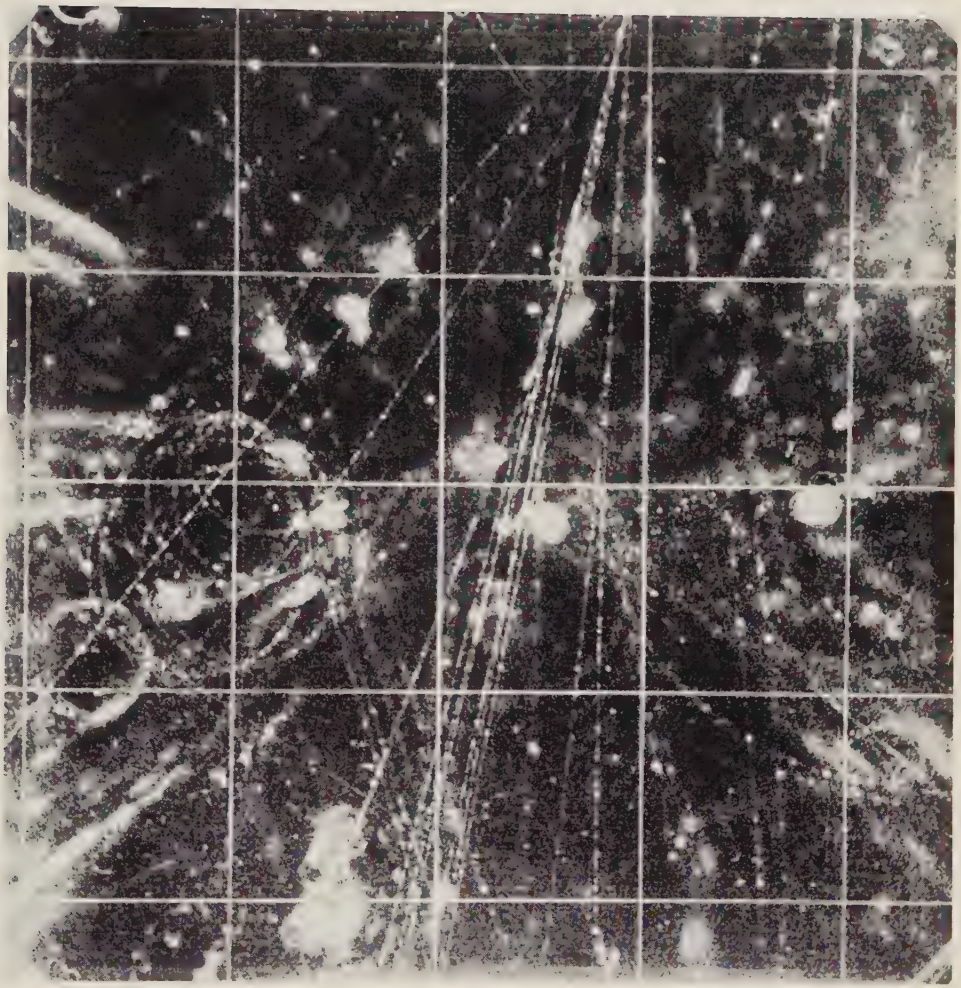

Plate 1. – *Event* XS 29. This event is listed in Table II and the determination of γ_c is shown in Fig. 3.

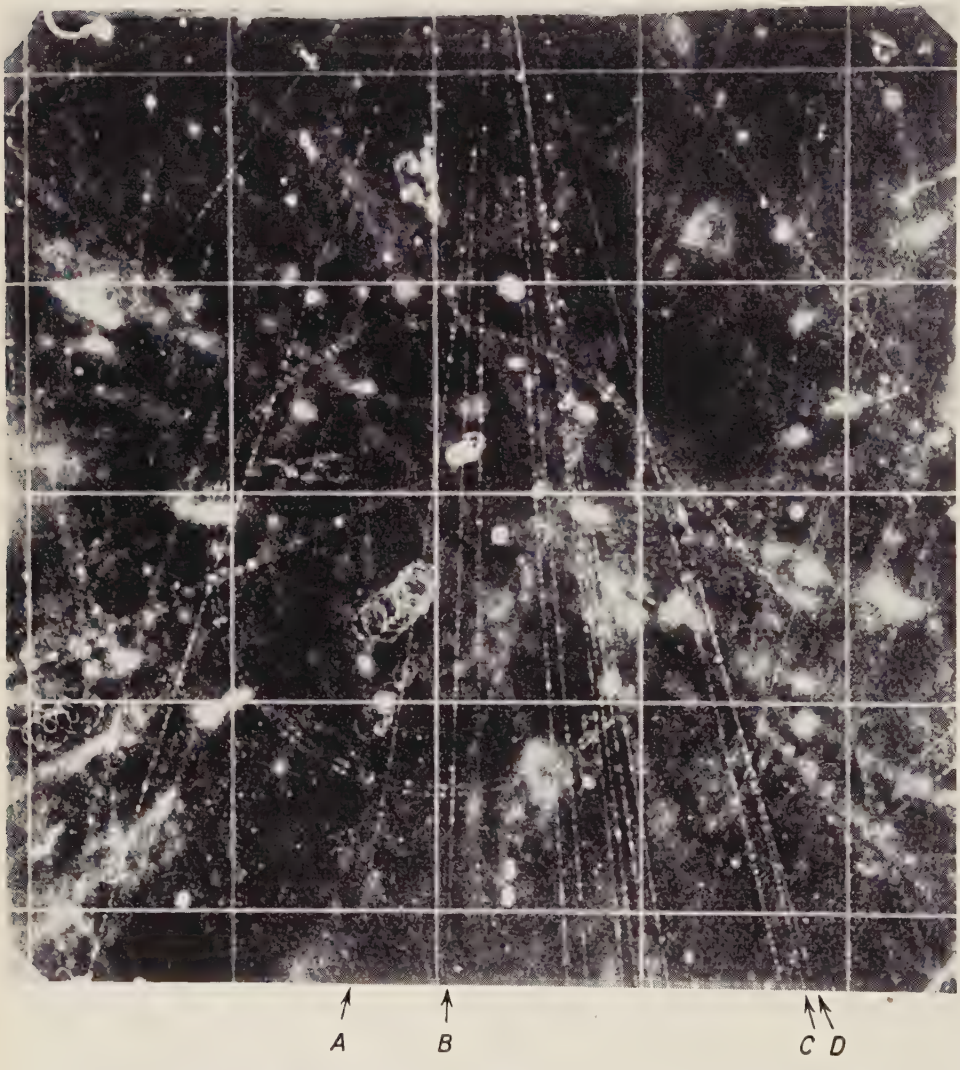

Plate 2. – *Event* XT 280. This event is listed in Table II and Table III. The tracks *A* and *B* come from a neutral V-decay while *C* and *D* are probably due to an electron pair produced in the gas of the cloud chamber.

errors in the determination when $n_s = 9$. Curve 3 in Fig. 3 shows a similar determination for an artificial event that was constructed by assuming ten secondary π-mesons to be emitted isotropically with a constant p^* in a system for which γ_c was 10 (*).

The method of finding γ_c outlined above was used on 41 interactions with $n_s \geq 5$ listed in Table II. For the first 36 events the results were straightforward. For four events the deduced values of γ_c were extremely low. It was impossible to interpret these four events as nucleon-nucleon collisions since the *visible* energy of the interaction was greater than that corresponding to a N-N collision with a C-system velocity of β_c ($E_{\text{lab}} = (2\gamma_c^2 - 1)m_N$). For the last interaction the high multiplicity made measurements difficult and a reliable value of γ_c could not be obtained.

The spectrum of the 36 values of γ_c is shown in Fig. 4.

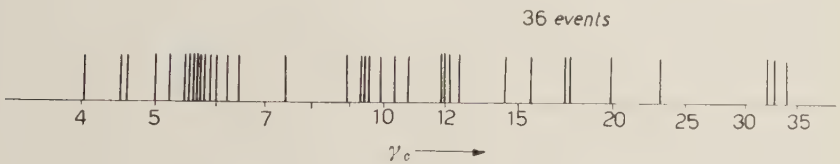

Fig. 4. – The distribution of values of γ_c found by the criterion $\sum \cos\theta^* = 0$ for the first 36 interactions listed in Table II. For a simple nucleon-nucleon interaction the laboratory energy is related to γ_c by the equation $E_{\text{lab}} = (2\gamma_c^2 - 1)M_N c^2$. Thus a value of 100 GeV for E_{lab} would correspond to $\gamma_c = 7.3$ and 200 GeV to $\gamma_c = 10.4$.

4. – The distribution of transverse momenta.

The 36 interactions for which a value of γ_c could be found without difficulty contain 273 charged secondary particles. Of these 102 were positive, 64 negative and 107 had momenta too great for their signs to be determined.

Before considering the distributions of momenta and angles of emission in the C-system we describe the distribution of transverse momenta ($p_t = p_i \sin\theta_i = p_i^* \sin\theta_i^*$). This is invariant under the transformation from L-system to C-system and is unaffected by errors in γ_c.

For the 166 particles whose momenta were measured the distribution of p_t is given in Fig. 5. This shows clearly that the vast majority of the *measured* particles (that is, at least 50 % of *all* the charged secondaries) have transverse

(*) In Fig. 3 the errors have been found assuming an isotropic distribution of the secondary particles. The observed anisotropy in our events led us to assume a value $m = 1$ in (2*a*). The error in γ_c for event XS 29 is then increased to the figure in Table II.

momenta less than 400 MeV/c. The number of particles with measured values of p_t greater than 400 MeV/c is very small.

Since only 60% of the charged secondaries are measured, it is important to consider whether the remaining 40% of particles could all have very different values of p_t. In general, the unmeasured momenta belong to particles in two classes; those giving long straight tracks at very small angles to the axis and those at large angles to the axis where the visible track is very short. Those wide-angle secondaries whose tracks lie nearly in the plane of the cloud chamber are measurable and Fig. 5 includes values from many such tracks. It is unreasonable to imagine that the wide-angle secondaries giving short tracks have different momenta from those giving long tracks and we can therefore ignore the bias due to the exclusion of wide-angle secondaries from the distribution of Fig. 5.

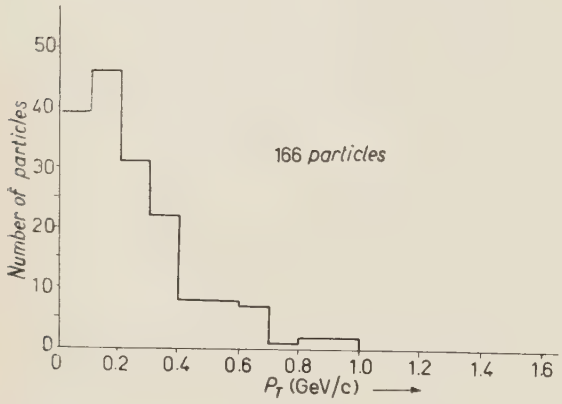

Fig. 5. – The distribution of transverse momenta for 166 measured secondary particles. This distribution is biased since, in the same interactions there are 107 particles whose momenta were too high to measure. This bias is discussed in the text.

The p_t-values from the high-momentum (> 10 GeV/c) particles inclined at small angles to the axis are a more serious difficulty since quite small changes in the assumed axis direction give large changes in p_t. The choice of axis —described in Section 2—essentially leads to small values of p_t (*). Without observing the direction of the primary particle it is very difficult to assess the error involved in our method of choosing the axis. What we have done is to investigate, in particular cases, the effect of altering the momenta assumed for very energetic particles. The resulting change in the axis direction is generally small ($\sim 2°$) and the corresponding alteration in the values of p_t is of the order of 200 MeV/c for a particle with a momentum of 5 GeV/c.

Our conclusion from this discussion is that at least half of the secondary charged particles have transverse momenta less than 400 MeV/c. We have no reason to think that our results are strongly biased by the exclusion of the particles whose momenta could not be measured. We therefore expect about

(*) Considering the p_t-values as vectors in the plane of the « target diagram » it is clear that our choice of axis makes $\sum \boldsymbol{p}_t = 0$ and makes the sum $\sum p_t^2$ a minimum.

80 % of all the secondary particles to have p_i below 400 MeV/c. The errors in the determination of the axis direction make it impossible to say anything about the distribution of the p_i-values below 400 MeV/c.

5. – The momentum spectra in the *C*-system.

The momentum of a particle in the *C*-system is obtained from the laboratory measurements by the Lorentz transformation

$$p_i^* = p_i \left\{ \sin^2 \theta_i + \gamma_c^2 \left(\cos \theta_i - \frac{\beta_c}{\beta_i} \right)^2 \right\}^{\frac{1}{2}}, \tag{3}$$

where β_c, γ_c are the constants of the transformation and β_i is the particle's velocity in the laboratory system. The above transformation was carried out for all the 166 measured secondary particles assuming, for the calculation of β_i, that every particle was a π-meson.

The resulting momentum spectra for positive and negative secondary particles are shown in Fig. 6 (*a* and *b*). Both spectra show that the majority of the measured secondaries have p^* less than 1 GeV/c; only 2 out of 64 negative particles and 9 out 102 positive particles have momenta above this limit.

The criterion of measurability used in selecting the particles whose momenta are plotted in Fig. 6 may well lead to a serious bias in the distribution. This is because both the classes of unmeasured particles referred to in Section **4** may consist of particles whose momenta in the *C*-system were high. For very high energy particles near to the axis of the interaction ($\cos \theta_i = \beta_i = 1$) equation (3) reduces to $p_i^* = p_i / 2\gamma_c$ and, with our values of γ_c, we obtain large values of p^* when p_i is greater than 20 or 30 GeV/c. For the wide-angle particles of low momentum the quantity $(\cos \theta_i - \beta_c/\beta_i)$ in (3) is negative and can easily be large enough to give a high value for p^*. In fact, of the 11 measured particles with high values of p^*, 8 are slow, wide-angle particles of this type.

As far as the measured particles are concerned, it is clear from (3) that the large error ($\sim 25\,\%$) in γ_c will be transferred nearly directly to give similar errors in the values of p^*. Moreover, even if the hypothesis that all the negative particles are π-mesons is reasonable, among the positive particles there are certainly many protons. The errors in p^* due to a wrong assignment of mass can be found from (3).

The only difference in the two momentum spectra of Fig. 6 is the suggestion of a larger proportion of positive particles with p^* above 1 GeV/c. If the nine positive particles with high p^* are assumed to be protons and β_i is reduced

accordingly, it is found that, in eight cases, the altered values of p^* are even greater than the original values.

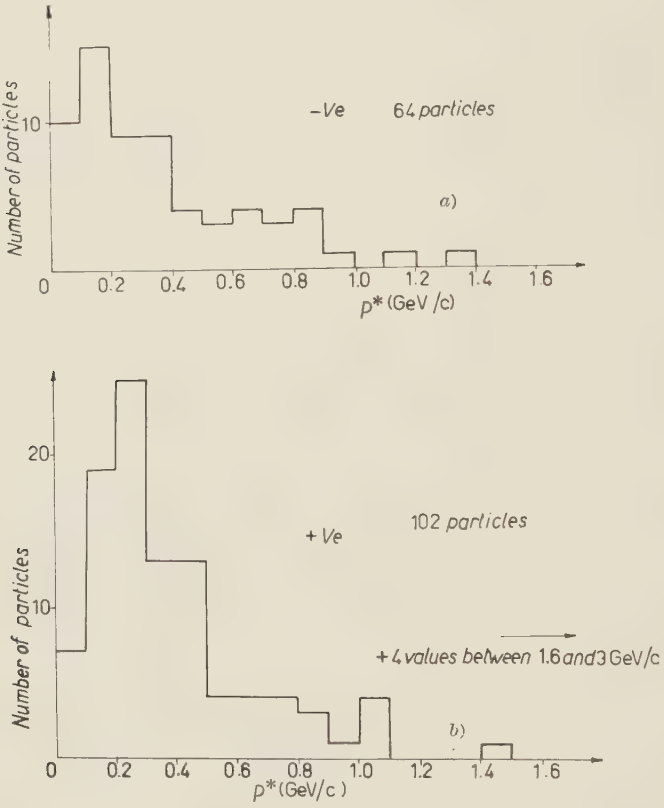

Fig. 6. – The values of p^* for 64 negative particles (*a*) and 102 positive particles (*b*) from the first 36 interactions of Table II. These values have been calculated using the best values of γ_c and on the assumption that all the particles are π-mesons. The error due to this assumption and the effect of the 107 unmeasurable particles are discussed in the text.

From the above discussion we conclude first that more than 50 % of the charged secondary particles have momenta in the *C*-system of less than 1 GeV/c. Secondly, we attribute large errors to the momenta shown in the spectra of Fig. 6 and fear that the unmeasured secondaries could alter their shapes significantly. Finally, we observe some indication of a positive excess among the particles with high p^*; if these particles are protons, their momenta in the *C*-system are very high ($\gtrsim 5$ GeV/c).

2386

6. – The angular distribution in the C-system.

The angle of emission (θ^*) of a particle in the C-system is related to the quantities we have determined by

$$\text{tg}\,\theta_i^* = \frac{\sin\theta_i}{\gamma_c\,(\cos\theta_i - \beta_c/\beta_i)}\,. \tag{4}$$

This involves the laboratory momentum and the mass of the secondary particle only through the value of β_i. Since p_i does not appear explicitly, it is possible to find values of θ^* even for unmeasured secondaries by assuming that β_i lies between unity and some lower limit set by the maximum detectable momentum. In nearly all cases the uncertainty in θ^* is only a few degrees although in rare cases it can be 30° or more.

The values of θ^* calculated from (4) were, of course, used to determine γ_c from the condition $\sum \cos\theta_i^* = 0$. When this condition is satisfied some measure of forward-backward symmetry of the angular distribution is demanded. The anisotropy of the distribution can be conveniently specified by the quantity $1/n_s \sum |\cos\theta_i^*| - A$. The expected value of A for a distribution proportional to $\cos^m\theta^*$ is:

$$A = \frac{m+1}{m+2} \pm \sqrt{\frac{m+1}{4n_s(m+3)}}\,, \tag{5}$$

which, for isotropic emission ($m = 0$) reduces to

$$A = 0.5 \pm 1/\sqrt{12\,n_s}\,. \tag{6}$$

In our experiment the value of A was calculated for each event during the determination of γ_c. The results are given in Table II and the distribution of values of A is shown in Fig. 8. The statistical errors are so large that the value of A obtained from a single interaction rarely differs significantly from 0.5 but the distribution of Fig. 8 shows a clear tendency for A to be greater than 0.5 (the mean value is 0.61, corresponding to $m = 1$). Further evidence for the existence of anysotropy is show in Fig. 7 where the angular distribution of all 273 secondary particles is shown.

There are two sources of error in the determination of A that should be considered. The first is the error due to the large uncertainty in γ_c. In Fig. 3 (curves 2 and 4) the value of A is plotted as a function of γ and it is clear that the variation is extremely slow. There is, moreover, a systematic tendency for A to have a minimum value when $\gamma = \gamma_c$. Thus there is a small syste-

matic error which tends to underestimate the anisotropy of the angular distribution.

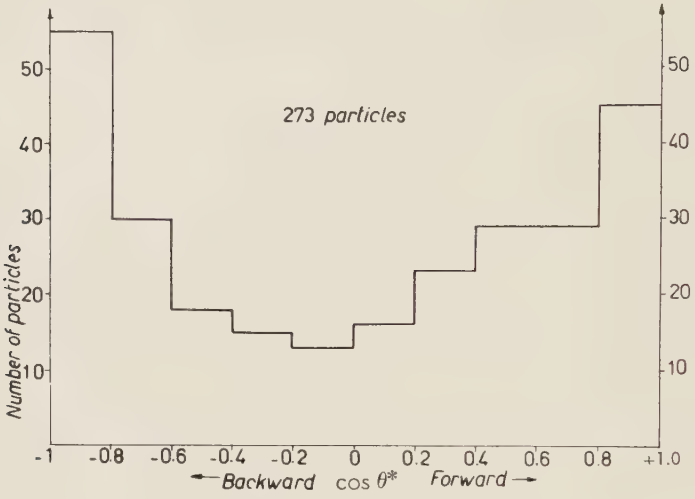

Fig. 7. – The angular distribution of the secondary particles in the first 36 interactions of Table II. There is no *significant* forward-backward asymmetry but the anisotropy of the distribution is clear.

The second source of error is important for interactions of low multiplicity and is associated with the determination of the axis direction. It can most easily be visualized by imagining an interaction with only two fast secondary

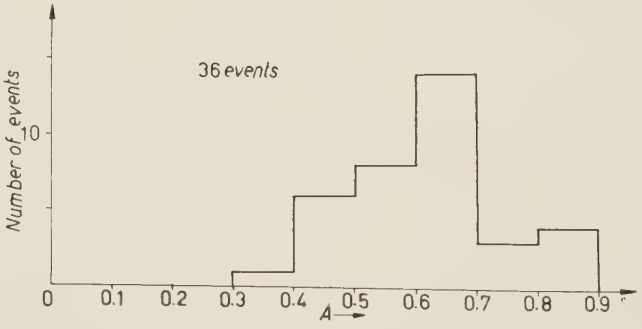

Fig. 8. – The distribution of the anisotropy A ($=|\overline{\cos\ \theta^*}|$) for the first 36 showers of Table II. $A=0.5$ is expected for an isotropic distribution.

particles ($p > 10$ GeV/c) which are inclined at an angle 2θ to one another. A strict application of our analysis procedure to such an interaction would lead to the results: $\gamma_c = \operatorname{cosec}\theta$, and $A = 0$. This arises from our inability to

measure momenta above 10 GeV/c — the axis is therefore chosen to make the angles θ_i equal. Any other choice of axis would lead to a smaller value of γ_c and, of course, a larger value of A. It is difficult to estimate the size of this bias in interactions with higher multiplicities but we excluded all interactions with multiplicity less than 5 from our analysis. The residual bias is probably small and, in any case, it again leads to an underestimate of the anisotropy.

Taking into account the statistical error in A (using $m = 1$ in equation (5)) and the error arising from the uncertainty in γ_c we obtain for all our interactions a weighted mean value of $\bar{A} = 0.61 \pm 0.025$. We consider this to be proof of an anisotropic angular distribution in the C-system.

7. – The production of strange particles.

Among the 36 well analysed interactions of Table II there are only two (XT 123 and XT 280) that show the decay of a strange particle. To obtain better statistical information about the frequency of production of strange particles, all the 188 interaction (Table I) were searched for V-particle decays. A further nine were found and the interactions were measured. The results for the eleven interactions are given in Table III.

TABLE III. – *Interactions in which V-particles are observed.*

Event no.	Origin	Nature of the V-event	n_T	n_H
XT 123	M	V^0	11	0
XT 232	M	$V^\pm$	11	1
XT 280	P	not Λ^0	10	1
XW 64	P	V^0	11	0
XW 660	P	Λ^0	11	0
XX 392	P	V^0	5	0
XX 399	P	V^0	~ 45	1
XX 731	P	V^0	11	1
XX 1425	P	Λ^0	10	0
XY 1370	?	V^0?	5	0
XZ 448	M	V^0	4	0

The interactions listed here include all those observed in the 9.153 photographs referred to in Table I. The origin *P* indicates the paraffin target, *M* indicates a doubtful origin that could be in aluminium, copper or paraffin. « V^0 » means a neutral V-decay that cannot be separated as Λ^0 or θ^0-decay. For event XY 1370 the origin is not coplanar with the V^0-decay. This could be an example of anomalous, 3-body decay or could be due to the presence of a second, unseen, interaction.

Little comment is required. There is a tendency for the interactions to have higher multiplicities than the average but the difference is barely significant statistically. A high proportion of the interactions occur in the paraffin target; this could be due, in part, to the higher probability of observing a V^0-decay when the V-particle is produced close to the sensitive volume of the cloud chamber.

If we confine attention to the interactions with between 5 and 15 secondary particles we find the following results. There are 129 interactions with a total of 953 fast charged secondary particles. The observed number of V^0-decays is 8. Making approximate allowance for the particles decaying outside the cloud-chamber and for those decaying into neutral secondaries, we estimate that about 40 V^0-particles must have been produced in the interactions. This corresponds to about 4% of the charged secondary particles — a similar proportion to that found in many experiments concerned with interactions of much lower energy ([3]).

8. – The nature of the interactions.

8·1. *The significance of* γ_c. – The physical meaning of γ_c depends upon the nature of the interacting particles and on the model that is adopted for the description of high-energy nuclear interactions ([4]).

In a collision between two protons the secondary particles must, statistically, be symmetrically emitted in the centre-of-mass frame of reference. If this symmetry, which is demanded by the principle of special relativity for an ensemble of interactions, is assumed to exist in every individual interaction then the C-system that we have considered is the centre-of-mass system of reference. The relation between γ_c and the energy (E_L) of the primary protons in the laboratory system is then

$$E_L = (2\gamma_c^2 - 1)\, M_N \approx 2\gamma_c^2 M_N \,, \tag{7}$$

where M_N is the rest-energy of the proton.

If a primary π-meson of high energy strikes a proton there is no *a priori* reason to assume forward-backward symmetry of the secondary products in any frame of reference. However, symmetry of the *produced* particles in the centre-of-mass frame of reference is a not unreasonable hypothesis and for an interaction with large multiplicity our C-system may again be identified with

---

([3]) C. FRANZINETTI and G. MORPURGO: *Suppl. Nuovo Cimento*, **6**, 469 (1957).

([4]) Article by D. H. PERKINS in *Progress in Elementary Particle and Cosmic-Ray Physics*, vol. **5** (Amsterdam).

2390

the centre-of-mass system of reference. The laboratory energy of the π-meson is again given by $2\gamma_c^2 M_N$ for values of γ_c such that $\gamma_c^2 \gg 1$.

The third type of collision we consider is that between a single primary proton and a number of nucleons inside a target nucleus. If the interaction can be separated into a number of distinct nucleon-nucleon and π-nucleon reactions occurring successively in a cascade process, no single frame of reference can be used to describe the complete interaction. If, instead, the incident proton can be assumed to interact simultaneously with a group of n nucleons in the target, a centre-of-mass frame of reference exists. If n is small compared with the multiplicity of secondary particles and if the *produced* particles are symmetrically emitted in the centre-of-mass system there will again be an approximate correspondence between this centre-of-mass system and our C-system.

If all these conditions are satisfied the relation between γ_c and the laboratory energy of the proton is $E_L \approx 2n\gamma_c^2 M_N$ if $\gamma_c^2 \gg 1$.

The above considerations show how important it is to decide on the nature of the interacting particles.

8·2. *The nature of the primary particles.* – Whatever the exact significance of γ_c there is no doubt that the primary particles responsible for our interactions have energies greater than 50 GeV—mostly in the range from 50 to 200 GeV. In principle, the counter tray A (Fig. 1) ensures that the primary particles are charged and not neutral although discharges in A may sometimes be due to an upward-moving secondary particle from an interaction produced by a neutral primary.

The only other direct information we have is that the primary particles are isolated in the sense that they are not accompanied by associated charged particles that traverse our cloud chamber. This suggests strongly that if our « primaries » are « secondaries » from atmospheric nuclear interactions the latter generally occur more than 50 m above our apparatus.

Indirectly, we may use the results of earlier experiments ([5]) on the « local penetrating showers » which showed that about half the primaries of such showers were charged and half neutral. From this fact it was inferred that they were high-energy protons and neutrons which, at this depth in the atmosphere, are expected in roughly equal numbers.

Our conclusion is, then, that the majority of our interactions are produced by high-energy protons and that these protons have travelled more than 50 m from the interactions in which they originate. A small proportion ($\sim 10\,\%$) of the interactions may be produced by π-mesons or other unstable particles.

([5]) W. D. Walker, S. P. Walker and K. Griesen: *Phys. Rev.*, **80**, 546 (1950).

8·3. *The number of target nucleons involved.* – For interactions that occur in paraffin with a geometrical cross-section about 40 % will be interactions with free protons and 60 % with carbon nuclei. Of the latter a considerable fraction (perhaps one third) should be « peripheral » and involve only a single nucleon in the carbon nucleus—apart from the transfer of some small excitation energy to the residual nucleus. The remaining interactions will be complex, involving several target nucleons intimately. Several different theories of complex interactions have been put forward and they predict very different values for the number of nucleons that take part in the interaction (6).

Ideally, the positive excess among the secondaries of each interaction gives directly the number of protons involved in that interaction. Since all our interactions show secondary particles whose charge cannot be determined we cannot use the positive excess in this way. Some idea of the average positive excess is given by the figures in Table IV. Despite the uncertainty due to the large number of unmeasured particles the figures suggest that the average number of target nucleons involved is not much greater than one.

TABLE IV. – *The positive excess in the analysable interactions.*

Number of interactions ($5 \leqslant n_T \leqslant 15$)	n_H	n_+	n_-	$n_?$	Mean + ve excess (deduced)
129	48	366	261	326	1.6

The interactions with n_T between 5 and 15 are collected together in order to find the mean positive excess. n_H is the number of slow, heavily ionizing, particles observed. n_+ and n_- refer to the fast positively and negatively charged particles and $n_?$ to the particles whose sign could not be determined.

The deduced positive excess is found by assuming first that 90 % of the heavily ionizing particles are protons and, second, that the ratio of positive to negative particles among $n_?$ is the same as the ratio $n_+ : n_-$.

It is clear that, assuming uniform detection efficiency, it is reasonable to suppose that more than half the interactions we observe in paraffin are nucleon-nucleon interactions. In the remainder, the number of target nucleons involved seems to be small.

8·4. *The laboratory energy of the primary particles.* – As a first approximation we assume that our interactions are simple nucleon-nucleon interactions and use (7) to calculate the primary energies from the values of γ_c: The results range from 30 GeV to 2 000 GeV with the majority of values between 70 GeV and 250 GeV.

(6) For example, T. GOZANI and K. SITTE: *Nuovo Cimento*, **11**, 26 (1959).

2392

In this range of energies the cosmic-ray protons have a steeply falling energy spectrum of the form $N(E)\,\mathrm{d}E \propto E^{-s}\,\mathrm{d}E$ with $s \sim 2.5$. If the interaction cross-section is independent of energy we can use (7) to find the expected spectrum of values of γ_c. We find $N(\gamma_c)\,\mathrm{d}\gamma_c \propto \gamma_c^{1-2s}\,\mathrm{d}\gamma_c$ which gives a power law with exponent -4 if $s = 2.5$.

The observed distribution of values of γ_c (Fig. 4) is certainly much more widely spread than the expected distribution. There are two effects that could account for the discrepancy. In the first place, the selection of our events discriminates against low-energy interactions but does not impose a sharp cut-off. This undoubtedly reduces the number of events with low values of γ_c.

Secondly, the large error in the determination of γ_c coupled with the steep form of the proton energy spectrum leads to a systematic tendency to overestimate the energy of interactions. The number of low-energy interactions is always greater than the number of high-energy interactions. As a result of fluctuations there will always be more low-energy interactions that appear to have a high energy than the reverse.

Some idea of the magnitude of this effect can be obtained in the following way. First, we note that a set of interactions with fixed true value of γ will give a distribution of values of γ_c that is symmetrical about the true value on a logarithmic scale. We therefore change to the quantities $l = \ln \gamma$ and $l_c = \ln \gamma_c$. We make the assumption that the distribution of l_c about l can be represented by a Gaussian with standard deviation σ. The true frequency distribution of l is obtained from the expected spectrum of γ and is $N(l)\,\mathrm{d}l = \exp[2l(1-s)]\,\mathrm{d}l$. The likelihood that an interaction with true value $(l, \mathrm{d}l)$ should occur and lead to an observed value $(l_c, \mathrm{d}l_c)$ is thus

$$\exp[2l(1-s)]\,\mathrm{d}l \exp\left[-\frac{(l_c-l)^2}{2\sigma^2}\right]\mathrm{d}l_c\,.$$

The logarithm of the likelihood function for l is

$$\log L = 2l(1-s) - \frac{(l-l_c)^2}{2\sigma^2} \tag{8}$$

and this has a maximum corresponding to

$$\frac{\gamma_c}{\gamma} = \exp[2(s-1)\sigma^2]$$

or, for $s = 2.5$,

$$\frac{\gamma_c}{\gamma} = \exp[3\sigma^2]\,. \tag{9}$$

For the majority of our events where the statistical error in γ_c is of the order of 25% the corresponding systematic overestimation of γ_c is less than 20%. However (9) shows that the bias rises rapidly with increasing error and it would be quite reasonable to take the few values of γ_c that we find to be greater than 20 as being spurious.

8·5. *The inelasticity of the interactions.* – For a nucleon-nucleon interaction the kinetic energy available for particle production is, in the center-of-mass system $2(\gamma_c - 1)M_N$. The energy radiated as π-mesons is $n_\pi \overline{E_\pi^*}$, where n_π includes both charged and neutral π-mesons and $\overline{E_\pi^*}$ is the average total energy of a π-meson in the center-of-mass system. If we neglect the nucleons and heavy mesons among the secondary particles from an interaction we may express the inelasticity (K) in the form

$$K \simeq \frac{1.5\, n_s \overline{E_\pi^*}}{2(\gamma_c - 1)M_N} . \tag{10}$$

Experimentally, $\overline{E_\pi^*}$ does not seem to vary much from one interaction to another. The quantity $n_s/(\gamma_c - 1)$ should therefore be closely related to K. The distribution of this quantity for our 36 interactions is shown in Fig. 9. If a reasonable value of $\overline{E_\pi^*}$ (~ 500 MeV) is inserted in (10) we find that a value of unity for $n_s/(\gamma_c - 1)$ corresponds to $K \sim 0.4$.

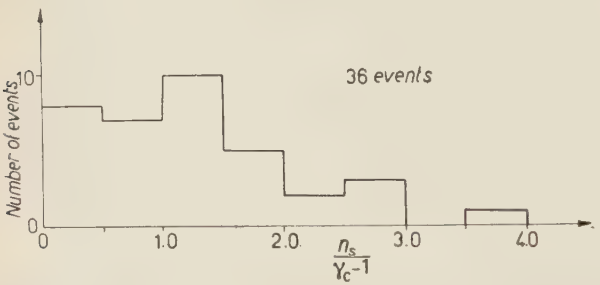

Fig. 9. – Distribution of the quantity $n_s/(\gamma_c - 1)$ for the first 36 interactions of Table II. n_s is the number of fast secondary particles from each interaction. The relation between $n_s/(\gamma_c - 1)$ and the inelasticity is discussed in the text.

The distribution of Fig. 9 must not be given too great an importance because of the very large errors in γ_c: In particular, the low values of $n_s/(\gamma_c - 1)$ correspond to the events that give very large values of γ_c and, as explained above, there is reason to think that these may be spurious.

The conclusion that we draw is that the inelasticity in the interactions we have studied is generally significantly below unity ($\sim 0.25 \div 0.75$) but we can say nothing about the form of the distribution.

2394

9. – Discussion and conclusions.

The first conclusion we would draw from our work is that a cosmic ray study of proton-proton interactions at energies of about 100 GeV is perfectly feasible. At an altitude of 3 500 m, using apparatus with an acceptance of 40 $cm^2 \times sr$ and a target thickness of 0.1 interaction length about one useful interaction with energy above 70 GeV was observed per day.

Secondly, the type of study we have made is severely limited by the large uncertainty involved in the indirect estimation of the energy of the interactions. The statistical error in γ_c amounts to about 25 % in our method of determination; for low multiplicities there is a tendency to choose the axis direction in such a way as to overestimate γ_c; finally, due to the shape of the spectrum of cosmic ray protons there is a systematic tendency to overestimate γ_c for all interactions.

With these errors, it is clear that no quantity that depends strongly on γ_c can be well determined. The inelasticity of the interactions is the most important and interesting such quantity. The quantities that are *not* dependent on γ_c or vary very slowly with the assumed value, are the transverse momenta and the anisotropy in the angular distribution of the secondary particles. For the transverse momenta, our results agree with many others in finding predominantly low values ([7]). For the angular distribution of the secondary particles we find a definite anisotropy in contrast to the results of DULLER and WALKER ([8]) and of LOHRMANN ([9]) who found no sign of anisotropy in interactions of comparable energy. We can find no satisfactory explanation of this discrepancy.

Concerning the various models that have been proposed to describe high-energy interactions there is little that we can say since we have made no attempt to obtain an unbiassed sample of interactions. In particular no variation of multiplicity with energy is found; our criteria of selection were such that interactions with low multiplicity were rejected or discriminated against.

We have, however, two indications that the inelasticity of the interactions is considerably less than unity. The first is the presence of positive particles (presumably protons) with high momenta in the C-system. The second is the distribution of $n_s/(\gamma_c - 1)$ discussed in Section 8.5. These indications are evidence against a model of the type proposed by FERMI ([10]) in which the entire

([7]) O. MINAKAWA, Y. NISHIMURA, M. TSUZUKI, H. YAMANOUCHI, H. AIZU, H. HASEGAWA, Y. ISHII, S. TOKUNAGA, Y. FUJIMOTO, S. HASEGAWA, J. NISHIMURA, K. NIU, K. NISHIKAWA, K. IMAEDA and M. KAZUNO: *Suppl. Nuovo Cimento*, **11**, 125 (1959).

([8]) N. M. DULLER and W. D. WALKER: *Phys. Rev.*, **93**, 215 (1954).

([9]) E. LOHRMANN: *Nuovo Cimento*, **5**, 1074 (1957).

([10]) E. FERMI: *Progr. Theor. Phys.*, **5**, 570 (1950).

2595

energy of the interacting particles is statistically distributed among the secondaries.

* * *

In the initial stages of the experiment we had the valued collaboration of Dr. H. FILTHUTH amd Mr. S. O. LARSON in CERN and much help from Mr. A. H. CHAPMAN of Imperial College, London.

At the Jungfraujoch Research Station Mr. HANS WIEDERKEHR gave us every assistance. We are indebted to him and to the Administration of the Research Station for providing us with facilities for ous work.

While considering the results of our experiment we had an extremely valuable discussion with the groups at the Ecole Polytechnique, Paris, and Imperial College, London, who are performing an experiment of a similar type. In particular this discussion made clear to us the importance of the argument summarized in Section 8·4.

Finally, we wish to record our debt to the late Professor C. J. BAKKER, the Director-General of CERN, and to Dr. L. KOWARSKI who encouraged our work and supported it whole-heartedly.

RIASSUNTO (*)

Si riferisce un esperimento con raggi cosmici per studiare interazioni nucleari di 100 GeV con una camera a nebbia in campo magnetico. Si descrive l'analisi delle interazioni e si discutono le ipotesi necessarie per interpretare le misure. Si danno i risultati di un primo campione di 41 interazioni. Essi dimostrano che: 1) gli impulsi trasversali delle particelle secondarie sono generalmente bassi (< 0.5 GeV/c) e 2) nel centro del sistema di riferimento degli impulsi le particelle emesse per la maggior parte hanno impulsi bassi e la loro distribuzione angolare è anisotropa. Ci sono anche prove che in una interazione nucleone-nucleo di questa intensità di energia il numero di nucleoni interessato è piccolo. La proporzione di particelle strane fra le particelle secondarie è analoga a quella che si riscontra in interazioni di energia molto inferiore.

(*) *Traduzione a cura della Redazione.*

2396

Internal Conversion Coefficients of $E2$ Transitions.

B. N. Subba Rao

Tata Institute of Fundamental Research - Bombay

(ricevuto il 18 Marzo 1960)

Summary. — A survey and analysis of all available data on internal conversion coefficients of pure $E2$ $(2+ \to 0+)$ transitions is presented. The results indicate the possibility of the internal conversion coefficients depending on the deformation of the nucleus.

1. – Introduction.

It is well established [1,2] that proper charge and current distributions of the nucleus in its finite dimensions should be taken into account in all calculations of internal conversion coefficients. Further theoretical work [3-5] has shown that internal conversion coefficients also depend upon the detailed nuclear dynamics. However, all these effects are considered to be negligible for $E2$ transitions. For this reason, sometimes theoretical conversion coefficients of $E2$ transitions are taken as a standard in order to evaluate conversion coefficients. But a few reports [6,7] indicate that some conversion coefficients of $E2$ transitions show $(10 \div 20)\%$ deviation from their corresponding theoretical value. All attempts [4,8] at understanding these deviations in terms of nuclear

(1) L. A. Sliv and M. Listengarten: *Žurn. Éksp. Teor. Fiz.*, **22**, 29 (1952); L. A. Sliv and I. M. Band: *Coefficients of Internal Conversion* (Moscow, 1956).

(2) C. Nordling, K. Siegbahn, E. Sokolowski and A. H. Wapstra: *Nucl. Phys.*, **1**, 326 (1956).

(3) E. L. Church and J. Weneser: *Phys. Rev.*, **104**, 1382 (1956).

(4) T. A. Green and M. E. Rose: *Phys. Rev.*, **110**, 105 (1958).

(5) A. Reiner: *Nucl. Phys.*, **5**, 544 (1958); S. G. Nilsson: UCRL-3803 (1957)

(6) F. K. McGowan and P. H. Stelson: *Phys. Rev.*, **107**, 1674 (1957); M. C. Joshi, B. N. Subba Rao and B. V. Thosar: *Nuovo Cimento*, **10**, 775 (1958).

(7) G. J. Nijgh and A. H. Wapstra: *Nucl. Phys.*, **9**, 545 (1959).

(8) L. S. Kisslinger: *Phys. Rev.*, **114**, 292 (1959).

2397

structure effects have failed, because these $E2$ transitions are enhanced by large factors. These considerations prompted a survey of all experimental data on pure $E2$ transitions and an analysis of it to be made.

2. – Analysis of data and results.

Table I shows most of the available data ([9]) on K-shell internal conversion coefficients (α^K) of pure $2+ \rightarrow 0+$ $E2$ transitions. In the first column, the nucleus and the energy in (keV) of the transition are shown. In the second column, experimental values (α^K_{exp}) are shown together with the reference. In the third column the mean of all observed values weighted according to the inverse of errors are shown. In doing this, a 12% error was assigned wherever errors were uncertain or were not available, since this appears to be the normal range of experimental error. The fourth column gives the theoretical values obtained by numerical log-log interpolation of the values tabulated by ROSE ([10]), and SLIV and BAND ([1]). In almost all cases, these tabulated values do not differ by more than a few per cent. The fifth column gives the ratio $R(\alpha^K)$ of the experimental to theoretical values. The last column shows the deformation parameter obtained from $E2$ transition probabilities ([11]). In Fig. 1

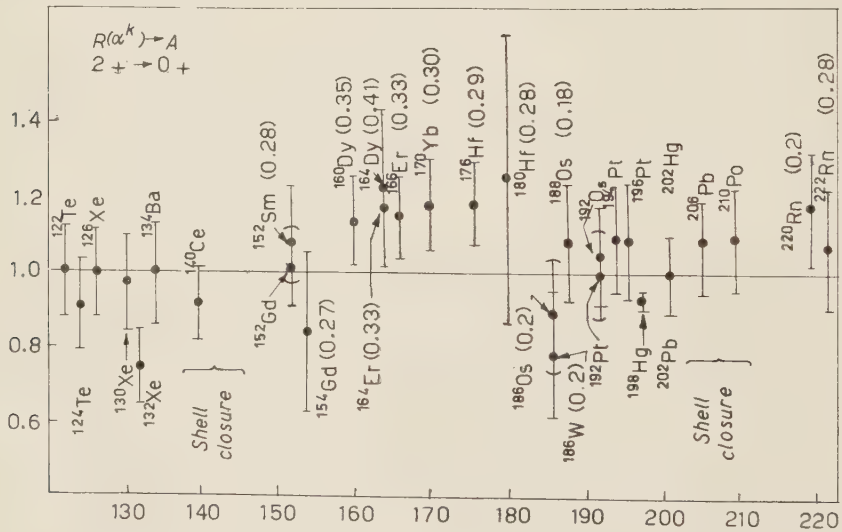

Fig. 1. – Variation of $R(\alpha^K)$ with mass number.

([9]) Data were obtained in many cases from: D. STROMINGER, J. M. HOLLANDER and G. T. SEABORG: *Rev. Mod. Phys.*, **30**, 585 (1958); B. S. DZELEPOV and L. K. PEKER: *Schemes of Radioactive nuclei* (Moscow, 1958).

([10]) M. E. ROSE: *Internal Conversion Coefficients* (Amsterdam, 1958).

([11]) K. ALDER, A. BOHR, T. HUUS, B. MOTTELSON and A. WINTHER: *Rev. Mod. Phys.*, **28**, 432 (1956).

2308

TABLE I. – *Conversion coefficients.*

Nucleus (E keV)	$\alpha^K_{exp.}$ Observed	Ref.	Adopted	$\alpha^K_{Theor.}$	$R(\alpha^K)$	Deformation parameter, β
^{122}Te (564)	$5.2\cdot10^{-3}$	(1)	$(5.42\pm0.6)\cdot10^{-3}$	$5.3\cdot10^{-3}$	1.02 ± 0.11	—
	$(5.2\pm0.4)\cdot10^{-3}$	(2)				
	$(6.6\pm1.7)\cdot10^{-3}$	(3)				
^{124}Te (603)	$3.4\cdot10^{-3}$	(4)	$(3.8\pm0.5)\cdot10^{-3}$	$4.15\cdot10^{-3}$	0.92 ± 0.12	—
	$3.7\cdot10^{-3}$	(5)				
	$4.3\cdot10^{-3}$	(6)				
^{126}Xe (386)	$(1.6\pm0.2)\cdot10^{-2}$	(7)	$(1.65\pm0.2)\cdot10^{-2}$	$1.65\cdot10^{-2}$	1.00 ± 0.12	—
	$1.7\cdot10^{-2}$	(8)				
^{130}Xe (528)	$6\cdot10^{-3}$	(9)	$(6.5\pm0.8)\cdot10^{-3}$	$6.6\cdot10^{-3}$	0.98 ± 0.12	—
	$7\cdot10^{-3}$	(10)				
^{132}Xe (673)	$2.7\cdot10^{-3}$	(41)	$(2.7\pm0.32)\cdot10^{-3}$	$3.6\cdot10^{-3}$	0.75 ± 0.09	—
^{134}Ba (605)	$(4.7\pm0.3)\cdot10^{-3}$	(11)	$(5.1\pm0.8)\cdot10^{-3}$	$5.10\cdot10^{-3}$	1.00 ± 0.16	—
	$(5.7\pm0.7)\cdot10^{-3}$	(43)				
	$(4.6\pm0.4)\cdot10^{-3}$	(12)[a], (13)				
	$(6.1\pm0.7)\cdot10^{-3}$	(44)[a]				
^{140}Ce (1597)	$6.3\cdot10^{-4}$	(59)	$(6.3\pm0.76)\cdot10^{-4}$	$6.9\cdot10^{-4}$	0.91 ± 0.11	—
^{152}Sm (122)	0.80	(14)	0.7 ± 0.11	0.65	1.08 ± 0.16	0.28
	0.6 [b]	(45)				
^{152}Gd (344)	$(3.2\pm0.5)\cdot10^{-2}$	(14)	$(3.25\pm0.3)\cdot10^{-2}$	0.032	1.02 ± 0.1	0.2
	$(3.3\pm0.1)\cdot10^{-2}$	(15)				
^{154}Gd (123)	(0.54 ± 0.13)	(16)	0.54 ± 0.13	0.64	0.84 ± 0.21	0.27
^{160}Dy (87)	1.65 ± 0.2	(17)	1.75 ± 0.20	1.55	1.14 ± 0.12	0.35
	1.6	(18)				
	1.5	(19)				
	2.0 ± 0.2	(20)				

(*a*) These were obtained from α, using $(K/L+M=6.7)$.
(*b*) This is derived, assuming the theoretical value for the α^K of the 344 keV transition in ^{152}Gd.

2399

TABLE I (*continued*).

Nucleus (E keV)	$\alpha^K_{exp.}$ Observed	Ref.	Adopted	$\alpha^K_{Theor.}$	$R(\alpha^K)$	Deformation parameter, β
^{164}Dy (73)	(2.7 ±0.5)	(21)	2.7 ±0.5	2.19	1.23±0.22	0.41
^{164}Er (91)	1.9 ±0.2	(21)	1.9 ±0.20	1.60	1.18±0.12	0.33
^{166}Er (80)	1.9 ±0.3	(17)	1.88±0.18	1.65	1.15±0.11	0.33
	1.9 ±0.2	(23)				
	1.9	(24)				
	1.85±0.13	(22)				
^{170}Yb (84)	1.5 ±0.2	(17)	1.6 ±0.15	1.36	1.18±0.12	0.30
	1.6 ±0.15	(25)				
	1.56±0.15	(26)				
	1.6	(27)				
	1.69	(28)				
	1.70±0.20	(46)				
	1.65±0.12	(22)				
^{176}Hf (89)	1.3	(17)	1.31±0.11	1.12	1.18±0.1	0.29
	1.32±0.11	(22)				
^{180}Hf (93)	1.30±0.4	(60)	1.30±0.4	1.04	1.25±0.38	0.20
^{186}Os (137)	0.37±0.08	(29)	0.39±0.06	0.43	0.90±0.14	0.20
	0.35±0.10	(30)				
	0.45±0.03	(31)				
	0.36	(32)				
^{186}W (123)	0.45±0.10	(29)	0.45±0.10	0.57	0.79±0.17	0.20
^{188}Os (155)	0.40±0.05	(31)	0.36±0.05	0.33	1.09±0.16	0.18
	0.32±0.05	(33)				
^{192}Os (206)	0.16	(47)	0.16 ±0.02	0.152	1.05±0.13	0.18

2400

TABLE I (*continued*).

Nucleus (E keV)	$\alpha_{exp.}$ Observed	Ref.	Adopted	$\alpha^K_{Theor.}$	$R(\alpha^K)$	Deformation parameter, β
^{192}Pt (317)	0.054	(34)	0.054	0.054	1.00±0.12	0.2
^{194}Pt (328)	0.056 ±0.006	(42)	0.056 ±0.006	0.051	1.09±0.12	0.2
^{196}Pt (354)	0.042 ±0.003	(35)	0.046 ±0.006	0.042	1.09±0.15	0.2
	0.059	(42)				
	0.05	(36)				
^{198}Hg (411)	0.037	(53)	0.0281±0.0005	0.0302	0.93±0.02	0.2
	0.03	(54)				
	0.028 ±0.007	(36)				
	0.026	(55)				
	0.025	(37)				
	0.029	(56)				
	0.0281±0.0005	(38)				
^{202}Hg (439)	0.034	(48)	0.034	0.027	1.26	—
^{202}Pb (961)	0.0055	(57)	0.0058±0.0007	0.0058	1.00±0.11	—
	0.006	(58)				
^{206}Pb (803)	$9 \cdot 10^{-3}$	(49)	$(9 \pm 1) \cdot 10^{-3}$	$8.3 \cdot 10^{-3}$	1.08±0.12	—
^{210}Pb (1181)	$4.8 \cdot 10^{-3}$	(50)	$(4.8 \pm 0.6) \cdot 10^{-3}$	$4.4 \cdot 10^{-3}$	1.09±0.13	—
^{220}Rn (24)1	0.13	(39)	0.13	0.111	1.17±0.14	0.2
^{222}Ra (111)	<0.4	(52)	—	—	—	0.2
^{222}Rn (187)	0.15	(51)	0.19±0.03	0.180	1.06±0.16	0.28
	0.22 ±0.02	(40)				

TABLE I (*continued*).

([1]) B. FARRELY *et al.*: *Phys. Rev.*, **99**, 1440 (1955).
([2]) M. J. GLAUBMAN: *Phys. Rev.*, **98**, 645 (1955).
([3]) R. ROHR and R. BIRKHOF: *Phys. Rev.*, **98**, 1266 (1955).
([4]) L. LANGER *et al.*: *Phys. Rev.*, **91**, 000 (1953).
([5]) D. HUTCHINSON and M. WIDENBECK: *Phys. Rev.*, **88**, 699 (1952).
([6]) F. R. METZGER: *Phys. Rev.*, **90**, 328 (1953).
([7]) L. KOERTS *et al.*: *Phys. Rev.*, **98**, 1230 (1955).
([8]) N. MARTY *et al.*: *ñourn. Phys. et Rad.*, **14**, 663 (1953).
([9]) R. S. CAIRD and A. C. G. MITCHELL: *Phys. Rev.*, **93**, 175 (1954).
([10]) A. ROBERTS *et al.*: *Phys. Rev.*, **64**, 268 (1943).
([11]) G. BERTOLINI *et al.*: *Nuovo Cimento*, **2**, 273 (1955).
([12]) Z. O'FRIEL and A. WEBER: *Phys. Rev.*, **10ò**, 1076 (1956).
([13]) G. KEISTER *et al.*: *Phys. Rev.*, **97**, 451 (1955).
([14]) S. K. BHATTACHERJEE *et al.*: *Nuovo Cimento*, **7**, 501 (1958).
([15]) P. N. MUKHERJEE *et al.*: *Proc. Ind. Sci. Congr.*, part II (1960), p. 77.
([16]) J. JULIANO and F. STEPHENS: *Phys. Rev.*, **108**, 341 (1957).
([17]) F. K. MCGOWAN: *Phys. Rev.*, **85**, 151 (1952).
([18]) O. NATHAN: *Nucl. Phys.*, **4**, 125 (1957).
([19]) M. CLARK and J. KNOWLES: *Bull. Amer. Phys. Soc.*, **2**, 231 (1957).
([20]) M. C. JOSHI, B. N. SUBBA RAO and B. V. THOSAR: *Nuovo Cimento*, **10**, 775 (1958).
([21]) H. BROWN and R. BECKER: *Phys. Rev.*, **96**, 1372 (1954).
([22]) F. K. MCGOWAN and P. H. STELSON: *Phys. Rev.*, **97**, 1674 (1957).
([23]) A. W. SUNYAR: *Phys. Rev.*, **93**, 1345 (1954).
([24]) R. L. GRAHAM *et al.*: *Phys. Rev.*, **98**, 1173 (1955).
([25]) R. L. GRAHAM *et al.*: *Can. Journ. Phys.*, **30**, 459 (1952).
([26]) K. LINDEN and N. STARFELT: *Ark. Fys.*, **7**, 109 (1954).
([27]) N. JAFFE: *Nucl. Sci. Abstr.*, **9**, no. 24B (1955).
([28]) A. BISI *et al.*: *Nuovo Cimento*, **3**, 1007 (1956).
([29]) R. M. STEFFEN: *Phys. Rev.*, **82**, 827 (1951).
([30]) F. METZGER and R. HILL: *Phys. Rev.*, **82**, 646 (1951).
([31]) M. JOHNS *et al.*: *Can. Journ. Phys.*, **34**, 69 (1956).
([32]) F. PORTER *et al.*: *Phys. Rev.*, **103**, 921 (1956).
([33]) V. R. POTNIS: *Phys. Rev.*, **104**, 722 (1956).
([34]) L. BAGGERLEY *et al.*: *Phys. Rev.*, **100**, 1364 (1955).
([35]) M. THIEME and E. BLEULER: *Phys. Rev.*, **101**, 1031 (1956).
([36]) R. M. STEFFEN *et al.*: *Helv. Phys. Acta*, **22**, 167 (1949).
([37]) R. G. WILKINSON *et al.*: *Phys. Rev.*, **74**, 1250 A (1948).
([38]) A. H. WAPSTRA and G. J. NIJGH: *Nucl. Phys.*, **9**, 545 (1959).
([39]) S. ROSENHUM *et al.*: *Journ. Phys. et Rad.*, **15**, 129 (1954).
([40]) M. JURIA and D. STANOJEVIA: *Bull. Inst. Nucl. Sci. Boris Kidric*, **5**, 15 (1956).
([41]) H. FINSTON and W. BERNSTEIN: *Phys. Rev.*, **96**, 71 (1954).
([42]) M. THIEME and E. BLEULER: *Phys. Rev.*, **101**, 1031 (1956).
([43]) C. L. PEACOCK and J. L. BRAND: *Phys. Rev.*, **83**, 484 A (1952).
([44]) H. H. HORSTER *et al.*: *Nuovo Cimento*, **2**, 854 (1955).
([45]) O. NATHAN and M. A. WAGGONER: *Nucl. Phys.*, **2**, 548 (1957).
([46]) M. C. JOSHI, B. N. SUBBA RAO and B. V. THOSAR: unpublished results.
([47]) L. BAGGERLY *et al.*: *Phys. Rev.*, **100**, 1364 (1955).
([48]) P. KRAMER, H. C. HAMERS and G. MEIJER: *Physica*, **22**, 208 (1956).
([49]) T. NOVAKOV *et al.*: *Ark. Fys.*, **13**, 113 (1958).
([50]) R. HOFF: *Nat. Soc. Amer.*, **9**, no. 24B (1955).
([51]) R. ROY and M. GOES: *Compt. Rend. Acad. Sci.*, **238**, 469 (1954).
([52]) F. S. STEPHENS *et al.*: *Phys. Rev.*, **96**, 1568 (1954).
([53]) D. SAXON and R. HELLER: *Phys. Rev.*, **75**, 909 (1949).
([54]) K. SIEGBAHN and A. HEDGRAN: *Phys. Rev.*, **75**, 523 (1949).
([55]) B. S. DZELEPOV *et al.*: *Izv. Akad. Nauk USSR*, **14**, 299 (1950).
([56]) C. Y. FAN: *Phys. Rev.*, **87**, 252 (1953).
([57]) D. MAEDER *et al.*: *Physica*, **20**, 521 (1954).
([58]) K. BERGVIST *et al.*: *Phil. Mag.*, **46**, 65 (1955).
([59]) V. P. PRIKODSCHEVA and U. V. CHOLVNOV: *Izv. Akad. Nauk*, **22**, 176 (1958).
([60]) V. S. GVOZDEV *et al.*: *Nuclear Spectroscopy Conference* (Moscow, 1958). Reference ([29]) in M. A. LINTENGARTEN: *Izv. Akad. Nauk*, **22**, 759 (1958).

2402

$R(\alpha^K)$ is plotted against the nucleon number A, in order to bring out the possible dependence of $R(\alpha^K)$ on nuclear structure, in a good approximation. In this figure, the values of the deformation parameter, β, are given within brackets against the nucleus concerned.

It is seen from this figure and Table I that in the region of nearly spherical nuclei (in the neighbourhood of $A - 140$, 208), $R(\alpha^K)$ is approximately unity with much scatter on both sides and there is a trend of α^K_{exp} being slightly lower than α^K_{Theor}. This is in particular supported by the well studied ([7]) 412 keV transition in ^{198}Hg, as also by the transition in ^{140}Ce. But the more impressive trend is the systematically higher values of most of the α^K_{exp} in the highly deformed nuclei. Many of them have been determined by different methods and different groups, as shown in Table I. Thus the possibility of a constant error entering the experimental values seems to be reduced. It was for this purpose that in the analysis of data the weighted mean procedure was adopted. Moreover the deviation of α^K_{exp} of the 122 keV transition in ^{152}Sm is larger than in the 344 keV transition in ^{152}Gd. Similarly, the deviation in the transition of ^{164}Dy is higher than that in the transition of the less deformed ^{164}Er. The general situation shows that experimental errors are rather large to permit a quantitative evaluation of the dependence on deformation. It may be emphasized that apart from the cases which had been specifically reported ([6,7]) to be deviating from theoretical values, many other experimental data are in good agreement with the general trends of the large positive deviations in the highly deformed nuclei and a small and sometimes negative deviation in the near-closed shell nuclei.

Most of the $(2+ \rightarrow 0+)$ transitions in the deformed actinide nuclei fall below the threshold for K-conversion, so that not much information can be obtained in this region of nuclei. The dependence of conversion coefficients on the nuclear structure is expected to be prominent in heavy nuclei. In addition, due to the high energy of such transitions in light nuclei and the low conversion in these light nuclei, not many cases have been studied accurately. For this reason, the survey and analysis have been limited to the rare earth and neighbouring nuclei.

Similar analysis of conversion ratios K/L and $(L_{\text{I}} + L_{\text{II}})/L_{\text{III}}$ showed that no systematic deviations are clearly observable.

3. – Discussion.

There are a few cases in which the generalization that conversion coefficients of transitions in deformed nuclei is higher, appears to fail. These are the 123 keV transitions in ^{154}Gd and ^{186}W. No particular comments seem to

be relevant, since both these transitions have been studied in a rather approximate way and only one measurement for each of them is available at present. It is interesting that both of them are on the borders of the region of large deformation. The conversion coefficients of transitions in ^{202}Hg and ^{132}Xe, similarly, show large deviations compared to others in that region. Again only one measurement is available in these cases. Thus, while more accurate determinations are indicated by this survey for almost all transitions, these singular cases deserve particular attention.

Experimental errors in conversion coefficients depend to a large extent on the particular experimental procedure adopted. There are many direct and indirect procedures ([12]) of evaluating conversion coefficients. But the most favourable method which can lead to very small errors is to be decided for the particular case. Thus, as pointed out above, while the magnetic spectrometric measurement of conversion line intensities and the corresponding β-group intensities has led to accurate values ([7]) in many instances, for highly converted and low energy transitions this method is very unfavourable. McGowan and Stelson ([6]), who first reported about the systematic deviations in a few nuclei, pointed out that systematic errors in their method could be a reason for such deviations. As has been stressed earlier, the consideration of values obtained by different methods obviates this doubt to a large extent.

From such considerations, it is seen that possibly the conversion coefficients are nearly normal with a tendency to being slightly lower in the closed shell nuclear region, and are mostly above the present theoretical values in the highly deformed region.

Most of $E2$ transition probabilities in the deformed nuclei are enhanced by large factors due to collective motion of nucleons. This makes the dynamic nuclear structure contribution ([4]) very small. The same conclusions were arrived at from considerations of nuclear configuration mixing ([8]). Thus, nuclear dynamics may not be contributing appreciably to such deviations. However, effects of static structure due to nuclear deformation can present themselves through electron wave functions entering into calculations of conversion coefficients (*).

It should be quite interesting, therefore, to understand the cause of these apparent anomalies from theoretical and more accurate experimental investigations.

([12]) D. Alburger: *Handb. d. Phys.*, **42**, 26 (1957).

(*) Recent investigations of the influence of nuclear deformation on electron wavefunctions by P. Vainer *et al.*: *Žurn. Eksp. Teor. Fiz.*, **38**, 870 (1960) and A. S. Meligy: *Nucl. Phys.*, **14**, 248 (1959) adduce further support for such a proposal.

* * *

I am very thankful to Dr. B. V. THOSAR for many helpful discussions. My thanks are also due to Drs. M. E. ROSE, E. L. CHURCH and J. M. HOLLANDER for helpful communications.

RIASSUNTO (*)

Si presenta una rassegna analitica di tutti i dati disponibili sui coefficienti interni di conversione delle pure transizioni $E2$ $(2+ \to 0+)$. I risultati mostrano la possibilità che i coefficienti interni di conversione dipendano dalla deformazione del nucleo.

(*) *Traduzione a cura della Redazione.*

Nuclear Magnetic Relaxation Times T_1 and T_2 in Some Liquids.

G. Bonera, L. Chiodi, G. Lanzi and A. Rigamonti

Istituto di Fisica dell'Università - Pavia

(ricevuto il 30 Marzo 1960)

Summary. — Nuclear relaxation times T_1 and T_2 of a set of pure liquids have been measured. The results we have obtained give in general for low viscosity liquids, according to theory, $T_1 = T_2$ within the experimental error. We then examine the possibility that in some liquids having more than one chemical type of protons, different longitudinal relaxation times are present.

1. – Introduction.

It is known that nuclear relaxation times have a fundamental importance in describing the nuclear magnetic resonance in condensed matter.

The reciprocal of the longitudinal relaxation time T_1 gives a valuation of the interaction between the nuclear spin system and the lattice; the reciprocal of the transversal relaxation time T_2 gives a valuation of the spin-spin interaction.

The nuclear relaxation theory in liquids has been developed by various authors [1-9] and foresees $T_1 = T_2$ for pure liquids of low viscosity in which

[1] N. Bloembergen, E. M. Purcell and R. V. Pound: *Phys. Rev.*, **73**, 679 (1948).
[2] R. K. Wangsness and F. Bloch: *Phys. Rev.*, **89**, 728 (1953).
[3] A. Abragam and R. V. Pound: *Phys. Rev.*, **92**, 953 (1953).
[4] R. Kubo and K. Tomita: *Journ. Phys. Soc. Japan*, **9**, 888 (1954).
[5] I. Solomon: *Phys. Rev.*, **99**, 559 (1955).
[6] F. Bloch: *Phys. Rev.*, **102**, 104 (1956).
[7] N. Bloembergen: *Phys. Rev.*, **104**, 1542 (1956).
[8] E. M. Purcell: *Suppl. Nuovo Cimento*, **3**, 961 (1957).
[9] K. Tomita: *Progr. Theor. Phys.*, **19**, 541 (1958).

the relaxation is due only to a pure dipole-dipole interaction between the protons. The main aim of this work is to verify this expectation of the theory (*). A comparison between the two relaxation times in liquids has been already made by some authors ([10-16]). However the results till now published are not in good agreement with one another. Therefore we think that the present work can bring a contribution to the question.

In this work we have then examined some liquids that have protons in non equivalent positions in order to verify the possible presence of more than one longitudinal relaxation time.

2. – Experimental apparatus.

The measurement of the relaxation times has been carried out with the methods we have described in previous works ([17,14]).

The measurement of the longitudinal relaxation time T_1 is based on the recording of a sequence of nuclear signals in phase with the rotating magnetic field $\boldsymbol{H}_1$, due to the complete reversal of nuclear magnetization. This reversal is obtained performing adiabatic fast passages through resonance.

The transversal relaxation time T_2 is measured observing the nuclear magnetization decay when it precesses together with the rotating field in a plane normal to the constant magnetic field $\boldsymbol{H}_0$. The magnetization $\boldsymbol{M}$ is set parallel with $\boldsymbol{H}_1$ stopping an adiabatic fast passage in resonance.

The measurements of T_1 and T_2 are made with a magnetic field H_0 of 1650 gauss.

The precision we have in comparing the two relaxation times in a liquid is determined in practice by the precision obtained in the measurement of T_2.

(*) If a scalar interaction with another spin is present and if the correlation time relative to this interaction is great enough T_1 can be greater than T_2. Furthermore in this case the value of T_2 can depend in a very remarkable way on the magnitude of the rotating magnetic field. [J. M. Winter: *Compt. Rend.*, **249**, 1346 (1959); I. Solomon: *Compt. Rend.*, **249**, 1631 (1959)].

([10]) J. G. Powles and D. Cutler: *Nature*, **180**, 1344 (1957).

([11]) S. Meiboom and D. Gill: *Rev. Sci. Instr.*, **29**, 688 (1958).

([12]) J. G. Powles and D. Cutler: *Arch. des Sci.*, **12**, fasc. spéc., 135 (1959).

([13]) G. Hochstrasser: *Arch. des Sci.*, **12**, fasc. spéc., 132 (1959).

([14]) G. Bonera, L. Chiodi, L. Giulotto and G. Lanzi: *Nuovo Cimento*, **14**, 119 (1959).

([15]) J. G. Powles and D. Cutler: *Nature*, **184**, 1123 (1959).

([16]) I. Solomon: *Journ. Phys. Rad.*, **20**, 768 (1959).

([17]) G. Chiarotti, G. Cristiani, L. Giulotto and G. Lanzi: *Nuovo Cimento*, **12**, 519 (1954).

Indeed the measurement of the transversal relaxation time presents greater experimental difficulties mainly if this time has a magnitude of several seconds.

One could expect that in liquids having protons in non-equivalent positions more than one longitudinal relaxation time and more than one transversal relaxation time are present. We have performed a research of this type for longitudinal relaxation times only, because of the greater precision we can obtain in this measurement.

The investigation of more than one longitudinal relaxation time in liquids has been performed observing the return to the equilibrium value of the nuclear magnetization $\boldsymbol{M}$ after it has been reversed by means of a fast adiabatic passage. If many longitudinal relaxation times T_1 are present, M reaches the equilibrium value M_0 according to the law:

$$M(t) = M_0 \sum_i A_i(1 - 2 \exp[-t/T_i]) ,$$

t being the time elapsed after the reversal and A_i the fraction of protons having longitudinal relaxation time T_i.

From the behaviour of M as function of t it is possible in practice to obtain the values of relaxation times only if they are two or three different ones. To this object it is convenient to set $\ln \frac{1}{2}(1 - M(t)/M_0)$ *versus* t. A sufficiently sure experimental datum is then given by the slope of the tangent at the curve for $t = 0$. This slope is equal to $\sum_i A_i/T_i$.

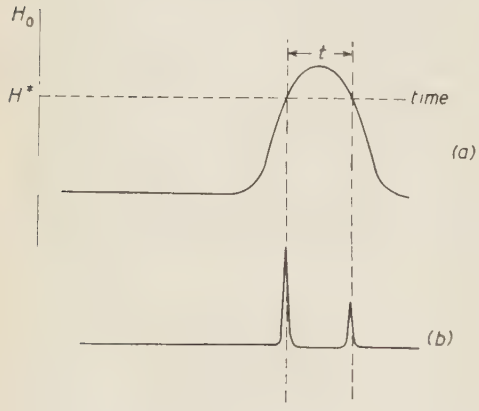

Fig. 1. – *a*) Magnetic field *vs.* time; *b*) record of nuclear signal.

We have measured the rate $M(t)/M_0$ relative to different values of t modulating the constant magnetic field H_0 throughout the resonance value H^* as is shown in Fig. 1-*a*. One obtains in such a way two fast adiabatic passages elapsed in time of t.

The height of the first signal (Fig. 1-*b*) is proportional to M_0 and that of the second one to $-M(t)$.

We have obtained a modulation like that of Fig. 1 by means of the electrolytic bridge described in a previous work ([17]).

The central electrode of the electrolytic bridge is stopped outside the resonance during a quite long time in order that the nuclear magnetization reach the equilibrium value. Then by means of a particular device the central electrode makes a rotation of 360° with a suitable angular speed.

3. – Experimental results.

We plot in Table I the values of the longitudinal and transversal relaxation times in some pure liquids we have measured in order to verify the equality between this two times foreseen by theory. In the same table some of the data obtained by other authors are plotted.

TABLE I.

Liquid	T_1 at 1650 G (s)	T_2 at 1650 G (s)	temp. (°C)	Literature values T_1 (s)	field (G)	temp. (°C)	Literature values T_2 (s)	field (G)	temp. (°C)
Water	3.2	3.1	23°	3.2 *a*	1650	23°	3.1 *a*	1650	20°
				3.2 *b*	2000 and 7000	23°	2.7 *e*	0.5	20
				3.6 *c*	250 and 5000	25°	2.7 *c*	0.75	25°
				3.3 *d*	6500	24°	2.65 *d*	6500	24°
Cyclopentane	12.8	10.5	20°						
Cyclohexane	6.2	5.5	23°	6.5 *f*	1650	(*)			
				5.5 *c*	250	25°	3.5 *c*	0.75	25°
				7.1 *c*	5000	25°			
Cycloheptane	4.4	4.4	21°						
Methyl-alcohol	7.5	6.5	22°	8 *f*	1650	(*)			
				(2.5-8.5) *g*	250	25°	2.5 *g*	0.75	25°
Ethyl-alcohol	3	3.1	22°	3.5 *f*	1650	(*)			
				2.2 *g*	250	25°	2.3 *g*	0.75	25°
				2.2(**) *h*	6800 and 1100	20°			
Propyl-alcohol	1.1	1.1	23°	2 *g*	250	25°	1.9 *g*	0.75	25°
Butyl-alcohol	0.6	0.6	19°	1.4 *g*	250	25°	1.5 *g*	0.75	25°

References for literature values in Table I:
a = [18] and [14]; *b* = [19]; *c* = [15]; *d* = [16]; *e* = [13]; *f* = [20]; *g* = [12]; *h* = [1].

(*) These results, obtained some years ago with the same experimental apparatus, are relative to a temperature that had not been exactly measured, but which was probably quite greater than 20 °C.

(**) This measurement has been accomplished in presence of oxygen in solution.

[18] L. GIULOTTO, G. LANZI and L. TOSCA: *Arch. des Science*, **10**, fasc. spéc., 250 (1957).
[19] J. H. SIMPSON and H. Y. CARR: *Phys. Rev.*, **111**, 5 (1958).
[20] G. CHIAROTTI, G. CRISTIANI and L. GIULOTTO: *Nuovo Cimento*, **1**, 863 (1955).

2409

We can remark in some cases remarkable differences between the results relative to the same liquids. Only in part these differences can be due to differences of temperature or to the presence of oxigen in solution.

If we restrict our considerations only to the results we have obtained at present, we can observe that in general the equality between the two nuclear relaxation times is well verified for liquids whose relaxation times are less or equal to about 4 s. For T_1 and T_2 greater than 4 s we can remark that our measurements should give for T_2 a value slightly less than T_1. However it is probable that such a result can be due to a systematic error. These differences could at least be partially due to surface effects. A systematic study of surface effects in nuclear magnetic relaxation is now in progress.

We can remark besides that for some liquids plotted in the table (methyl-alcohol, ethyl-alcohol, propyl-alcohol and butyl-alcohol) many chemical types of protons are present. However, the return of nuclear magnetization to equilibrium value we have examined for these liquids with the method previously described, looks still exponential within the experimental error (see Fig. 2).

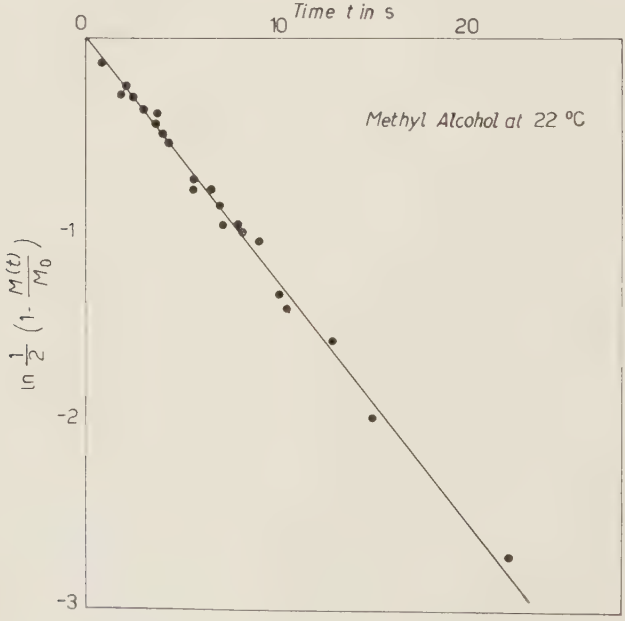

Fig. 2. - $\ln \frac{1}{2}[1 - M(t)/M_0]$ *vs.* t for Methyl-Alcohol.

This result seems to prove that for the primary alcohols we have studied, the longitudinal relaxation times of the various groups of protons in non-equivalent positions, are not very different from one another. However this con-

clusion does not seem in good agreement with the results recently obtained by POWLES and CUTLER [12].

On the contrary an analogous research we have performed on toluene has shown in a rather evident way the presence of two longitudinal relaxation times as one sees in Fig. 3. The dotted line is the tangent at the origin of the

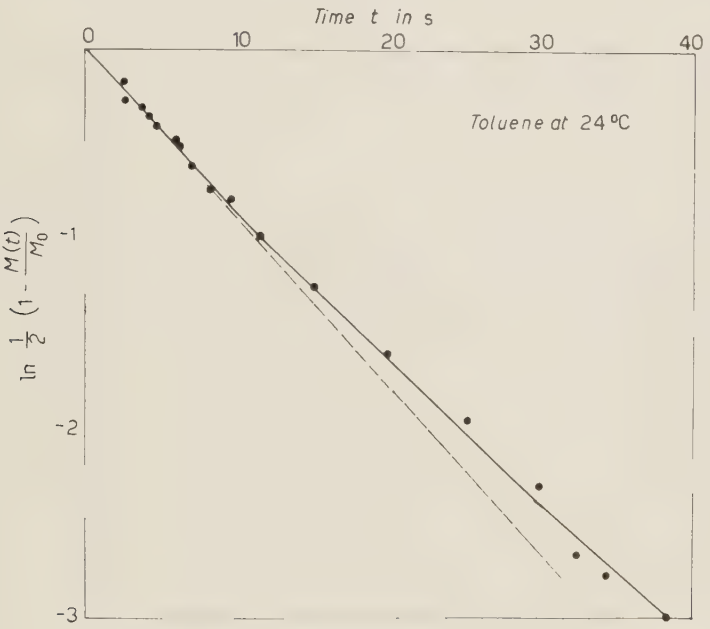

Fig. 3. - $\ln \frac{1}{2}[1 - M(t)/M_0]$ *vs.* t for Toluene.

curve which represents $\ln \frac{1}{2}(1 - M(t)/M_0)$ as a function of t; the continuous line is the theoretical plot for two longitudinal relaxation times $(T_1)_{C_6H_5} = 15$ s and $(T_1)_{CH_3} = 8$ s. This line is quite well adherent to the experimental results. We can observe that these values of the two longitudinal relaxation times of toluene are in good agreement with the results obtained by NEDERBRAGT and REILLY [21] with a high resolution device $((T_1)_{C_6H_5} = 16$ s; $(T_1)_{CH_3} = 9$ s at 25 °C).

* * *

The authors are grateful to Professor L. GIULOTTO for most helpful discussions and valuable suggestions.

[21] G. W. NEDERBRAGT and C. A. REILLY: *Journ. Chem. Phys.*, **24**, 1110 (1955).

The authors also wish to express their gratefulness to the Consiglio Nazionale delle Ricerche for its grant, and to the Office, Chief of Research and Development, U.S. Department of Army, who has sponsored in part this work through its European Office.

RIASSUNTO

Sono stati misurati i tempi di rilassamento nucleare T_1 e T_2 per una serie di liquidi puri. I risultati da noi ottenuti danno in generale per liquidi puri a bassa viscosità, in accordo con la teoria, $T_1 = T_2$ nei limiti dell'errore sperimentale. È stata inoltre esaminata la possibilità che in alcuni liquidi aventi protoni in posizioni non equivalenti siano presenti più tempi di rilassamento longitudinale.

The Characteristic-Functional Method in Cascade Theory.

J. W. Gardner

Atomic Power Division, English Electric Co., Ltd. - Whetstone, Leicester

(ricevuto il 30 Marzo 1960)

Summary. — In a previous paper the last-collision equation treatment of the general Markoff cascade was developed and applied to examples drawn from cosmic radiation and nuclear reactor theory. The present paper gives an alternative approach via the characteristic functional, the latter being introduced as a logical extension of the concept of a moment-generating function. Potentially the C.F. embodies complete information about all the probability relations of the stochastic process in question; in practice the extraction of information about any particular distribution depends on a suitable choice of the arbitrary auxiliary function occurring in the definition of the C.F. The power and versatility of the method are illustrated by reference to both point-source and extended-source cascades; it is particularly suited to the treatment of cascades from line sources, examples of which would be, in descending order of energy: a high energy nuclear «jet»; the track of an ionising particle; the source representation in the Feinberg-Galanin method of nuclear reactor theory.

1. – Introduction.

In a previous paper (1) the present author has given a general mathematical solution for the probability distributions of a Markoff cascade, the latter being defined as any multiplying system (physical, biological, etc.) whose growth can be characterized by parameters defining a Markoff process. An example chosen for illustration was the longitudinal development of the nucleon cascade with general source terms and certain simplifying, albeit inessential assumptions.

(1) J. W. Gardner: *Nuovo Cimento*, **16**, 977 (1960). This paper will be designated hereinafter as I.

The method adopted was that of the so-called « last collision equation », which is itself a particular form of the Chapman-Kolmogoroff equation, relating the state of the system at $t+\Delta t$ to the state at t. (Here t is the parameter with respect to which the process develops; conventionally it is referred to as « time » in the mathematical treatment although in physical applications it may be depth, energy, etc.)

General solutions were obtained for the distribution functions p_n and q_n whose definitions are here recapitulated for convenience: $p_n(\eta_1, ..., \eta_n; x)\,\mathrm{d}\eta_1 ... \mathrm{d}\eta_n$ is defined as the differential probability that the postulated source distribution give rise at depth x to n particles with energies in the ranges η_k, $\eta_k + \mathrm{d}\eta_k$ with $k = 1, ..., n$ in any order; $q_n(\eta_1, ..., \eta_n; x)\,\mathrm{d}\eta_1 ... \mathrm{d}\eta_n$ is defined as the differential probability that the postulated source distribution give rise at depth x to n particles with energies specified as above, plus any number of particles with arbitrary energies, including if we wish the same energies specified above.

In addition to p_n and q_n a further function of considerable practical interest was defined, to wit $\varphi_n(\eta; x)$ expressing the probability that the postulated source distribution give rise at depth x to n particles with energies greater than η and any number of particles with energies less than η. Although it was pointed out that the moments of φ_n are simply related to the q_n no equation was established for φ_n itself. This was because the Chapman-Kolmogoroff equations in question apply only to Markoff processes and the function $\varphi_n(\eta; x)$ does not define a Markoff process since the information that there are n particles above energy η at depth x is insufficient to predict the state of the system at $x+\Delta x$.

However, $\varphi_n(\eta; x)$ is still a *stochastic* variable and it will be shown in what follows that it can be extracted from another quantity, the « characteristic functional », which obeys the Chapman-Kolmogoroff equations (*) and which contains in portmanteau form as it were, all the probability relationships associated with the state of the population of particles at a particular value of the parameter t (or x). Whether these probability relationships can be extracted in explicit analytical form from the characteristic functional will depend on the particular application envisaged; in general one must not expect to avoid considerable numerical work with this method, as with other methods of solving the cascade problem, in any but a few mathematically favourable cases. This necessity for extensive computational work appears to be an ineluctable concomitant of the physical nature of the problem. What is claimed, rather, for the characteristic functional is that it provides a convenient means of handling in one package operation any or all of the probability distributions of the

(*) In the present paper we shall use only the first-collision equation satisfied by the characteristic functional; a subsequent publication will extend the discussion to other equations.

cascade, some of which are extremely intractable to handle by other means. From this it also follows that hitherto unsuspected, or at least unformulated, relationships between the various distributions may well be disclosed by the characteristic functional method.

Rather than proceed immediately to the details of the method, it may be to some heuristic and epistemological advantage to review certain other methods of cascade theory which have been used with varying success in their own particular fields. This we do in the next section.

2. – Previous methods.

Each of the distribution functions q_n, p_n and φ_n represents a historically different approach to the cascade problem: the product density q_n is associated primarily with the work of BHABHA ([2]) and of RAMAKRISHNAN ([3]), and the p_n and φ_n with the work of JÁNOSSY ([4,5]), although subsequent developments have of course been made by many authors, see for example the bibliography given by GARDNER *et al.* ([6]).

The Jánossy function p_n, could it be determined, would provide complete information about the longitudinal development of the cascade since it specifies precisely the energies of *all* particles at depth x, arising from a given source distribution. However, just because it contains potentially so much information the function p_n is in general enormously complex, and its diffusion equations can be solved directly in only a very few ideal cases. This led Jánossy to develop and apply to cascade theory the method of regeneration points, already a familiar tool in other contexts to statisticians, see for example the review by BARTLETT *et al.* ([7]). The method uses the following argument: at some point (the « regeneration » point) located in the interval $d\xi$ at depth $x - \xi$ a primary particle undergoes a collision, giving rise to two secondaries (*)

([2]) H. J. BHABHA: *Proc. Roy. Soc.*, A **202**, 301 (1950).

([3]) A. RAMAKRISHNAN: *Proc. Camb. Phil. Soc.*, **46**, 595 (1950); **48**, 451 (1952).

([4]) L. JÁNOSSY: *Proc. Phys. Soc.*, A **63**, 241 (1950).

([5]) L. JÁNOSSY and H. MESSEL: *Proc. Roy. Irish Acad.*, A **54**, 245 (1951).

([6]) J. W. GARDNER, H. GELLMAN and H. MESSEL: *Nuovo Cimento*, **2**, 58 (1955).

([7]) M. S. BARTLETT *et al.*: *Proc. Camb. Phil. Soc.*, **47**, 65 (1951).

(*) *Note*: (i) As in I, we use the word « collision » only to fix our ideas: the multiplication could occur for example by spontaneous fission, or some other process not involving a collision in the conventional sense.

(ii) One of the « secondaries » is the original primary.

(iii) We neglect ternary and higher order collisions which could however be accommodated by an obvious extension of the notation.

which become independent primaries of stochastic processes; the first-generation secondaries of these new processes become primaries of further processes, and so on. This argument leads to the following well known first-collision equation for a point-source cascade:

$$(2.1) \qquad \varphi_n(\eta; x) = \sum_{k+m=n} \int_0^x \int_\eta^1 \exp\left[-(x-\xi)\right] \varphi_k(\eta_k; \xi) \varphi_m(\eta_m; \xi) \omega(\eta_k, \eta_m) \, \mathrm{d}\eta_k \, \mathrm{d}\eta_m \, \mathrm{d}\xi ,$$

where $\omega(\eta_k, \eta_m) \, \mathrm{d}\eta_k \, \mathrm{d}\eta_m \, \mathrm{d}\xi$ denotes the appropriately normalized (*) probability for a primary particle of unit energy to have in distance $\mathrm{d}\xi$ a collision resulting in two secondaries with energies in the intervals $\mathrm{d}\eta_k$ at η_k and $\mathrm{d}\eta_m$ at η_m.

Equation (2.1) may be formally solved either directly by means of multiple Mellin-Laplace transforms ([8]), or indirectly using the generating functions introduced by JÁNOSSY ([4,5]).

Despite the fact that φ_n contains only the one energy variable η, contrasted with the n energy variables $\eta_1, \ldots, \eta_n$ of p_n, its practical evaluation is still in general a formidable computational task even with modern automatic equipment. Means of approximating to it have consequently been considered with varying success by a number of authors, a favoured method being an expansion of φ_n in terms of its moments which may be, at least in principle, computed from the product densities q_n. The limitations of this method have been discussed elsewhere by the present autor ([9]): its usefulness is for practical purposes restricted to rather small energy ranges and numbers of particles (n not more than 2 or 3, say).

Summarizing then the results of earlier work on q_n, p_n and φ_n it may be said that while formal solutions have been obtained for all three distributions the numerical evaluation of these solutions is practically limited, with existing computing facilities, to a rather small range of cases. This range may be extended somewhat—usually at a certain cost to accuracy—by employing an expansion of φ_n in terms of its moments.

Naturally the quantities q_n, p_n and φ_n are not independent and for completeness we recapitulate below the well known relations between them, the most widely useful of which is (2.4) expressing the moments of φ_n in terms

(*) The normalisation in (2.1) is such that the Ω defined in (4.10) below is unity. We shall later remove this restriction.

([8]) J. W. GARDNER and H. MESSEL: *Phys. Rev.*, **86**, 808 (1952).

([9]) J. W. GARDNER: *Nuovo Cimento*, **5**, 1368 (1957).

of the q_n,

$$\varphi_n(\eta; x) = \frac{1}{n!}\int_{\eta}^{\infty}\dots\int_{\eta}^{\infty} p_{n+m}(\eta_1, \dots, \eta_n, \eta_{n+1} \dots, \eta_{n+m}; x)\, \mathrm{d}\eta_n \dots \mathrm{d}\eta_1 , \tag{2.2}$$

$$p_n(\eta_1, \dots, \eta_n; x) = \frac{1}{n!} P(n, x)\, q_n(\eta_1, \dots, \eta_n; x) , \tag{2.3}$$

with

$$P(n, x) = \int_{0}^{\infty}\dots\int_{0}^{\infty} p_n(\eta_1, \dots, \eta_n; x)\, \mathrm{d}\eta_n \dots \mathrm{d}\eta_1 , \tag{2.3a}$$

$$T_n(\eta; x) = \int_{\eta}^{\infty}\dots\int_{\eta}^{\infty} q_n(\eta_1, \dots, \eta_n; x)\, \mathrm{d}\eta_n \dots \mathrm{d}\eta_1 , \tag{2.4}$$

where $T_n(\eta; x)$ is the n-th factorial moment of $\varphi_n(\eta; x)$ defined by:

$$T_n(\eta; x) = \sum_{a=0}^{\infty} \frac{(n + a)!}{a!} \varphi_{n+a}(\eta; x) . \tag{2.4a}$$

The above are general mathematical results which are not restricted to any particular cascade model or source distribution; however, in physical applications it is standard practice to express energies as fractions of the highest primary energy, so that the upper integration limits would then be unity rather than infinity.

The remainder of this paper will be devoted to consideration of the characteristic functional as an alternative description of the cascade.

3. – Characteristic functional - general definitions.

The concept of the characteristic *functional* of a distribution is a logical extension of the ideas of the moment-generating function and the characteristic *function*, familiar from standard statistical theory ([10]). We recall first of all the definition of the moment-generating function of some stochastic variable ζ, having a distribution $F(\zeta)$. In terms of some auxiliary variable ν the moment-generating function $M(\nu)$ say, is defined:

$$M(\nu) = E\{\exp[\nu\zeta]\} , \tag{3.1}$$

([10]) See for example: M. G. KENDALL: *Advanced Theory of Statistics* (1955).

where $E\{z\}$ means the expectation value of z. The function $M(\nu)$ always exists; moreover when ν is imaginary, say $i\mu$, the moment-generating function is then a function $c(\mu)$ of the real variable μ. This *characteristic function* $c(\mu)$ is related to the distribution function $F(\zeta)$ by the wellknown formula ([11]):

$$\Delta F(\zeta) = \lim_{L\to\infty} \frac{1}{2\pi} \int_{-L}^{L} \frac{\Delta\{\exp[-i\mu\zeta]\}}{-i\mu} c(\mu)\,\mathrm{d}\mu\,, \tag{3.2}$$

where

$$\Delta y(\zeta) \equiv y(\zeta + h) - y(\zeta) \tag{3.3}$$

for any function y, and where $F(\zeta)$ is assumed continuous at ζ and $\zeta+h$. The n-th derivative (if it exists) of $c(\mu)$ at $\mu = 0$ gives the quantity $i^n E\{\zeta^n\}$.

It is possible to generalize $c(\mu)$ by replacing the argument μ by the product-sum:

$$\sum_j R_j \Gamma_j\,, \tag{3.4}$$

where the R_j are values of any random variable extracted from the stochastic process $\zeta(t)$ and the Γ_j are corresponding values of some arbitrary function $\Gamma(t)$. In practical applications Γ would be chosen to facilitate the evaluation of whatever parameters of the distribution one is particularly interested in; moreover both ζ and Γ may be—and in practice often are—continuous variables, in which case the product-sum is replaced by the integral $\int R[\zeta(t)]\,\mathrm{d}\Gamma(\zeta)$. The *characteristic functional*, denoted by C, is then defined as $c(\mu)$ with μ replaced by the above integral; it may be considered as an alternative theoretical specification of the stochastic process. While having a less direct interpretation, it is potentially useful as a concise form of definition which moreover lends itself to mathematical manipulations, especially linear transformations or operations on the random function $\zeta(t)$. BARTLETT *et al.* in references ([7]) and ([11]) have discussed the application of characteristic functionals to a variety of stochastic processes, including such disparate examples as the turbulent flow of a fluid and the ageing of a biological population.

We conclude the present section by remarking that the complete characteristic functional with respect to the distribution function $F(\zeta)$ automatically contains all the factorial moments. For the case in which $F(\zeta)$ is a step function, say b for ζ between u and $u+h$ and 0 otherwise, the verification of this statement follows immediately from expanding the exponential in the

([11]) See for example: M. S. BARTLETT: *Stochastic Processes* (Cambridge, 1956).

definition

$$C(\Gamma, t) = E\left\{\exp\left[i\int \Gamma(\zeta)\,\mathrm{d}F(\zeta)\right]\right\}. \tag{3.4}$$

From this result and (2.4) of the preceding section it is clear that the characteristic functional also contains all the product densities q_n, although not necessarily in such a way that they can be explicitly extracted in closed form. We shall revert to this point in the next section.

4. – Application to point-source cascades.

Although the definitions given above permit one immediately to write down the formal expressions for the characteristic functionals of any arbitrary cascade, a better insight into their properties and general usefulness can be obtained by considering first the characteristic functional of a point-source cascade. Let us consider therefore the cascade initiated by a primary particle of unit energy, at depth $x = 0$, and having the multiplication cross-section ω defined in Section **2** above.

The quantity R with respect to which the characteristic functional is taken can in principle, as we saw in Section **3** above, be any random variable of the cascade. For simplicity and definiteness we shall in the present context take it to be the number $N(\eta, x)$ of particles having energies $\geqslant \eta$ at depth x, arising fom the specified primary. Then if $\Gamma(\eta)$ is an arbitrary real function of η the characteristic functional is given by:

$$C\,[\Gamma(\eta), x] = E\left\{\exp\left[i\int_0^1 \Gamma(\eta)\,\mathrm{d}N\,(\eta, t)\right]\right\}. \tag{4.1}$$

We may note at once from the definition (4.1) a relation between C and the p_n defined in Section **1**, *viz*:

$$C[\Gamma, \eta), x] = \frac{1}{n!}\sum_{n=1}^{\infty}\int_0^{\eta}\int_0^{\eta_n}\cdots\int_0^{\eta_2}\exp\,[i\sum_{k=1}^{n}\Gamma(\eta_k)]\cdot p_n(\eta_1, \ldots, \eta_n; x)\,\mathrm{d}\eta_n \ldots \mathrm{d}\eta_1\,. \tag{4.2}$$

As in the case of the relation between C and q_n mentioned above, the value of (4.2) as a means of determining p_n must depend on the distribution law; both relations simplify considerably for the case of a Poisson law. (See for example Bartlett, reference [11], chapter 3).

From C can also be obtained the probability generating function and mo-

ment generating function of the cascade. Thus the probability generating function for the number of particles of energy $\geqslant \eta$ is:

$$G(z, \eta, x) \equiv \sum_{n=0}^{\infty} z^n \varphi_n(\eta, x) = C[\Gamma_z(u), x], \tag{4.3}$$

where

$$\Gamma_z(u) = \begin{cases} \dfrac{1}{i} \ln z & \text{when } u \geqslant \eta, \\ 0 & \text{when } u < \eta. \end{cases} \tag{4.4}$$

The moments of this distribution are given by:

$$U_n(\eta, x) \equiv \bar{N}^k(\eta, x) = \left[\left(-\frac{\partial}{\partial s}\right)^k M(s, \eta, x)\right]_{s=0}, \tag{4.5}$$

where

$$M(s, \eta, x) = G(e^{-s}, \eta, x) = C[\Gamma_s(u), x], \tag{4.6}$$

with

$$i\Gamma_s(u) = \begin{cases} -s & \text{when } u \geqslant \eta, \\ 0 & \text{when } u < \eta. \end{cases} \tag{4.7}$$

Yet another property of the cascade which can be obtained from C is the total energy distribution $\varrho(\eta, x)$, whose Laplace inverse $L(\alpha, x)$ is given by

$$L(\alpha, x) \equiv \int_0^{\infty} \exp[-\alpha\eta]\, \varrho(\eta, x)\, \mathrm{d}\eta = C[\Gamma_\alpha(\eta), x], \tag{4.8}$$

with

$$i\Gamma_\alpha(\eta) = -\alpha\eta. \tag{4.9}$$

The above examples illustrate the usefulness and versatility of the characteristic functional in yielding any distribution of interest connected with the cascade by an appropriate choice of the arbitrary function Γ.

We now proceed to show that the characteristic functional satisfies the first collision equation. Since the auxiliary function Γ does not enter into the ensuing argument, which is quite general, we shall for the remainder of this, section use the abbreviated notation $C(\eta, x)$ for the functional of a cascade initiated by a primary of energy η. Let us consider the change in $C(x)$ in the initial small interval $(0, \Delta x)$. In this interval there is a probability $\omega(\eta_m, \eta_k)\, \mathrm{d}\eta_m\, \mathrm{d}\eta_k\, \Delta x$ for the primary to suffer a collision giving rise to two

secondaries having energies in the intervals $\mathrm{d}\eta_m$ at η_m and $\mathrm{d}\eta_k$ at η_k, with $\eta_m + \eta_k = 1$. The probability for the primary to suffer no collision in Δx is $(1 - \Omega)\,\Delta x$ where, as in I,

$$\Omega = \int_0^1 \omega(\eta_k, \eta_m)\,\mathrm{d}\eta_k + \int_0^1 \omega(\eta_k, \eta_m)\,\mathrm{d}\eta_m = \tag{4.10}$$

$$= 2\int_0^1 \omega(\eta_k, \eta_m)\,\mathrm{d}\eta_k = 2\int_0^1 \omega(\eta_k, \eta_m)\,\mathrm{d}\eta_m\,.$$

Since any secondaries produced in the interval Δx may be regarded as the primaries (with energies η_k, η_m) of two independent cascades, we have:

$$C(1, x) = (1 - \Omega\,\Delta x)\,C(1,\ x - \Delta x) + \Omega\,\Delta x \int_0^1 C(v,\ x - \Delta x)\,\omega(\eta_1\eta_2)\,\mathrm{d}\eta_1\,, \tag{4.11}$$

where v has been written for $1 - \eta_1 - \eta_2$. On dividing throughout by Δx and proceeding to the limit in the usual way we obtain the first collision equation for C, *viz.*:

$$\left(\frac{\partial}{\partial x} + \Omega\right) C(1, x) = \Omega \int_0^1 C(v, x)\,\omega(\eta_1\eta_2)\,\mathrm{d}\eta_1\,. \tag{4.12}$$

The solution of (4.12) will of course depend on the functional form of the cross-section ω, which is assumed to be specified either empirically, or by a suitable mathematical model for the cascade under consideration. It will be convenient to postpone further discussion of the solution of (4.12) until we have set up the corresponding equation for the general-source cascade, and can then discuss the solution of both equations together.

5. – Application to general-source cascades.

As in I we postulate a source function $S(\eta, x)$ representing the probability of a primary particle's being « emitted » with energy η at depth x. Thus, for the case considered in Section 4 of a primary having unit energy at zero depth, $S(\eta, x)$ obviously has the form $\delta(\eta - 1)\,\delta(x)$, where the deltas are Dirac functions. For the cascade having more general source terms there are two alternative methods of setting up the characteristic functional equations. The first and more obvious method is simply a generalization of that given in Section 4, with the auxiliary function redefined to secure consistency with the new boun-

dary conditions. The second method utilizes the fact that in the present one-dimensional treatment the most general source can consist only of point-sources and line sources, and that the latter can be considered as generated by rectilinear motion of the former. We shall consider each of these approaches in turn and discuss their equivalence.

Let us write $\Psi[\chi(\eta), x]$ for the characteristic functional of the cascade arising from the source distribution $S(\eta, x)$; here $\chi(\eta)$ is a new auxiliary function replacing the $\Gamma(\eta)$ of the previous sections: it must obviously satisfy the boundary conditions imposed by $S(\eta, x)$ but is other wise arbitrary. The familiar arguments of the regeneration-point method may now be used to express the change in Ψ in the interval Δx. It must be borne in mind of course, in applying these arguments to the present case that a change in Ψ can arise not only from the primary's undergoing a collision in the interval Δx but from the emission of $\int_0^{\Delta x} (\eta, x)\,\mathrm{d}x$ new « primaries » from the source S. However, this latter possibility can be accomodated, formally at least, by a redefinition of the collision cross-section ω to include particles emitted by S. We shall denote by β this redefined cross-section which may be regarded as an empirically, if not analytically known quantity. Thus $\beta(\eta_k, \eta_m)\,\mathrm{d}\eta_k\,\mathrm{d}\eta_m\,\mathrm{d}x$ denotes the probability for two « secondaries » with energies in the intervals $\mathrm{d}\eta_k$ at η_k and $\mathrm{d}\eta_m$ at η_m to be generated in the depth interval $\mathrm{d}x$ at x, *regardless* of whether these arise from collision of the primary or emission from the source S. By analogy with (4.10) we may also define a total cross-section B thus

$$B = \int_0^\infty \beta(\eta_k, \eta_m)\,\mathrm{d}\eta_k + \int_0^\infty \beta(\eta_k, \eta_m)\,\mathrm{d}\eta_m = 2\int_0^\infty \beta(\eta_k, \eta_m)\,\mathrm{d}\eta_k = 2\int_0^\infty \beta(\eta_k, \eta_m)\,\mathrm{d}\eta_m \,. \tag{5.1}$$

The upper limit of integration, formally taken as infinity above, would in practice be determined by the highest energy of particles emitted by S.

The equation satisfied by Ψ is then, by regeneration-point arguments, found to be:

$$\Psi[\chi(\eta); \eta_0, x] = \int_0^{\eta_0}\int_0^{x} \exp[-B\tau]\,\Psi[\chi(\eta); \eta_1, x-\tau]\,\beta(\eta_1, \eta_2)\,\mathrm{d}\eta_1\,\mathrm{d}\tau \,. \tag{5.2}$$

If we now differentiate this equation with respect to x, at the same time suppressing the auxiliary function and defining our energy scale so that the maximum energy η_0 is taken as unity, equation (5.2) becomes

$$\left(\frac{\partial}{\partial x} + B\right)\Psi(1, x) = B\int_0^1 \Psi(v, x)\,\beta(\eta_1, \eta_2)\,\mathrm{d}\eta_1 \,, \tag{5.3}$$

which compares with equation (4.12) for the point-source cascade, showing that the characteristic functional satisfies the same type of first-collision equation in either case.

We now proceed to the alternative approach in which the extended source S is supposed to be generated by the motion of a point source, Q, say. This latter must have a certain probability, P, say, to emit in a small interval Δx a primary particle of given energy which will then originate a point source cascade, described by a characteristics functional C as in Section 4 above. In general P will be a function of the energy η of the emitted primary, and of the depth x; in fact it is immediately apparent that it is only necessary to identify $P(\eta, x)$ with $S(\eta, x)$ to ensure that the moving point-source Q fully reproduces the cascade of the stationary extended-source S. (Things would not be so simple of course if we were concerned with the temporal as well as the spatial development of the cascade, but that is outside the scope of the present paper.)

As before, we consider the variation of $\Psi[x]$ in the interval Δx. There is a probability $1 - W(x)\,\Delta x$ that Q emit no primary in the interval Δx, where

$$W(x) = \int_0^\infty S(\eta, x)\,\mathrm{d}\eta\ ; \tag{5.4}$$

and there is a probability $S(\eta, x)\,\mathrm{d}\eta \cdot \Delta x$ that it emit a primary in the energy interval $\mathrm{d}\eta$ at η, in the detph interval Δx. Such a primary can then initiate an independent point-source cascade whose characteristic functional at depth x is $C[\eta, x]$. Hence

$$\Psi(x) = [1 - W(x)\,\Delta x]\,\Psi[x - \Delta x] + \\ + W(x)\,\Delta x\,\Psi[x - \Delta x]\int_0^\infty C(\eta, x - \Delta x)\,S(\eta, x)\,\mathrm{d}\eta\ . \tag{5.5}$$

The upper limit on the energy integral is replaced by unity if we use the same energy scale as in (5.3), and it then follows from (5.5) that $\Psi[x]$ satisfies the first-collision equation

$$\left[\frac{\partial}{\partial x} + W(x)\right]\Psi[x] = W(x)\int_0^1 C[\eta, x]\,S(\eta, x)\,\mathrm{d}\eta\ . \tag{5.6}$$

Equations (5.3) and (5.6) will be equivalent if the auxiliary function $\chi(\eta)$ in $\Psi[\chi(\eta), x]$ is appropriately chosen; in fact these equations may be regarded as defininig a relation between χ and C for the cascade in question.

The solution of (4.12), (5.3) and (5.6) will be discussed in the next section, and some applications considered.

6. – Solutions and discussion.

As has already been mentioned the methods to be used for solving integro-differential equations such as (4.12), (5.3) and (5.6) will be selected in the light of the analytical or empirical forms of the functions ω and S, which are assumed to be known. In view or this it would scarcely be profitable to proceed further with our (hitherto) completely general discussion, leaving ω and S unspecified. We shall first of all therefore suppose ω and S to be such that known functions $K(\eta, x)$ and $H(\eta, x)$ can be found to satisfy

$$K(\eta, x) = \int_0^{\eta} C[\eta - u, x]\, \omega(u, \eta)\, \mathrm{d}u\,, \tag{6.1}$$

and

$$H(\eta, x) = \int_0^{\eta_0} \Psi[\eta - u, x]\, \beta(u, \eta)\, \mathrm{d}u\,.$$

Thus, for example, in the ionization cascade discussed in I and elsewhere [12-14] if $C[\eta, x]$ is known for $\eta < kI_0$, where k is an integer and I_0 is the ionization potential, $K(\eta, x)$ for given x is known as a function of η in the range $kI_0 \leqslant \eta < (k+1)I_0$, and hence by iteration in the range $(k+1)I_0 \leqslant \eta < (k+2)I_0$, and so on.

Assuming then that $K(\eta, x)$ and $H(\eta, x)$ are available in analytic or tabular form the solutions of (4.12) and (5.3) for the specified initial conditions can be written respectively:,

$$C[\eta, x] = \exp[i\Gamma(\eta) - \Omega(\eta)x] + \Omega(\eta)\int_0^x \exp[-\Omega(\eta)[x-\tau]]K(\eta, \tau)\, \mathrm{d}\tau; \tag{6.3}$$

$$\Psi[\eta, x] = \exp[i\chi(\eta) - B(\eta)x] + B(\eta)\int_0^x \exp[-B(\eta)[x-\tau]]H(\eta, \tau)\, \mathrm{d}\tau\,. \tag{6.4}$$

To express the solution of (5.6) it is convenient to define a function $Y(\eta, x)$ as follows:

$$Y(\eta, x) = \int_0^{\eta} C[u, x]\, S(u, x)\, \mathrm{d}u\,. \tag{6.5}$$

(12) J. W. Gardner: *Phys. Rev.*, **94**, 764 (1954).
(13) J. W. Gardner: *Proc. Phys. Soc.*, A **68**, 1072 (1955).
(14) J. E. Moyal: *Nucl. Phys.*, **1**, 180 (1956).

2124

Then, for the same initial conditions as applied above to (6.4), the solution of (5.6) is

$$\Psi[\eta, x] = \exp\left[W(x)\int_0^x [Y(\eta, \tau) - 1]\,\mathrm{d}\tau\right]. \tag{6.6}$$

The use of expression (6.6) to compute Ψ requires Y, and hence C, to be known. In other words, one must in this case solve the point source cascade first and then feed the solution into the general-source cascade equations. This would seem a tiresome procedure if one were interested only in the general-source cascade and one might try to avoid the computation of C by using the expression (6.4) for Ψ. Naturally both (6.4) and (6.6) must give the same ultimate answer and since the latter depends on C so, somehow, must the former. As we saw in the previous section this dependence enters in (6.4) via the choice of the auxiliary function χ. In principle χ can always be obtained if we know C; in practice χ can often be much more expeditiously obtained by applying simple trial and error procedure to a few likely-looking functions. If χ cannot be obtained by trial and error then the computation of C cannot be avoided, and if one has C computed it is probably better to proceed via formula (6.6) for the computation of Ψ.

7. – Conclusion.

We conclude with a few remarks about other forms in which the characteristic-functional method might be applied to cascade theory. In the definition of Section 3 above the R_j occurring in the product sum $\sum_j R_j \Gamma_j$ are values of any random variable extracted from the stochastic process $\zeta(t)$. For the applications considered in this paper we have taken R to be continuous and have in fact replaced it by the average-number distribution. It would however have been perfectly legitimate mathematically to replace it by any other distribution, continuous or discrete, extracted from the random variable $\zeta(t)$; one could for example define the characteristic functional with respect to any of the distributions p_n, q_n, φ_n introduced in Section 1. It might well be asked of course, in view of the complexity of these functions themselves, whether a characteristic functional so constructed would be of any value for the practical computation of quantities of physical interest. It has already been remarked that p_n, could it be determined, would give all the physical information about a cascade, but that this very fact means that p_n must be an enormously complicated function. Would not this same limitation apply also to the characteristic functional constructed from p_n? Not necessarily: the virtue of the characteristic functional method is that one can often choose the auxiliary

function I in such a way as to suppress parameters not of immediate interest, leaving a relatively simple, or at least computable expression in the others.

It should also be remarked that in the present paper we have concentrated on the first-collision equations satisfied by the characteristic functional. These equations correspond to the Chapman-Kolmogoroff equations relating the state of the system at time Δt to its state at time zero. For the applications discussed in Sections 4-6 above this seemed the most direct and useful approach; for other applications some other forms of the equation satisfied by the characteristic functional might be preferable.

It is hoped to publish in a subsequent paper a more detailed development of the alternative forms of the characteristic-functional method adumbrated in this section.

* * *

The author is indebted to Dr. J. Bunbury for valuable discussion, and to The English Electric Co., Ltd., for permission to publish.

RIASSUNTO (*)

In uno scritto precedente si sviluppava e si applicava ad esempi tratti dalla radiazione cosmica e dalla teoria dei reattori nucleari, il trattamento dell'equazione della ultima collisione. Il presente scritto dà, in alternativa al precedente, un altro metodo di affrontare il problema a mezzo del funzionale caratteristico, il quale ultimo viene introdotto come un'estensione logica del concetto di funzione generatrice di impulso. Potenzialmente il funzionale caratteristico contiene informazioni complete su tutte le relazioni di probabilità del processo stocastico in questione, in pratica il ricavare informazioni su una distribuzione particolare dipende da una opportuna scelta della funzione ausiliaria arbitraria presente nella definizione del funzionale caratteristico. Le possibilità e la versatilità del metodo sono illustrate facendo riferimento a cascate sia con sorgente puntiforme sia con sorgente estesa; esso è particolarmente adatto al trattamento di cascate con sorgenti lineari, come per esempio, in ordine decrescente di energia: un getto nucleare ad alta energia; la traccia di una particella ionizzante; la rappresentazione di sorgente nel metodo Feinberg-Galanin per la teoria dei reattori nucleari.

(*) *Traduzione a cura della Redazione.*

Production of Bremsstrahlung by Longitudinally Polarized Electron-Proton Collisions.

Sasabindu Sarkar

Department of Theoretical Physics,
Indian Association for the Cultivation of Science - Jadavpur, Calcutta

(ricevuto il 6 Aprile 1960)

Summary. — The purpose of this paper is to calculate the differential cross section for the production of bremsstrahlung in the high energy collisions of longitudinally polarized electrons and protons considering the effect of the anomalous magnetic moment and the recoil of the proton. We have neglected the matrix element for the bremsstrahlung of the proton and so our formula will be valid when the angle between the directions of the electron and the photon will be of the order of mc/p (m and p being the mass and momentum of the electron respectively).

1. – Introduction.

In this paper we intend to calculate the cross-section of radiative collisions between a longitudinally polarized electron and a nucleon polarized in the same or opposite direction. Several authors, *e.g.* Bincer [1], Ford, Mullin [2] and Scofield [3] have investigated different cases of the differential cross-section of scattering of two polarized fermions. The effects of polarization in the case of bremsstrahlung production becomes important when the kinetic energy of the recoil proton is comparable to its rest energy. Rzewuski [4], Drell [5], Berg and Lindner [6] have studied high energy electron proton bremsstrahlung. In our case there will be two matrix elements one of which

(1) A. M. Bincer: *Phys. Rev.*, **107**, 1467 (1957).
(2) G. W. Ford and C. I. Mullin: *Phys. Rev.*, **108**, 477 (1957); **110**, 1485 (E) (1958).
(3) J. H. Scofield: *Phys. Rev.*, **113**, 1599 (1959).
(4) J. Rzewuski: *Acta Phys. Pol.*, **9**, 121 (1948).
(5) S. D. Drell: *Phys. Rev.*, **87**, 753 (1952).
(6) R. A. Berg and C. N. Lindner: *Phys. Rev.*, **112**, 2072 (1958).

corresponds to the radiation emitted by the electron (M_{I}) and the other by the proton (M_{II}). There is a sharp rise in the value of the differential cross-section of ultra relativistic energy of the electron when the bremsstrahlung photon emerges nearly parallel to either the incident or the final electron. It can be shown that when the angle of emergence is of the order of mc/p (m and p being electron mass and momentum respectively), and the electron energy is of the order of the rest energy of the proton (Mc^2), the contribution to the differential cross-section from $|M_{\text{II}}|^2$ and that from the product of M_{I} and M_{II} is smaller than that from $|M_{\text{II}}|^2$ by factors of the order of $(m/M)^2$ and m/M respectively as observed by RZEWUSKI ([4]). We have considered only M_{I} and so our formula for the differential cross-section is valid when the emerging photon makes an angle of the order of mc/p or the kinetic energy acquired by the proton is small compared to its rest energy. The formula for the differential cross-section can be verified by coincidence experiments. The formula for the total cross-section obtained after integrating the differential cross-section over the momenta of the proton and the photon will be fairly correct because BERG and LINDNER ([6]) have estimated that in their case the product of M_{I} and M_{II} contributes at most 3% to the final integrated cross-section when the maximum of the momentum transferred to the proton is of the order of 500 MeV. In our calculation we have taken into account the effect of the anomalous magnetic moment of the proton which is taken to be g in units of nuclear magneton.

2. – Calculation.

Let $\boldsymbol{p}_0(E_0)$, $\boldsymbol{p}(E)$, $\boldsymbol{k}(k)$ and $\boldsymbol{q} = \boldsymbol{p}_0 - \boldsymbol{p} - \boldsymbol{k}(E_2)$ momenta (the corresponding energies) of the incident electron, final electron, the photon and the recoil proton respectively. For convenience of calculation we introduce unit vectors $\boldsymbol{e}_z$, $\boldsymbol{e}_y$ and $\boldsymbol{e}_x$ in the direction of $\boldsymbol{p}_0$, $\boldsymbol{p}_0 \times \boldsymbol{q}$ and $(\boldsymbol{p}_0 \times \boldsymbol{q}) \times \boldsymbol{p}_0$.

Taking $\sigma_{p_0} = \boldsymbol{\sigma}_0 \cdot \boldsymbol{p}_0 / |\boldsymbol{p}_0|$, the spin projection operator for the initial state of the electron is $\frac{1}{2}(1 + \varepsilon_1 \sigma_{p_0})$ where $\varepsilon_1 = 1$ or -1 according as the electron is polarized in the forward or backward direction. The corresponding operator for the initial state of the proton at rest is taken to be $\frac{1}{2}(1 + \varepsilon_2 \sigma_z)$.

The required differential cross-section $\mathrm{d}\Phi(\varepsilon_1, \varepsilon_2)$ considering the matrix element M_{I} of BERG and LINDNER ([6]) is evaluated in the usual way and is given by (putting $\hbar = c = 1$).

$$(1) \qquad \mathrm{d}\Phi(\varepsilon_1, \varepsilon_2) = \frac{e^6}{8\pi^2} \frac{i'}{p_0 q^4} \left\{ \left(1 + g^2 \frac{E_2 - M}{2M} \right) q_1 + \right.$$

$$\left. + \frac{E_2 - M}{2M} (1 + g)^2 q_2 + \varepsilon_1 \varepsilon_2 (1 + g) \left[\frac{q_x}{M} q_3 + \frac{E_2 - M}{M} (1 + g) q_4 \right] \right\} \int \frac{E_2 \, \mathrm{d}E \, \mathrm{d}\Omega \, \mathrm{d}\Omega_k}{kE_2 - \boldsymbol{k} \cdot \boldsymbol{q}},$$

2425

where

$$\varphi_1 = p_{0l}^2 \frac{4E(E_0-k)+(E_2-M)^2-q^2}{2\Delta_0^2} - p_{0l}p_l \frac{4E_0E+(E_0-E)^2+k^2-q^2}{\Delta_0\Delta} + \\ + k^2\frac{p_{0l}^2+p_l^2}{\Delta\Delta_0} + p_l^2\frac{4E_0(E+k)+(E_2-M)^2-q^2}{2\Delta^2},$$

$$\varphi_2 = (q^2-2m^2)\left(\frac{p_l^2}{\Delta^2} - \frac{2p_{0l}p_l}{\Delta\Delta_0} + \frac{p_{0l}^2}{\Delta_0^2}\right) + k^2\left(\frac{\Delta_0}{\Delta}+\frac{\Delta}{\Delta_0}\right),$$

$$\varphi_3 = -q_x\left(\frac{p_l^2E_0}{\Delta^2} - \frac{p_{0l}p_l(2E_0-k)}{\Delta\Delta_0} + \frac{(E_0-k)p_{0l}^2}{\Delta_0^2}\right) + \frac{k_xq_l}{\Delta_0}\left(\frac{p_lE_0}{\Delta} - \frac{E_0-k}{\Delta_0}p_{0l}\right) + \\ + k\frac{k_x+2p_le_{xl}}{2\Delta}\left(E_0 - \frac{(E_0-k)\Delta-q^2/2}{\Delta_0}\right) + \frac{k_y^2E_0-k^2\Delta_0}{2\Delta_0}\left(\frac{q_x-2e_{xl}q_l}{\Delta_0} - \frac{q_x}{\Delta}\right) - \\ - k\frac{k_x+2e_{xl}p_{0l}+2e_{yl}(\boldsymbol{k}\times\boldsymbol{e}_z)_l}{2\Delta_0}\left(\frac{q^2-2(E_0-k)\Delta}{2\Delta_0}+E_0\right) + \\ + e_{yl}\frac{q_lk_xk_yE_0+p_{0l}kk_yq_x+e_{yl}k^2\Delta_0q_x}{\Delta_0^2},$$

$$\varphi_4 = -\frac{q^2+2k\Delta}{2}\left(\frac{p_l^2}{\Delta^2} - \frac{2p_{0l}p_l}{\Delta\Delta_0} + \frac{p_{0l}^2}{\Delta_0^2} + \frac{(\boldsymbol{k}\times\boldsymbol{e}_z)_l^2}{\Delta_0^2} + \frac{k^2-k_z^2}{2\Delta_0}\left(\frac{1}{\Delta}-\frac{1}{\Delta_0}\right)\right) + \\ + \frac{k_xq_x-k\Delta}{\Delta_0}\left(\frac{p_{0l}p_l}{\Delta} - \frac{p_{0l}^2+p_{0l}e_{yl}k_y+k\Delta_0(e_{yl}^2-\frac{1}{2})}{\Delta_0}\right) + k^2e_{zl}^2 + \\ + \frac{e_{xl}p_{0l}(kk_x\Delta+k_y^2q_x)-p_{0l}q_l(k^2-k_z^2)}{\Delta_0^2} + k\frac{2p_{0l}p_l-k_xq_x-2p_le_{zl}q_z-k\Delta_0}{2\Delta} - \\ - k\frac{p_{0l}^2-p_{0l}e_{zl}(2k_z+q_z)+p_le_{zl}k_z-e_{xl}e_{yl}k_yq_x-k\Delta e_{xl}^2}{\Delta_0},$$

where the suffixes x, y, z and l denote the components of the quantities in the direction of $\boldsymbol{e}_y$, $\boldsymbol{e}_x$, $\boldsymbol{e}_z$ and the polarization vector of the photon respectively. If we do not want to observe the polarization of the photon we have to sum the above expression over all its states of polarization. In the eq. (1) $\Delta = (kE-\boldsymbol{k}\cdot\boldsymbol{p})/k$, $\Delta_0 = (kE_0-\boldsymbol{k}\cdot\boldsymbol{p}_0)/k$, $\mathrm{d}\Omega$ and $\mathrm{d}\Omega_k$ are the elements of solid angles about the directions of $\boldsymbol{p}$ and $\boldsymbol{k}$.

The expression (1) clearly shows that the effect of polarization increases with q/M.

The above expression can be simplified by taking $\boldsymbol{p}_0$, $\boldsymbol{p}$, $\boldsymbol{k}$ and the polarization vector of the photon to be observed to be in the same plane, then terms involving k_y, $e_{yl}p_l$, $e_{yl}p_{0l}$, $e_{yl}e_{xl}$, e_{yl}^2, $e_{yl}(k\times e_z)_l$ will all vanish.

When the angle between $\boldsymbol{p}$ and $\boldsymbol{k}$ is of the order of m/p, the expression (1) can be put in the following simple form

$$(2)\quad \mathrm{d}\Phi(\varepsilon_1,\varepsilon_2)\approx\frac{e^6}{8\pi^2}\frac{p}{p_0q^4}\frac{p_l^2}{\Delta^2}\left\{\left(1+g^2\frac{E_2-M}{2M}\right)(4E_0(E+k)+(E_2-M)^2-q^2)/2+\right.$$
$$\left.+\frac{E_2-M}{2M}(1+g)^2q^2-\frac{\varepsilon_1\varepsilon_2}{M}(1+g)\,(q_x^2E_0+(1+g)(E_2-M)q^2/2)\right\}\frac{E_2\,\mathrm{d}E\,\mathrm{d}\Omega\,\mathrm{d}\Omega_k}{kE_2-\boldsymbol{k}\cdot\boldsymbol{q}}\,.$$

Further for $E_0=M$, $k=1$ MeV, the angle between $\boldsymbol{p}$ and $\boldsymbol{k}$ is of the order of m/p, $\boldsymbol{p}\perp\boldsymbol{p}_0$ and $1+g=2.793\,4\pm0.000\,3$

$$\frac{\mathrm{d}\Phi_p}{\mathrm{d}\Phi_a}=0.031\,5\qquad\text{using eq. (2)}$$

where suffixes p and a correspond to cases where the spins of the proton and electron in the initial state are parallel and antiparallel respectively.

When q is small compared to M, $k\ll1$ MeV and the angle between photon and the electron (both initial and final) is not necessarily small, expression (1) can also be put in the following simple form

$$(3)\quad \mathrm{d}\Phi(\varepsilon_1,\varepsilon_2)\approx\frac{e^6}{8\pi^2}\frac{p}{p_0q^4}\left(\frac{p_{0l}^2}{\Delta_0^2}-\frac{2p_{0l}p_l}{\Delta\Delta_0}+\frac{p_l^2}{\Delta^2}\right)\left\{\left(1+g^2\frac{E_2-M}{2M}\right)((E_0+E)^2-q^2)/2+\right.$$
$$\left.+\frac{E_2-M}{2M}q^2(1+g)^2-\frac{\varepsilon_1\varepsilon_2}{M}(1+g)\,(q_x^2E_0+(1+g)(E_2-M)q^2/2)\right\}\frac{E_2\,\mathrm{d}E\,\mathrm{d}\Omega\,\mathrm{d}\Omega_k}{kE_2-\boldsymbol{k}\cdot\boldsymbol{q}}\,.$$

Finally the formulae (1), (2) and (3) should all be multiplied by the square of the form factor of the proton which is same for both its charge and magnetic moment distribution.

In the experiment of high energy electron-proton scattering some soft photons which escape detection are emitted by electrons which are counted in the experiment as having been elastically scattered, though, actually, they are not. For this case SCHIFF [7] has given a correction term which is obtained by integrating the differential cross-section for the production of bremsstrahlung over the momenta of soft photons and recoil protons. A similar correction to the experiment of high energy longitudinally polarized electron-proton scattering can be obtained by integrating eqs. (2) and (3).

We find that the radiative and non-radiative scattering in the forward direction is nearly the same for the two cases of the spins being parallel or anti-

---

[7] L. I. SCHIFF: *Phys. Rev.*, **87**, 750 (1952).

2430

parallel, in these cases the influence of the interaction is not much felt. However, the difference between them is most prominent when the influence of the interaction is most felt, *i.e.* the value of the cross-section of the scattering of the electron in the backward direction for the case when the spins are antiparallel is very much larger than when the spins are parallel. From this it appears that the interaction between an electron and a proton is much stronger when the spins are antiparallel than when they are parallel.

* * *

The author is greatly indebted to Professor D. Basu for his constant help and guidance throughout the progress of the work.

RIASSUNTO (*)

Lo scopo di questo lavoro è di calcolare la sezione trasversale differenziale per la produzione di bremsstrahlung nelle collisioni di alta energia di elettroni e protoni polarizzati longitudinalmente, tenendo conto dell'effetto del momento magnetico anomalo e del rinculo del protone. Abbiamo trascurato l'elemento di matrice per la bremsstrahlung del protone e quindi la nostra formula sarà valida quando l'angolo fra le direzioni dell'elettrone e del protone è dell'ordine di mc/p (m e p sono rispettivamente la massa e l'impulso dell'elettrone).

(*) *Traduzione a cura della Redazione.*

IL NUOVO CIMENTO Vol. XVII, N. 2 16 Luglio 1960

Pion Photon Scattering.

M. Gourdin

Faculté des Sciences - Orsay et Bordeaux

A. Martin

CERN, Theoretical Study Division - Geneva

(ricevuto l'8 Aprile 1960)

Summary. — Combining the assumption of a Mandelstam representation with approximate unitarity one can get the pion-photon scattering amplitude in terms of the pion-pion scattering amplitude in even states and of the matrix element forp hotoproduction of pions on pions. In solving this problem attention must be paid to the fact that in the low energy limit this amplitude should become equal to the classical amplitude. With some simplifying assumptions we obtain an expression which contains four quantities: the two pion S-phase shifts, the total cross-section for photoproduction of pions on pions, and the electromagnetic coupling constant. Numerical estimates will be given later. The interest of studying this process lies in its possible influence on the nucleon-photon scattering.

1. – Introduction.

In a preceding paper [1] the authors have studied the reaction $\gamma+\pi\to\pi+\pi$, using the Mandelstam representation and assuming a pion-pion resonance in the $T=1$, $J=1$ pion-pion state. From this reaction amplitude and the pion-pion scattering amplitude in even angular momentum states one can get the amplitude for pion-photon scattering, using again the Mandelstam representation, and neglecting, in the application of unitarity, all the processes other than two-body two-body.

[1] M. Gourdin and A. Martin: *Nuovo Cimento* **16**, 78 (1960). See also: H. S. Wong: *Bull. Am. Phys. Soc.*, **4**, 407 (1959).

The pion-photon scattering amplitude cannot be directly confronted with experiment, but it plays a role in the nucleon-photon scattering, when the photon is scattered by the meson cloud of the nucleon. More precisely, when one tries to apply the Mandelstam technique to the process $\gamma+\mathcal{N}\to\gamma+\mathcal{N}$, one has to know the imaginary part of the reaction amplitude in the channel $\gamma+\gamma\to\mathcal{N}+\bar{\mathcal{N}}$; the lowest intermediate state is, apart from the π_0 giving rise to a pole, the two-pion state. This is the main motivation of the present work. On the other hand, the present problem constitutes a good illustration of the Mandelstam technique where an explicit solution of the equations can be given.

In the body of the paper several simplifying assumptions have been made, but we show in the appendices how one can solve the problems in the general case. First, we only retain the $J=1$ part of the $\gamma+\pi\to\pi+\pi$ amplitude, neglecting contributions from $J\geqslant 3$; second, we neglect the D waves and higher waves in pion-pion scattering, because this is essentially a low energy treatment, and, due to the range of the forces, these waves are expected to be very small. Then it is possible to express the γ-π scattering amplitude in terms of three quantities:

— the electromagnetic coupling constant which enters as a multiplying factor in the low energy limit of the charged scattering amplitude (this limit has to coincide with the Thompson amplitude);

— the total cross-section σ_T for the process $\gamma+\pi\to\pi+\pi$;

— the two S phases of pion-pion scattering in $T=0$ and $T=2$ isospin states.

In the present paper we make no attempt to replace these quantities by numbers. We feel that for the moment it is not really worthwhile. One could in principle use the figures proposed by FRAZER and FULCO [2] in the $T=1$ $J=1$ pion-pion state, which gives, up to a factor, σ_T, and try to estimate the $T=0.2$, $J=0$ pion-pion amplitudes by inserting the $T=1$, $J=1$ data in the Chew-Mandelstam [3] or Cini and Fubini [4] equations for the pion-pion scattering. This will be done later.

2. – Structure of the matrix elements.

We define p_1 p_2 as the incoming four momenta of the pions, k_1 k_2 as the coming momenta of the photons with polarizations e_1 and e_2. The relevant

(2) W. FRAZER and J. FULCO: UCRL 8880, to be published.
(3) G. F. CHEW and S. MANDELSTAM: UCRL 8728, to be published.
(4) M. CINI and S. FUBINI: to be published in *Ann. of Phys.*

channels are indicated in Fig. 1. We introduce the three invariants:

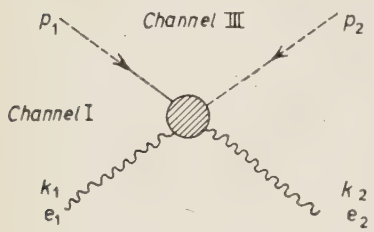

Fig. 1.

$$(1)\qquad \begin{cases} s_1 = -(k_1+p_1)^2 = -(k_2+p_2)^2\,, \\ s_2 = -(k_1+p_2)^2 = -(k_2+p_1)^2\,, \\ t = -(k_1+k_2)^2 = -(p_1+p_2)^2\,, \end{cases}$$

with, on the mass shell:

$$(2)\qquad s_1+s_2+t = 2\mu^2\,,$$

where μ is the pion mass.

Due to energy momentum conservation all the quantities can be expressed in terms of three four-vectors: k_1, k_2 and $\Delta = p_2 - p_1$.

The matrix element $e_{1\mu}\, e_{2\nu}\, M_{\mu\nu}\,(k_1, k_2, \Delta)$ must fulfil the gauge invariance condition which can be expressed as well known by the following necessary requirements:

$$k_{1\mu} M_{\mu\nu} = 0 \qquad \text{and} \qquad k_{2\nu} M_{\mu\nu} = 0\,.$$

If we retain only the terms giving non vanishing contributions we can write the matrix element Φ as

$$(3)\qquad \Phi(e_1, e_2; k_1, k_2, \Delta) \equiv D_\alpha(s_1, s_2, t) I_\alpha + D_\beta(s_1, s_2, t) I_\beta\,,$$

where the two invariants I_α and I_β are given by:

$$(4)\qquad \begin{cases} I_\alpha = (e_1\cdot e_2) - \dfrac{(e_1\cdot k_2)(e_2\cdot k_1)}{k_1\cdot k_2}\,, \\ I_\beta = (e_1\cdot\Delta)(e_2\cdot\Delta)(k_1\cdot k_2) - (e_1\cdot k_2)(e_2\cdot\Delta)(k_1\cdot\Delta) - \\ \qquad - (e_1\cdot\Delta)(e_2\cdot k_1)(k_2\cdot\Delta) + \dfrac{(e_1\cdot k_2)(e_2\cdot k_1)(k_1\cdot\Delta)(k_2\cdot\Delta)}{(k_1\cdot k_2)}\,. \end{cases}$$

With the above notations the S-matrix element has the form

$$(5)\qquad \langle f|S|i\rangle = \frac{1}{4(2\pi)^2}\,\frac{1}{[k_1^0 k_2^0 p_1^0 p_2^0]^{\frac{1}{2}}}\,\delta_4(p_1+p_2+k_1+k_2)\Phi,$$

and we obtain for the differential cross-section $\gamma+\pi\to\gamma+\pi$ in the centre of mass system:

$$(6)\qquad \frac{\mathrm{d}\sigma}{\mathrm{d}\Omega} = \frac{1}{s_1}\left|\frac{\Phi}{8\pi}\right|^2.$$

2434

We notice that I_1 and I_2 are invariant in the exchange $p_1 \leftrightarrow p_2$, *i.e.* $\Delta \to -\Delta$. The matrix element Φ must be even in Δ by crossing property. It follows that D_α and D_β are symmetrical functions of s_1 and s_2. Then it is easy to see that in channel III only even angular momentum states of the pion-pion system are permissible; therefore the isotopic $T=1$ state is forbidden. Hence the two photons currents appearing in the matrix element are either both isoscalars or both isovectors.

Let us call Φ_C and Φ_N the matrix elements for the Compton effects on charged and neutral pions (by charge conjugation one sees that there is no difference between π^+ and π^-). The pions being in the $T=0$ and $T=2$ isotopic states, the corresponding reactions amplitudes are:

$$(7) \qquad \begin{cases} \Phi_0 = \dfrac{1}{\sqrt{3}}(2\Phi_C + \Phi_N) - \dfrac{2}{\sqrt{3}} F\,, \\ \Phi_2 = \sqrt{\tfrac{2}{3}}(\Phi_C - \Phi_N) = \sqrt{\tfrac{2}{3}} F_2\,. \end{cases}$$

Conversely $\Phi_N = \frac{2}{3}(F_0 - F_2)$ and $\Phi_C = \frac{1}{3}(2F_0 + F_2)$.

Let us now compute the matrix element Φ_C in the Born approximation. The three contributions indicated on Fig. 2 cannot be treated separately because of gauge invariance.

We find for the two functions D_1 and D_2 the following contributions:

Fig. 2.

$$(8) \qquad D_\alpha^B = 2e^2\,, \qquad D_\beta^B(s_1, s_2) = \frac{2e^2}{(s_1 - \mu^2)(s_2 - \mu^2)}\,,$$

where e is the rationalized electromagnetic coupling constant.

3. – Kinematics in the various channels.

Because of the crossing properties one has only to consider two independent channels (see Fig. 1).

3·1. *Channel I.* – If $\boldsymbol{k}$ and $\boldsymbol{k}'$ are momenta of the pions in the centre of mass system, the three invariants are given by:

$$(9) \qquad \begin{cases} s_1 = (k + \omega_k)^2\,, \\ s_2 = \mu^2 - 2k\omega_k - 2k^2\cos\theta\,, \\ t = -2k^2(1 - \cos\theta)\,, \end{cases}$$

where θ is the scattering angle.

Then

$$(10)\qquad \begin{cases} k^2 = \dfrac{(s_1-\mu^2)^2}{4s_1}\,, \\ \cos\theta = 1+\dfrac{2s_1 t}{(s_1-\mu^2)^2}\,. \end{cases}$$

If we choose the gauge to eliminate longitudinal photons we get the following expressions for I_α and I_β

$$(11)\qquad \begin{cases} I_\alpha = \boldsymbol{e}_1\cdot\boldsymbol{e}_2 - \dfrac{2}{t}\,(\boldsymbol{e}_1\cdot\boldsymbol{k}_1)(\boldsymbol{e}_2\cdot\boldsymbol{k})\,, \\ I_\beta = -\dfrac{2}{t}\,(s_1-\mu^2)^2(\boldsymbol{e}_1\cdot\boldsymbol{k}')(\boldsymbol{e}_2\cdot\boldsymbol{k})\,. \end{cases}$$

In spite of the presence of t in the denominators the invariants I_α and I_β are bounded in the limit $t\to 0$. In this limit $\boldsymbol{k}=\boldsymbol{k}'$; so $\boldsymbol{e}_1$ becomes orthogonal to $\boldsymbol{k}'$ and $\boldsymbol{e}_2$ to $\boldsymbol{k}$. In addition, it is easy to see that in the limit of zero energy, only I_α is non vanishing while I_β behaves like k^2.

3·2. *Channel III.* – $\boldsymbol{p}$ and $-\boldsymbol{p}$ are the photon momenta, $\boldsymbol{q}$ and $-\boldsymbol{q}$ the momenta; then the invariants take the form:

$$(12)\qquad \begin{cases} s_1 = -(q^2+\omega_q^2+2q\omega_q\cos\varphi)\,, \\ s_2 = -(q^2+\omega_q^2-2q\omega_q\cos\varphi)\,, \\ t = 4p^2 = 4\omega_q^2\,. \end{cases}$$

The pion-photon angle, φ, is given by:

$$(13)\qquad \cos\varphi = \frac{s_2-s_1}{[t(t-4\mu^2)]^{\frac{1}{2}}}\,,$$

and I_α and I_β can be written for transverse photons:

$$(14)\qquad \begin{cases} I_\alpha = \boldsymbol{e}_1\cdot\boldsymbol{e}_2\,, \\ I_\beta = 2t(\boldsymbol{e}_1\cdot\boldsymbol{q})(\boldsymbol{e}_2\cdot\boldsymbol{q})\,. \end{cases}$$

2436

4. – Mandelstam representation.

We assume for $D_\alpha(s_1, s_2)$ and $D_\beta(s_1, s_2, t)$ a Mandelstam representation:

$$(15)\qquad D_i(s_1, s_2, t) = D_i^B + \frac{1}{\pi}\iint \frac{\varrho_i(s_1', s_2')}{(s_1' - s_2)(s_2' - s_2)}\,\mathrm{d}s_1'\,\mathrm{d}s_2' + \\ + \frac{1}{\pi}\iint \frac{\sigma_i(s_1' \cdot t')}{(s_1' - s_1)(t' - t)}\,\mathrm{d}s_1'\,\mathrm{d}t' + \frac{1}{\pi}\iint \frac{\sigma_i(s_2', t')}{(s_2' - s_2)(t' - t)}\,\mathrm{d}s_2'\,\mathrm{d}t' \qquad i = \alpha, \beta\,.$$

Let us first consider the case of two isoscalar photons. It can be easily seen that the variables of integrations s_1' and s_2' or s' and t' cannot reach simultaneously their lower limit. More precisely if $(2\mu)^2 \leqslant s_1' \leqslant (4\mu)^2$ one has $s_2' \geqslant (4\mu)^2$, and conversely; the same result holds for s' and t'. So the Cini and Fubini technique can be applied ([4]), and we introduce unidimensional representations.

The situation is not the same for isovector photons. One can just say that the integration domains are limited by

$$s_1' \geqslant (3\mu)^2\,, \qquad s_2' \geqslant (3\mu)^2\,, \qquad t' \geqslant (2\mu)^2\,.$$

The weak dependence on s_1 and s_2 will be completely neglected. As will become clear later it is impossible to take this dependence into account as long as nothing is known on the reaction $\gamma + \pi \to \pi + \pi + \pi$.

The amplitude Φ_0 involves both isoscalar and isovector photons but Φ_2 corresponds only to isovector photons.

Under these assumptions one can write generally

$$(16)\qquad D(s_1, s_2, t) = D^B + \sum_n (s_1 - \mu^2)^{2n} P_n\left[1 + \frac{2s_1 t}{(s_1 - \mu^2)^2}\right] a^{(n)}(s_1) + \\ + \mathrm{Sym}\,(s_1 \to s_2) + \sum_n [t(t - 4\mu^2)]^n P_{2n}\left[\frac{s_2 - s_1}{[t(t - 4\mu^2)]^{\frac{1}{2}}}\right] b^{(n)}(t)\,,$$

where P_n is the ordinary Legendre polynomial.

This corresponds to a partial wave expansion in the various channels (see formulas (10) and (13)).

We assume for $a^{(n)}$ and $b^{(n)}$ a spectral representation

$$(16')\qquad \begin{cases} a^{(n)}(s) = \dfrac{1}{\pi}\displaystyle\int_{(2\mu)^2}^{\infty} \frac{\sigma^{(n)}(x)\,\mathrm{d}x}{x - s} & \text{for the } T = 0 \text{ amplitude}\,, \\ a^{(n)}(s) = 0 & \text{for the } T = 2 \text{ amplitude}\,, \\ b_T^{(n)}(t) = \dfrac{1}{\pi}\displaystyle\int_{(2\mu)^2}^{\infty} \frac{\tau_T^{(n)}(y)\,\mathrm{d}y}{y - t}\,. \end{cases}$$

The convergence of the integrals will be studied later. The low energy limits of D_α and D_β must, in addition, satisfy certain requirements [5] which will be taken into account later.

5. – Unitarity in Channel I.

In this Section we shall only be concerned with the F_0 amplitude. In channel I, F_0 is given by:

$$(17)\quad F_0 = (\boldsymbol{e}_1\cdot\boldsymbol{e}_2)D_{\alpha 0} + \frac{1}{k^2(1-\cos\theta)}(\boldsymbol{e}_1\cdot\boldsymbol{k}')(\boldsymbol{e}_2\cdot\boldsymbol{k}_2)[D_{\alpha 0} + 4k^2(k+\omega_k)^2 D_{\beta 0}]\,.$$

Application of the unitarity condition enables us to determine the imaginary part of this amplitude:

$$(18)\quad \operatorname{Im}\langle\gamma\pi|T|\gamma\pi\rangle = \sum_{(n)}\langle\gamma\pi|T|n\rangle\langle n|T^*|\gamma\pi\rangle\,.$$

The only intermediate state we retain is the two-pion state, because we are interested into an energy domain where s_1 is less than $(3\mu)^2$. The $\gamma+\pi\to\pi+\pi$ amplitude has been calculated in a preceding paper [1]. The structure of this matrix element is

$$(19)\quad M_{fi} = \frac{1}{(2\pi)^6}\frac{1}{4\omega_q(k\omega_k)^{\frac{1}{2}}}(\boldsymbol{e},\,\boldsymbol{k},\,\boldsymbol{q})H[k^2,\,(\boldsymbol{k}\cdot\boldsymbol{q}^2)]\,,$$

where $\boldsymbol{k}$ is the photon momentum and $\boldsymbol{q}$ the outgoing pion momentum in the centre of mass system. If one assumes that the reaction mainly occurs in the $T=1$, $J=1$ state, H does not depend on the angles (this approximation was done in [1]). Under this assumption the imaginary part of the $\gamma\pi\to\gamma\pi$ amplitude can be related to the total cross-section σ_T for $\gamma\pi\to\pi\pi$:

$$(20)\quad \operatorname{Im} F_0 = \frac{2(k+\omega_k)}{k}(\boldsymbol{e}_1\times\boldsymbol{k})\cdot(\boldsymbol{e}_2\times\boldsymbol{k}')\sigma_T\,,$$

with

$$\sigma_T = \frac{1}{48\pi}\frac{kq^3}{(k+\omega_k)^2}\,|H(k^2)|^2\,,$$

---

[5] M. GELL-MANN and M. L. GOLDBERGER: *Phys. Rev.*, **96**, 1433 (1954); M. GELL-MANN and V. GLASER: private communications.

2438

where $2\omega_q = k + \omega_k$. By comparison of formulae (17) and (20) one gets:

$$(21) \qquad \begin{cases} \operatorname{Im} D_{\alpha 0} = 2k(k+\omega_k)\cos\theta\,\sigma_T\,, \\ \operatorname{Im} D_{\beta 0} = -\dfrac{\sigma_T}{2k(k+\omega_k)}\,. \end{cases}$$

These formulae could have been obtained by use of the « optical » theorem.

The more general case where H possesses an angular dependence is considered in Appendix I.

If we return to formula (16) for functions D, the knowledge of (21) gives the values of the weight functions $\sigma^{(n)}$. Then one can write D_α and D_β as:

$$(22) \qquad \begin{cases} D_i(s_1 s_2 t) = D_i^B(s_1 s_2) + C_i(s_1 t) + C_i(s_2 t) + \\ \qquad\qquad + \sum_n [t(t-4\mu^2)]^n P_{2n}\left[\dfrac{s_2 - s_1}{\sqrt{t(t-4\mu^2)}}\right] b^{(n)}(t)\,, \qquad i = \alpha, \beta, \\ C_{\alpha 0}(s,t) = [2st + (s-\mu^2)^2]\,\dfrac{1}{\pi}\displaystyle\int_{(2\mu)^2}^{\infty} \frac{\sigma_T(x)\,\mathrm{d}x}{(x-\mu^2)(x-s)}\,, \\ C_{\beta 0}(s) = -\dfrac{1}{\pi}\displaystyle\int_{(2\mu)^2}^{\infty} \frac{\sigma_T(x)\,\mathrm{d}x}{(x-\mu^2)(x-s)}\,. \end{cases}$$

6. – Unitarity in Channel III.

In this channel the unitarity condition connects the reaction amplitude $\gamma+\gamma \to \pi+\pi$ to pion-pion scattering. Only even angular momenta are present, and we shall provisionally assume that the D-waves (and higher waves) of the pion-pion scattering can be neglected (the general case will be considered in Appendix II). The first invariant I_1 is isotropic but I_2 contains both S and D parts. Therefore, if $\operatorname{Im} D_2$ is non vanishing in channel III the $J \neq 0$ amplitudes have a non vanishing imaginary part in contradiction with the above assumption. It follows that all the functions appearing in D_β are zero and that in D_α the only non vanishing weight function, $\tau^{(0)}$ is proportional to the $J=0$ pion-pion scattering amplitude. We now extract the S part of F both in $T=0$ and $T=2$ states:

$$(23) \qquad (\boldsymbol{e}_1 \cdot \boldsymbol{e}_2) F^S_{0,2}(q^2) = \frac{1}{4\pi}\int F_{0,2}(\boldsymbol{e}_1;\, \boldsymbol{e}_2;\, \boldsymbol{q})\,\mathrm{d}\Omega_q\,.$$

Then, for $T=0$ or 2:

$$(24) \qquad \operatorname{Im} F^S_T(q^2) = \tau^{(0)}_T(4\omega_q^2) = F^{S}_{T}(q^2)\, h^{s*}_T(q^2)\,.$$

$h_T^s(q^2) = \exp[i\delta_T^s] \sin \delta_T^s$ is the pion-pion scattering amplitude for $J = 0$ and $T = 0$ or 2.

7. – Low energy requirements.

From the above equations we finally get the following representations:

$$(25)\quad D_{\alpha 0}(s_1; s_2; t) = D_\alpha^B(s_1; s_2) + [2s_1 t + (s_1 - \mu^2)^2] \frac{1}{\pi} \int_{(2\mu)^2}^{\infty} \frac{\sigma_T(x)\,dx}{(x-\mu^2)(x-s_1)} +$$

$$+ [2s_2 t + (s_2 - \mu^2)^2] \frac{1}{\pi} \int_{(2\mu)^2}^{\infty} \frac{\sigma_T(x)\,dx}{(x-\mu^2)(x-s_2)} + \frac{4}{\pi} \int_0^{\infty} \frac{F_0^S(q^2) h_0^{S*}(q^2)\,dq^2}{4(\mu^2+q^2) - t} ,$$

$$(26)\quad D_{\beta 0}(s_1; s_2; t) = D_\beta^B(s_1; s_2) - \frac{1}{\pi} \int_{(2\mu)^2}^{\infty} \frac{\sigma_T(x)\,dx}{(x-\mu^2)(x-s_1)} - \frac{1}{\pi} \int_{(2\mu)^2}^{\infty} \frac{\sigma_T(x)\,dx}{(x-\mu^2)(x-s_2)} ,$$

$$(27)\quad D_{\alpha 2}(s_1; s_2; t) = D_\alpha^B(s_1; s_2) + \frac{4}{\pi} \int_0^{\infty} \frac{F_2^S(q^2) h_2^{S*}(q^2)\,dq^2}{4(\mu^2+q^2) - t} ,$$

$$(28)\quad D_{\beta 2}(s_1; s_2; t) = D_\beta^B(s_1; s_2) .$$

It can be easily seen that in channel I (Compton scattering) $\lim_{\substack{s_1 \to \mu^2 \\ \cos\theta \text{ fixed}}} I_\alpha D_\alpha^B + I_\beta D_\beta^B$ is a finite quantity.

It is known that in the zero energy limit, for any charged system scattering photons [5], the cross-section becomes equal to the Thompson cross-section. Moreover the derivative with respect to k, at zero energy, is proportional to the magnetic moment of the system; here the magnetic moment is zero since we are dealing with spin zero particles; for the neutral case, the cross-section and its derivative should vanish. In fact the explicit proof was only given for spin $\frac{1}{2}$ particles but everybody believes that this result is independent of the spin of the particle. We shall not give here a justification of this statement but we shall take it for granted. Then one gets the following condition:

$$I_\alpha D_\alpha + I_\beta D_\beta - (I_\alpha D_\alpha^B + I_\beta D_\beta^B) \sim k \sim (s_1 - \mu^2)^2 \sim (s_2 - \mu^2)^2 \sim t ,$$

for $s_1 - \mu^2 \to 0$, $\cos\theta$ fixed.

Since I_β behaves like $(s_1 - \mu^2)^2$, the expressions (26) and (28) for $D_{\beta 0}$ and

$D_{\beta 2}$ are unaffected by this condition, but in $D_{\alpha 1}$ and $D_{\alpha 2}$ a subtraction is needed:

$$(29) \qquad D_{\alpha 0} = D_\alpha^B + [2s_1 t + (s_1 - \mu^2)^2]\frac{1}{\pi}\int_{(2\mu)^2}^{\infty}\frac{\sigma_T(x)\,\mathrm{d}x}{(x-\mu^2)(x-s_1)} +$$

$$+ [2s_1 t + (s_2 - \mu^2)^2]\frac{1}{\pi}\int_{(2\mu)^2}^{\infty}\frac{\sigma_T(x)\,\mathrm{d}x}{(x-\mu^2)(x-s_2)} + \frac{t}{\pi}\int_0^{\infty}\frac{F_0^S(q^2)\,h_0^{*S}(q^2)\,\mathrm{d}q^2}{(q^2+\mu^2)[4(q^2+\mu^2)-t]}\,,$$

$$(30) \qquad D_{\beta 2} = D_\beta^B + \frac{t}{\pi}\int_0^{\infty}\frac{F_2^S(q^2)\,h_2^{*S}(q^2)\,\mathrm{d}q^2}{(q^2+\mu^2)[4(q^2+\mu^2)-t]}\,.$$

These expressions still satisfy the unitarity requirements in channel III.

The very fact that subtractions are feasible in equations (25), (27) naturally leads to ask the question: why other subtractions should not be made?

Here, we have done the minimum number of necessary subtractions. It would look quite unnatural that the pion-pion interaction does not influence the k^2 dependence of the $\gamma\pi$ scattering cross-section, as viewed, for instance, in a perturbation approach.

8. – Equations for F_0^S and F_2^S and their solutions.

We take the average of the F_s' over angle φ in channel III as was done in Section 6 (see formula (23)). It is more convenient to write equations for $f_0^S = F_0^S/\omega_q^2$ and $f_2^S = F_2^S/\omega_q^2$:

$$(31) \qquad f_2^S(q^2) = \frac{1}{\pi}\int_0^{\infty}\frac{f_2^S(q'^2)\,h_2^{S*}(q'^2)\,\mathrm{d}q'^2}{q'^2 - q^2 - i\varepsilon} + \frac{e^2\mu^2}{\omega_q^2}\int_{-1}^{+1}\frac{\mathrm{d}\cos\varphi}{\omega_q^2 - q^2\cos^2\varphi}\,,$$

$$(32) \qquad f_0^S(q^2) = \frac{1}{\pi}\int_0^{\infty}\frac{f_0^S(q'^2)\,h_0^{S*}(q'^2)\,\mathrm{d}q'^2}{q'^2 - q^2 - i\varepsilon} + \frac{e^2\mu^2}{\omega_q^2}\int_{-1}^{+1}\frac{\mathrm{d}\cos\varphi}{\omega_q^2 - q^2\cos^2\varphi} +$$

$$+ \frac{2}{\pi}\int_{-1}^{+1}\mathrm{d}\cos\varphi\left[s_1\int_{(2\mu)^2}^{\infty}\frac{\sigma_T(x)\,\mathrm{d}x}{(x-\mu^2)(x-s_1)} + \mathrm{Sym}\,(1 \leftrightarrows 2)\right].$$

These equations are obtained after some manipulations using the expressions of q^2 and $\sin^2\varphi$ in terms of s_1, s_2, and t. These equations are of Omnès-

Mushkelishvili type (6); they could be solved directly but it is perhaps better to exhibit first the analytical structure of the inhomogeneous terms. By the change of variable $Z = -2/\sin^2\varphi$, one shows:

$$\int_{-1}^{+1} \frac{\mathrm{d}\cos\varphi}{\omega_q^2 - q^2\cos^2\varphi} = \int_{-\infty}^{-\mu^2} \frac{\mathrm{d}z}{(q^2 - z)\sqrt{z(z+\mu^2)}} \,. \tag{33}$$

One makes also use of the relation:

$$\int_{-1}^{+1} \frac{\mathrm{d}\cos\varphi}{x - s_1} = \int_{-1}^{+1} \frac{\mathrm{d}\cos\varphi}{x - s_2} = \int_{-\infty}^{-(x+\mu^2)^2/4x} \frac{\mathrm{d}z}{2(q^2 - z)\sqrt{z(z+\mu^2)}} \qquad \text{(see Appendix III).} \tag{34}$$

Then the equations become:

$$f_2^S(q^2) = \frac{1}{\pi}\int_0^\infty \frac{f_2^S(q'^2)\,\mathrm{d}q'^2}{q'^2 - q^2 - i\varepsilon} + \frac{e^2\mu^2}{\omega_q^2}\int_{-\infty}^{-\mu^2} \frac{\mathrm{d}z}{(q^2 - z)\sqrt{z(z+\mu^2)}} \,, \tag{35}$$

$$f_0^S(q^2) = \frac{1}{\pi}\int_0^\infty \frac{f_0^S(q'^2)\,\mathrm{d}q'^2}{q'^2 - q^2 - i\varepsilon} + \frac{e^2\mu^2}{\omega_q^2}\int_{-\infty}^{-\mu^2} \frac{\mathrm{d}z}{(q^2 - z)\sqrt{z(z+\mu^2)}} - \tag{36}$$

$$- \frac{1}{\pi}\int_{(2\mu)^2}^\infty \frac{8\sigma_T(x)\,\mathrm{d}x}{x - \mu^2} + \frac{1}{\pi}\int_{(2\mu)^2}^\infty \frac{2x\sigma_T(x)\,\mathrm{d}x}{x - \mu^2}\int_{-\infty}^{-(\mu^2+x)^2/4x} \frac{\mathrm{d}z}{(q^2 - z)\sqrt{z(z+\mu^2)}} \,.$$

Actually the two last terms in the last equation could be combined to show that it is still meaningful if $\sigma_T(x)$ increases like $x^{1-\varepsilon}$ at infinity.

Under the following assumptions:

$$\begin{cases} \delta_T^S(0) = \delta_T^S(\infty) = 0 \,, \\ \delta_T^S(q'^2) \sim q' & \text{as} \quad q' \to 0 \,, \\ \delta_T^S(q'^2) \sim \dfrac{A_T}{q'} + \dfrac{B_T}{q'^2} + \ldots & \text{as} \quad q' \to \infty \,. \end{cases} \tag{37}$$

One gets the solutions of equations (35), (36) (see Appendix III)

$$F_2^S(q^2) = \exp\left[\varrho_2^S(q^2) + i\,\delta_2^S(q^2)\right] e^2\mu^2 \cdot$$

$$\cdot \int_{-\infty}^{-\mu^2} \frac{\mathrm{d}z}{\sqrt{z(z+\mu^2)}} \left[\frac{\exp\left[-\varrho_2^S(z)\right]}{q^2 - z} + \frac{\exp\left[-\varrho_2^S(z)\right] - \exp\left[-\varrho_2^S(-\mu^2)\right]}{z + \mu^2}\right] ,$$

(6) R. OMNÈS: *Nuovo Cimento*, **8**, 316 (1958).

where

$$\varrho_2^S(q^2) = \frac{P}{\pi}\int_0^\infty \frac{\delta_2^S(q'^2)\,\mathrm{d}q'^2}{q'^2 - q^2}$$

and

$$(38)\quad \left\{\begin{aligned} F_0^S(q^2) &= \exp\left[\varrho_0^S(q^2) + i\,\delta_0^S(q^2)\right]\cdot \\ &\cdot\left[e^2\mu^2\int_{-\infty}^{-\mu^2}\frac{\mathrm{d}z}{\sqrt{z(z+\mu^2)}}\left(\frac{\exp[-\varrho_0^S(z)]}{q^2 - z} + \frac{\exp[-\varrho_0^S(z)] - \exp[-\varrho_0^S(-\mu^2)]}{z+\mu^2}\right) + \right. \\ &\left. + \frac{2\omega_q^2}{\pi}\int_{(2\mu)^2}^\infty \frac{\sigma_T(x)\,\mathrm{d}x}{x-\mu^2}\left(x\int_{-\infty}^{-(x+\mu^2)^2/4x}\frac{\exp[-\varrho_0^S(z)]\,\mathrm{d}z}{(q^2-z)\sqrt{z(z+\mu^2)}} - 4\right)\right], \end{aligned}\right.$$

with a similar definition of ϱ_0^S.

The advantage of putting the solution in this form, is that, apart $\varrho(q^2)$' there is no principal value integral to evaluate, which is a great advantage from a computational point of view. It can be seen that F_0^S exists even if $\sigma_T(x)$ behaves like $x^{1-\varepsilon}$ at infinity: the assumptions on δ show that $\varrho(z)$ behaves like $(\log z/z)$ at infinity; hence for $x \to \infty$

$$\left|\int_{-\infty}^{(x+\mu^2)^2/4x}\frac{\exp[-\varrho_0^S(z)]\,\mathrm{d}z}{(q^2-z)\sqrt{z(z+\mu^2)}} - \frac{4}{x}\right| < C\,\frac{\log x}{x^2}\,.$$

The assumptions on the phase shift behaviour at zero energy and at infinity permit to guarantee the uniqueness of the solutions of equations (35), (36) (see Appendix III).

By inserting F_0^S and F_2^S in the subtracted $D_{\alpha 0}$ and $D_{\alpha 2}$ (equations (29), (30)) and substituting these quantities in equation (17) one gets the Compton scattering amplitude.

9. – Concluding remarks.

We have given explicit expressions of F_0^S and F_2^S in terms of σ_T, δ_0^S, δ_2^S which permit to obtain the γ-π scattering amplitude or the $\pi+\pi \to \gamma+\gamma$ amplitude. However one cannot consider this problem as completely solved since we have not made any attempt of numerical evaluation of these amplitudes, because of the lack of information on pion-pion scattering. Nevertheless we felt it might be useful to give this algebraic solution. Of course it would

be very interesting to give numerical estimates of the deviations from Born approximation as the energy of the photon increases. This will be done in the future.

It is important to notice that the equations we solve have a unique solution if the S-phases of pion-pion scattering are such that $\delta(0) = \delta(\infty) = 0$, but that the equations are not really unique, because an arbitrary number of subtractions can be made before solving them. Here, we have done one subtraction, which is the minimum number of subtraction needed to ensure that the low energy cross-section for γ-π scattering is given by the Thompson formula. On the other hand one cannot see any mathematical argument to forbid a larger number of subtractions at $t = 0$; nevertheless this would give the result that the derivative of the amplitude F_2, related to the difference between the charged and neutral amplitude, with respect to k^2, at zero energy, would not be influenced by the pion-pion interaction, which looks rather unsatisfactory. So, on the basis of this argument and also for simplicity reasons we felt that one should not make more than one subtraction at zero energy.

* * *

The authors wish to thank Professor S. FUBINI for useful suggestions and comments. They are indebted to Professor GELL-MANN and Professor GLASER for clarifying discussions about the low energy limits. One of us (M.G.) would like to thank Professor FIERZ and Professor BAKKER for hospitality at CERN during the early stage of the present work.

APPENDIX I

Unitarity in Channel I.

The matrix element for the process $\gamma + \pi \to \gamma + \pi$ has been defined in the centre of mass system as:

$$\langle \boldsymbol{k}', \boldsymbol{e}_2 | T | \boldsymbol{k}, \boldsymbol{e}_1 \rangle = \frac{1}{(2\pi)^6} \frac{1}{4k\omega_k} \Phi(\boldsymbol{e}_1, \boldsymbol{e}_2, \boldsymbol{k}, \boldsymbol{k}') \,, \tag{I.1}$$

and for the process $\gamma + \pi \to \pi + \pi$

$$\langle q | T | \boldsymbol{k}, \boldsymbol{e} \rangle = \frac{1}{(2\pi)^6} \frac{1}{4(k\omega_k)^{\frac{1}{2}} \omega_q} \Psi(\boldsymbol{e}, \boldsymbol{k}, \boldsymbol{q}) \,. \tag{I.2}$$

2144

The unitarity condition has the simple form:

$$\text{(I.3)} \qquad \operatorname{Im} \Phi(\boldsymbol{e}_1, \boldsymbol{e}_2; \boldsymbol{k}, \boldsymbol{k}') = \frac{1}{(2\pi)^2} \frac{1}{8\omega_q^2} \int \mathrm{d}_3 \boldsymbol{q}\, \delta(2\omega_q - \omega_k - k) \cdot \cdot \Psi(\boldsymbol{e}_1, \boldsymbol{k}, \boldsymbol{q}) \Psi^*(\boldsymbol{e}_2, \boldsymbol{k}', \boldsymbol{q}),$$

and after integration over the modulus of q

$$\text{(I.4)} \qquad \operatorname{Im} \Phi(\boldsymbol{e}_1, \boldsymbol{e}_2; \boldsymbol{k}, \boldsymbol{k}') = \frac{1}{(8\pi)^2} \frac{q}{\omega_q} \int \Psi(\boldsymbol{e}_1, \boldsymbol{k}, \boldsymbol{q}) \Psi^*(\boldsymbol{e}_2, \boldsymbol{k}', \boldsymbol{q})\, \mathrm{d}\Omega_q$$

with $2\omega_q = k + \omega_k$.

From gauge and Lorentz invariance conditions, we know that $\Psi(\boldsymbol{e}, \boldsymbol{k}, \boldsymbol{q})$, has the form

$$\Psi(\boldsymbol{e}, \boldsymbol{k}, \boldsymbol{q}) = (\boldsymbol{e}, \boldsymbol{k}, \boldsymbol{q}) H[k^2, (\boldsymbol{k} \cdot \boldsymbol{q})^2] .$$

It follows that the integral over the $\boldsymbol{q}$ angle can be written as a linear combination of two invariants directly related to I_1 and I_2. By definition of U_1 and U_2

$$\text{(I.5)} \qquad \int \Psi(\boldsymbol{e}_1, \boldsymbol{k}, \boldsymbol{q}) \Psi^*(\boldsymbol{e}_2, \boldsymbol{k}', \boldsymbol{q})\, \mathrm{d}\Omega_q = \frac{4\pi}{3} q^2 \{(\boldsymbol{e}_1 \cdot \boldsymbol{e}_2)(\boldsymbol{k} \cdot \boldsymbol{k}') U_1(k^2, \cos^2\theta) - - (\boldsymbol{e}_1 \cdot \boldsymbol{k}')(\boldsymbol{e}_2 \cdot \boldsymbol{k}) U_2(k^2, \cos^2\theta)\} .$$

By comparing this expression of $\operatorname{Im} \Phi$ and the definition

$$\operatorname{Im} \Phi = I_1 \operatorname{Im} D_1 + I_2 \operatorname{Im} D_2 ,$$

we easily deduce by identification:

$$\text{(I.6)} \qquad \begin{cases} \operatorname{Im} D_1 = \dfrac{1}{24\pi} \dfrac{q^3 k^2}{k + \omega_k} \cos\theta\, U_1(k^2, \cos\theta) , \\ \operatorname{Im} D_2 = \dfrac{1}{96\pi} \dfrac{q^3}{(k + \omega_k)^3} [\cos\theta (U_2 - U_1) - U_2] . \end{cases}$$

At this stage, it is interesting to relate U_1 to the total cross-section for the reaction $\gamma + \pi \to \pi + \pi$. In order to obtain the latter we must calculate the integral

$$\int |\Psi(\boldsymbol{e}, \boldsymbol{k}, \boldsymbol{q})|^2\, \mathrm{d}\Omega_q \qquad \frac{4\pi}{3} q^2 k^2 U_1(k^2, 1) ,$$

and the total cross-section is given by

$$\text{(I.7)} \qquad \sigma_T = \frac{1}{48\pi} \frac{k q^3}{(k + \omega_k)^2} U_1(k^2, 1) .$$

In the particular case considered in this paper, where H does not depend of the angle between $\boldsymbol{k}$ and $\boldsymbol{q}$, we simply have

$$U_1(k^2, \cos^2\theta) = U_2(k^2, \cos^2\theta) = |H(k^2)|^2 . \tag{I.8}$$

From the general form given for D_1 and D_2 we can expand their imaginary parts in Legendre polynomials of $\cos\theta$

$$\operatorname{Im} D_i = \sum_n [2k(k+\omega_k)]^{2n} P_n(\cos\theta)\, \sigma_i^{(n)}(s_1),$$

and the unitarity condition permits to know the weight functions $\sigma_i^{(n)}(s_1)$:

$$\text{(I.9)} \quad \begin{cases} \sigma_\alpha^{(n)}(s_1) = \dfrac{2n+1}{48\pi} \dfrac{q^3 k^2}{k+\omega_k} \dfrac{1}{[2k(k+\omega_k)]^{2n}} \displaystyle\int_{-1}^{+1} U_1(k^2, u^2) u P_n(u)\, \mathrm{d}u , \\ \sigma_\beta^n(s_1) = \dfrac{2n+1}{192\pi} \dfrac{q^3}{(k+\omega_k)^3} \dfrac{1}{[2k(k+\omega_k)]^{2n}} \displaystyle\int_{-1}^{+1} [u(U_1 - U_2) - U_2] P_n(u)\, \mathrm{d}u . \end{cases}$$

Appendix II

For the channel III, φ is given by:

$$\varphi = (\boldsymbol{e}_1 \cdot \boldsymbol{e}_2) D_1 - 8\omega_q^2 (\boldsymbol{e}_1 \cdot \boldsymbol{q})(\boldsymbol{e}_2 \cdot \boldsymbol{q}) D_2 . \tag{II.1}$$

Taking the incident momentum $\boldsymbol{p}$ as z axis and the bissector of e_1 and e_2 as x axis, we have:

$$(\boldsymbol{e}_1 \cdot \boldsymbol{q})(\boldsymbol{e}_2 \cdot \boldsymbol{q}) = \frac{q^2}{2} \sin^2\varphi [\boldsymbol{e}_1 \cdot \boldsymbol{e}_2 + \cos 2\omega] ,$$

where φ and ω are the polar angles of the final momentum $\boldsymbol{q}$. Consequently the amplitude φ takes the form:

$$\varphi = (\boldsymbol{e}_1 \cdot \boldsymbol{e}_2)\{D_1 - \tfrac{8}{3}(q\omega_q)^2 [1 - P_2(\cos\varphi)] D_2\} - \tfrac{4}{3}(q\omega_q)^2 P_2^2(\cos\varphi) \cos 2\omega D_2,$$

where P_2 and P_2^2 are respectively the Legendre polynomial and the Legendre associated function of order 2.

The first part of φ contains only cylindrical symmetrical waves and the second part non cylindrical symmetrical waves. For one given value of the orbital angular momentum l we can define two partial waves (except for

2446

$l = 0$):

$$\text{(II.2)} \quad \begin{cases} F_{2l}(q^2) = \dfrac{4l+1}{2} \displaystyle\int_{-1}^{+1} [D_1 - \tfrac{8}{3}(q\omega_q)^2 D_2(1 - P_2(\cos\varphi))] P_{2l}(\cos\varphi)\, \mathrm{d}\cos\varphi\,, \\ f_{2l}(q^2) = \displaystyle\int_{-1}^{+1} D_2 P_2^2(\cos\varphi) P_{2l}^2(\cos\varphi)\, \mathrm{d}\cos\varphi\,, \end{cases}$$

corresponding to the following expansion for φ:

$$\varphi = (\boldsymbol{e}_1 \cdot \boldsymbol{e}_2) \sum_{l=0}^{\infty} F_{2l}(q^2) P_{2l}(\cos\varphi) - \tfrac{4}{3}(q\omega_q)^2 \sum_{l=1}^{\infty} f_{2l}(q^2) P_{2l}^2(\cos\varphi) \cos 2\omega\,.$$

The imaginary parts of $F_{2l}(q^2)$ and $f_{2l}(q^2)$ are easily related to the imaginary parts of D_1 and D_2. With the definitions given in the text

$$\operatorname{Im} D_{1,2} = \sum_l (4q\omega_q)^2 P_{2l}(\cos\varphi)\, \varrho_{1,2}^{(l)}(4\omega_q^2)\,,$$

It follows that angular integrations over φ can be performed and we define for the cylindrical part:

$$\begin{cases} \alpha_n = \displaystyle\int_{-1}^{+1} (1 - u^2) P_{2n}(u) P_{2n+2}(u)\, \mathrm{d}u\,, \\ \beta_n = \displaystyle\int_{-1}^{+1} (1 - u^2)[P_{2n}(u)]^2\, \mathrm{d}u, \end{cases}$$

and the imaginary part of $F_{2l}(q^2)$ appears as a linear combination of the unknown weight functions ϱ:

$$\text{(II.3)} \quad \operatorname{Im} F_{2l}(q^2) = (4q\omega_q)^2 \cdot \left\{ \varrho_1^{(l)}(4\omega q^2) - \frac{4l+1}{8} [\alpha_{l-1} \varrho_2^{(l-1)}(4\omega_q^2) + (4q\omega_q)^2 \beta_l \varrho_2^{(l)}(4\omega_q^2) + (4q\omega_q)^4 \alpha_l \varrho_2^{(l+1)}(4\omega_q^2)] \right\}.$$

In the same way, we obtain for the non cylindrical functions:

$$\text{(II.4)} \quad \operatorname{Im} f_{2l}(q^2) = (4q\omega_q)^{2l-2} [\gamma_{ll-1} \varrho_2^{(l-1)}(4\omega_q^2) + (4q\omega_q)^2 \gamma_{ll} \varrho_2^{(l)}(4\omega_q^2) + (4q\omega_q)^4 \gamma_{ll+1} \varrho_2^{(l+1)}(4\omega_q^2)]\,,$$

where

$$\gamma_{lm} = \int_{-1}^{+1} (1 - u^2) P_{2l}^2(u) P_{2m}(u)\, \mathrm{d}u\,.$$

3447

It is easy to apply the unitary condition for each partial wave. For a given isospin, we have:

$$\begin{cases} \operatorname{Im} F_{2l}(q^2) = F_{2l}(q^2) h^*_{2l}(q^2) , \\ \operatorname{Im} f_{2l}(q^2) \ = f_{2l}(q^2) h^*_{2l}(q^2) , \end{cases}$$

where $h_{2l}(q^2)$ is the pion-pion scattering amplitude for the angular momentum $2l$.

By inspection of equations (II.3) and (II.4) we see that $\varrho_1^{(l)}$ appears in $\operatorname{Im} F_{2l}(q^2)$ and $\varrho_2^{(l)}$ in $\operatorname{Im} F_{2l+2}$, $\operatorname{Im} F_{2l}$, $\operatorname{Im} F_{2l-2}$, $\operatorname{Im} f_{2l+2}$ $\operatorname{Im} f_{2l}$, $\operatorname{Im} f_{2l-2}$. If we assume the pion-pion scattering amplitude to be zero for the angular momenta higher than $2L$, we can conclude: $\varrho_1^{(l)} = 0$ for $l > L$ and $\varrho_2^{(l)} = 0$ for $l > L-1$. The non vanishing weight functions are solutions of a linear system of $(2L+1)$ equations (corresponding to $(2L+1)$ unitarity conditions) for $(2L+1)$ functions ($\varrho_1^{(l)}$ for $l = 0$, L and $\varrho_2^{(l)}$ for $l = 0$, $L-1$). In general we have a unique solution.

The particular case considered in the text corresponds to $L = 0$ and we have only one weight function $\varrho_1^{(0)}$ given by the unitarity conditions corresponding to the S-wave.

Appendix III

We first transform the integral (34). A general technique has been given by the authors in ref. (1), but here a trick due to S. Fubini gives the answer in a straightforward way:

$$\int_{-1}^{+1} \frac{\mathrm{d}\cos\varphi}{x - s_1} = \int_{x}^{\infty} \mathrm{d}y \int_{-1}^{+1} \frac{\mathrm{d}\cos\varphi}{[y - s_1]^2} .$$

Since s_1 is a linear function of $\cos\varphi$ the last integral can be performed and gives a rational expression:

$$\int_{x}^{\infty} \frac{\mathrm{d}y}{2y[q^2 + ((y+\mu^2)/4y)^2]} ,$$

which, by a trivial change of variable gives:

$$\int_{-\infty}^{-(x+\mu^2)^2/1x} \frac{\mathrm{d}z}{2(q^2 - z)\sqrt{z(z+\mu^2)}} . \tag{III.1}$$

Then we try to solve equations (35) and (36). Let us first solve the general equation

$$f(q^2) = \frac{1}{\pi}\int_0^{\infty} \frac{f(q'^2)\,h^*(q'^2)\,\mathrm{d}q'^2}{q'^2 - q^2 - i\varepsilon} + \int_{-\infty}^{-M<0} \frac{p(z)\,\mathrm{d}z}{z - q^2} + C\,, \tag{III.2}$$

where $h(q^2) = \exp[i\,\delta(q^2)]\sin\delta(q^2)$ and where $p(z)$ may include a finite number of δ-functions and behaves at most like $1/z$ at infinity.

Equation (III.2) defines an analytic function $f(Z)$ with the following properties:

— it is such that $\lim_{|Z|\to\infty} f(Z) = C$, if an oscillator behaviour of $f(q^2)\,h^*(q^2)$ at infinity is excluded;

— it is holomorphic everywhere except along two cuts from $-\infty$ to $-M$ and from 0 to $+\infty$;

— the discontinuity across the right hand cut is such that

$$f(q^2 + i\varepsilon)/f(q^2 - i\varepsilon) = \exp[2i\,\delta(q^2)]\,.$$

If

$$\begin{cases} \delta(0) = \delta(\infty) = 0 & \text{and} \\ \delta(q^2) \sim q & \text{as} \quad q \to 0\,, \\ \delta(q^2) \sim \dfrac{1}{q} & \text{as} \quad q \to \infty\,, \end{cases} \tag{III.3}$$

one can define

$$U(Z) = \frac{1}{\pi}\int_0^{\infty} \frac{\delta(q'^2)\,\mathrm{d}q'^2}{q'^2 - Z}\,, \qquad U(q^2 + i\varepsilon) = \varrho(q^2) + i\,\delta(q^2)\,.$$

Then the quantity

$$\exp[U(Z)]\left[C + \int_{-\infty}^{-M} \frac{\exp[-\varrho(z)]\,p(z)}{z - Z}\,\mathrm{d}z\right] = \exp[U(Z)]\,g(Z)\,, \tag{III.4}$$

fulfils all the above requirements. To check that this is a solution one can insert it in (III.2). Then one has to compute the integral

$$\frac{1}{\pi}\int_0^{\infty} \frac{\exp[U(x + i\varepsilon)]\,g(x)\,h^*(x)\,\mathrm{d}x}{x - Z_0} = \frac{1}{2i\pi}\int_0^{\infty} \frac{(\exp[U(x + i\varepsilon)] - \exp[U(x - i\varepsilon)])\,g(x)\,\mathrm{d}x}{x - Z_0}$$

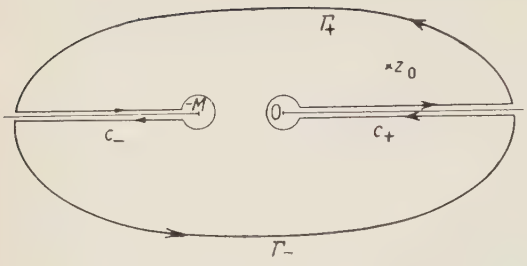

Fig. 3.

This integral can be computed by following C_+ (Fig. 3) (the contribution from the circle surrounding the origin vanishes). Then

$$\int_{C_+} = \text{Residue } (Z_0)\times 2\pi i - \int_{C_-} - \int_{\Gamma_-} - \int_{\Gamma_+} .$$

$$\frac{1}{\pi}\int_0^\infty \frac{\exp[u(x+i\varepsilon)]h^*(x)g(x)\,\mathrm{d}x}{x-Z_0} = \exp[u(Z_0)]\,g(Z_0)\,\frac{1}{2\pi i}\int_{C_-}\frac{\exp[u(Z)]g(Z)\,\mathrm{d}Z}{Z-Z_0} - C .$$

Now, if $g(Z)$ is *regular* at $Z=-M$ (which is the case here)

$$\text{(III.5)}\qquad \int_{C_-}\frac{\exp[u(Z)g(Z)]\mathrm{d}Z}{Z-Z_0} = \int_{-\infty}^{-M}\frac{\exp[\varrho(z)]\,[g(z+i\varepsilon)-g(z-i\varepsilon)]}{z-Z_0}\,\mathrm{d}z = 2\pi i\int_{-\infty}^{-M}\frac{p(z)\,\mathrm{d}z}{z-Z_0} .$$

Then it can be seen that the equation is satisfied. The multiplicity of the solutions has already been discussed elsewhere ([7]). The homogeneous equation has *no solution* when the hypothesis (III.3) are made on the phase shift. This is shown by inserting in the homogeneous equation the *possible* solutions, *i.e.* $Z^m\exp[U(Z)]$, m integer ([6]), and using contour integration.

The equations we have to solve in the present paper can be *formally* written in the form (III.2), but the singularities of the weight functions make the integral divergent: one writes the term arising from Born approximation as

$$\text{(III.6)}\qquad \frac{e^2\mu^2}{q^2+\mu^2}\int_{-\infty}^{-\mu^2}\frac{\mathrm{d}z}{(q^2-z)\sqrt{z(z+\mu^2)}} = -e^2\mu^2\left[-\frac{1}{q^2+\mu^2}\int_{-\infty}^{-\mu^2}\frac{\mathrm{d}z}{(\mu^2+z)\sqrt{z(z+\mu^2)}} + \int_{-\infty}^{-\mu^2}\frac{\mathrm{d}z}{(q^2-z)(z+\mu^2)\sqrt{z(z+\mu^2)}}\right] .$$

If we disregard the divergences and apply formula (III.4) we finally get for the solutions *convergent* expressions. Though this procedure is not well justified we can see by contour integration that the result is correct. As we said the only trouble comes from the term (III.6) which appears both in the equation for f_0^S and in the equation for f_2^S. The contribution of (III.6) to the solution

([7]) M. GOURDIN and A. MARTIN: *Nuovo Cimento*, **8**, 699 (1958).

is found to be

$$f_B(q^2) = \exp\left[u(q^2 + i\varepsilon)\right] \cdot$$
$$\cdot \frac{e^2\mu^2}{q^2+\mu^2} \int_{-\infty}^{-\mu^2} \left[\frac{\exp\left[-\varrho(z)\right]}{q^2 - z} + \frac{\exp\left[\quad \varrho(z)\right] - \exp\left[-\varrho(-\mu^2)\right]}{z+\mu^2} \right] \frac{\mathrm{d}z}{\sqrt{z(z+\mu^2)}} .$$

Now

$$\frac{1}{\pi} \int_0^\infty \frac{f_B(q'^2)\, h^*(q'^2)\, \mathrm{d}q'^2}{q'^2 - Z_0} = f_B(Z_0) - \frac{e^2\mu^2}{2\pi i} \cdot$$
$$\cdot \int_C \frac{\exp\left[u(Z)\right]}{Z - Z_0} \frac{\mathrm{d}Z}{(Z+\mu^2)} \int_{-\infty}^{-\mu^2} \left[\frac{\exp\left[-\varrho(z)\right]}{Z - z} + \frac{\exp\left[-\varrho(z) - \exp\left[-\varrho(-\mu^2)\right]\right.}{z+\mu^2} \right] \frac{\mathrm{d}z}{\sqrt{z(z+\mu^2)}} =$$
$$= f_B(Z_0) - \frac{e^2\mu^2}{2\pi i} \int_{C_-} \frac{\mathrm{d}Z}{(Z - Z_0)(Z+\mu^2)} \int_{-\infty}^{-\mu^2} \frac{\mathrm{d}z}{(Z - z)\sqrt{z(z+\mu^2)}} - \frac{e^2\mu^2}{2\pi i} \int_{C_-} \frac{\mathrm{d}Z}{(Z - Z_0)(Z+\mu^2)} \cdot$$
$$\cdot \int_{-\infty}^{-\mu^2} \left[\frac{\exp\left[-\varrho(z)\right] - \exp\left[-u(Z)\right]}{Z - z} + \frac{\exp\left[-\varrho(z)\right] - \exp\left[-\varrho(-\mu^2)\right]}{z+\mu^2} \right] \frac{\mathrm{d}z}{\sqrt{z(z+\mu^2)}} .$$

In the first part of the integral the path C_- can be obviously replaced by a contour surrounding Z_0. In the second part of the integral the integrand has no discontinuity across the left hand cut and the only possible singularity inside C_- lies at $Z = -\mu^2$, but the residue is zero, so, finally

$$\frac{1}{\pi} \int_0^\infty \frac{f_B(q'^2)\, h^*(q'^2)\, \mathrm{d}q'^2}{q'^2 - Z_0} = f_B(Z_0) - \frac{e^2\mu^2}{(Z_0+\mu^2)} \int_{-\infty}^{-\mu^2} \frac{\mathrm{d}z}{(Z_0 - z)\sqrt{z(z+\mu^2)}} . \qquad q.e.d.$$

RIASSUNTO (*)

Accoppiando i presupposti di una rappresentazione di Mandelstam con una unitarietà approssimata si può ottenere l'ampiezza di scattering pione-fotone in termini dell'ampiezza di scattering pione-pione in stati pari e degli elementi di matrice per la fotoproduzione di pioni su pioni. Nel risolvere questo problema si deve fare attenzione al fatto che nel limite della bassa energia questa ampiezza potrebbe divenire uguale all'ampiezza classica. Con alcune posizioni semplificatrici otteniamo un'espressione che contiene quattro quantità: gli spostamenti della fase S di due pioni, la sezione trasversale totale per la fotoproduzione di pioni su pioni, e la costante elettromagnetica di accoppiamento. Stime numeriche saranno date in un secondo tempo. L'interesse dello studio di questo problema sta nella sua possibile influenza sullo scattering nucleone-fotone.

(*) *Traduzione a cura della Redazione.*

IL NUOVO CIMENTO Vol. XVII, N. 2 16 Luglio 1560

Formulas for the Matrix Elements of Connected Diagrams in Field Theories.

F. R. Halpern (*)

Scuola di Perfezionamento in Fisica Teorica e Nucleare dell'Università - Napoli

(ricevuto il 9 Aprile 1960)

Summary. — A concise formula for an element of the S-matrix has been given by Caianiello in terms of the real particles appearing in the process. This formula contains in addition to the contributions of the diagrams that describe mutual interactions of all the interacting particles with each other, the contributions of disjoint processes occurring simultaneously. In the present note a method of factoring out unwanted disconnected pieces is given. As an example the removal of vacuum-vacuum transitions in quantum electrodynamics is carried out.

1. – Introduction.

A compact formula for S-matrix elements in quantum-electrodynamics has been given by Caianiello [1]. This expression contains the contributions of all diagrams with a prescribed number of external lines. Among these are found not only those that describe interactions of all the particles but also those that describe the simultaneous interaction of two or more disjoint sets of particles, *i.e.* disjoint graphs. The most common example of this situation is the occurrence of vacuum-vacuum transitions in the conventional expressions for the S-matrix. In low order calculations where only a small number of graphs are encountered it is a simple matter to discard these irrelevant diagrams. However if a serious attempt is to be made to present the renor-

(*) Fulbright Fellow on leave from Princeton University, Princeton, N. J.

The research reported in this document has been sponsored in part by the Office Chief of Research and Development, U. S. Department of Army, through its European Office under contract no. DA-91-591-EUC-1096.

[1] E. R. Caianiello: *Nuovo Cimento*, **11**, 492 (1954).

malized perturbation series it may be desireable to start by discovering expressions for an S-matrix element that is free of vacuum fluctuations.

It has been shown [1] that several algebric algorithms are sufficient to express the general S-matrix element. In the present development a new expansion is introduced for determinants and with the help of this it will be possible to start at any point in a matrix element, internal or external and to determine which other points are connected to it. A formula will be given for the S-matrix element that is free of vacuum-vacuum transitions. There is no unique formulae for this since it is possible to begin at any point or group of points and find all the connected points, and for each such choice a new formula results.

A typical matrix element M_{FI} will be the product of the vacuum-vacuum transition V and $\bar{M}_{FI}$, the vacuum free matrix element. If each of these three quantities is expanded in a power series in e, the n-th order matrix element $M_{FI}^{(n)}$ is given by

$$M_{FI}^{(n)} = \sum_{s=0}^{[n/2]} \binom{n}{2s} \bar{M}_{FI}^{(n-2s)} V^{(2s)} . \tag{1}$$

Equation (1) is a typical convolution type sum and may be solved for $\bar{M}_{FI}^{(n)}$ in terms of the other quantities quite easily. This solution although apparently more compat than the one to be presented is a typical combinatorial one in which a particular piece is added in and subtracted out many times to achieve a small net result, and thus will not be particularly useful for computational purposes. However if the matrix element M_{FI} can be displayed in the form of (1) the identification of $\bar{M}_{FI}^{(n)}$ will be possible. The occurrence of an equation like (4) is one of the reasons that makes the separation of vacuum pieces much simpler than the separation of pieces connected by several lines self-energy and vertex parts.

2. – An expansion theorem for determinants.

The formula for the S-matrix in quantum-electrodynamics is [1]

$$M_{FI} = \frac{(-1)^{p_{FI}}}{\sqrt{\sigma_1' \dots \tau_\alpha!}} \sum_{n=0}^{\infty} \frac{(-ie)^n}{n!} \int \mathrm{d}x_1 \dots \int \mathrm{d}x_n \, \gamma^{(1)} \dots \gamma^{(n)} \cdot \tag{2}$$

$$\cdot \begin{pmatrix} x_1 \dots x_n & u^{(1)} \dots u^{(N_0)} \\ x_1 \dots x_n & p^{(1)} \dots p^{(N_0)} \end{pmatrix} [x_1 \dots x_n \, z^{(1)} \dots z^{(P_0)}] .$$

The following expansion theorem for hafnians is contained in [1],

$$[x_1, x_2, \ldots, x_n] = \sum_{s=r}^{n} \sum_{C_{n-r}^{n-r}} [x_1, \ldots, x_r, \overset{0}{x}_{i_{r+1}} \ldots \overset{0}{x}_{i_s}][x_{i_{s+1}} \ldots x_{i_n}] . \tag{3}$$

The first sum is over the $\binom{n-r}{n-s}$ ways of separating $x_{r+1} \ldots x_n$ into two groups. One containing $n-s$ elements and the other $s-r$. This expansion requires that the points $x_{i_{r+1}} \ldots x_{i_s}$ are connected to the points $x_1 \ldots x_r$. This follows since in the expansion of the hafnian

$$[x_i x_j] = [\overset{0}{x}_i x_j] = [x_i \overset{0}{x}_j] = D_F(x_i - x_j) , \qquad [\overset{0}{x}_i \overset{0}{x}_j] = 0 . \tag{4}$$

A somewhat similar expansion is required for determinants. However the nature of the connection generated by the electron-positron line is somewhat different than that for the photon line since it proceeds either straight through the graph or is a closed loop. The set of all points connected to a given point by an electron line is the set of points on the line or loop containing the given point. The considerations lead to the following classification of the terms in the expansion of a determinant. Consider the determinant

$$\begin{pmatrix} a_1, & a_2, & a_n \\ a_1, & a_2, & a_n \end{pmatrix} ! .$$

In the expansion of this determinant the $n!$ products are to be arranged in cycles. All of the cycles are to be divided up into two groups, those that contain the elements $a_1, \ldots, a_r$, and those that don't. The products are to be arranged according to the number of elements a's there are in the cycles of the second type. There is a minimum of none, for example all the elements are in one cycle, and a maximum of $n-r$. A particular set of cycles of the first kind does not occur only once but will occur in fact in $(n-s)!$ products if there are $n-s$ a's not included in the cycles of the first type. The cycles of the second type are exactly those occurring in the expansion of the determinant composed of the $n-s$ elements in the cycles of the second type. In a similar way a particular set of elements does not give rise to just one set of cycles of the first type but to several. In this case the determinant of this group of elements is not formed since at least one of the first r a's must occur in each cycle of the first type. However all the terms in the expansion of the determinant of this group of elements consistent with this restriction does occur. For this reason a determinant with a modified expansion rule is introduced as follows.

24654

The determinant

$$\begin{pmatrix} a_1, & a_r, & \overline{a_{r+1}, & a_s} \\ a_1, & a_r, & \overline{a_{r+1}, & a_s} \end{pmatrix},$$

is to be expanded according to the conventional rules for determinants and then any term in the expansion that has at least one cycle composed entirely of the variables $a_{r+1} \dots a_s$ is to be discarded.

Thus the above discussion leads to the expansion of a conventional determinant as a sum of products consisting of one conventional determinant (cycles of the second kind) and one with the new rule for development (cycles of the first kind); more formally we have,

$$(5) \qquad \begin{pmatrix} a_1 \dots a_n \\ a_1 \dots a_n \end{pmatrix} = \sum_{s=r}^{n} \sum_{C_{n-s}^{n-r}} \begin{pmatrix} a_1 \dots a_r & \overline{a_{i_{r_n}} \dots a_{i_s}} \\ a_1 \dots a_r & \overline{a_{i_{r_n}} \dots a_{i_s}} \end{pmatrix} \begin{pmatrix} a_{i_s} \dots a_{i_n} \\ a_{i_s} \dots a_{i_n} \end{pmatrix}.$$

The inner sum is over the $\binom{n-r}{n-s}$ ways of dividing the $a_{r+1} \dots a_n$ into two groups. A more formal proof may be given by counting terms on both sides. There are $r(s-1)!$ in the barred determinant, $(n-s)!$ in the unbarred and

$$\sum_{s=0}^{n} \binom{n-r}{n-s} r!\,(s-1)!\,(n-s)! = n!$$

No signs occur because the structure of the cycles is left undisturbed in this expansion. The virtue of this expansion is that the points under the bar must be connected with the unbarred parts.

3. – Separation of the vacuum-vacuum amplitude in electrodynamics.

A systematic application of the two lemmas (3) and (5) to the S-matrix (2) permits it to be cast into the form (1). The first step is the expansion of the determinant. Only the determinant and hafnian are exhibited in what follows since no alteration is made in the other quantities. Advantage will be taken of the x's being dummy variables and the symmetry of the expressions to always replace the inner sums in (3) and (5) by a binomial coefficient. Expansion of the determinant using the external variable as the unbarred lines

yields,

$$(6)\qquad \begin{pmatrix} u^{(1)} \dots u^{(N_0)} & x_1 \dots x_n \\ v^{(1)} \dots v^{N_0)} & x_1 \dots x_n \end{pmatrix} [z^{(1)} \dots z^{(P_0)} \quad x_1 \dots x_n] =$$

$$= \sum_{a=0}^{n} \binom{n}{a} \begin{pmatrix} u^{(1)} \dots u^{(N_0)} & \overline{x_1 \dots x_a} \\ v^{(1)} \dots v^{(N_0)} & \overline{x_1 \dots x_a} \end{pmatrix} \begin{pmatrix} x_{a+1} \dots x_n \\ x_{a+1} \dots x_n \end{pmatrix} [z^{(1)} \dots z^{(P_0)} \quad x_1 \dots x_n] .$$

Because of Furry's theorem the second determinant must be of even order. If it is of odd order there is at least one closed cycle with an odd number of elements which vanishes. Thus $n - a = 2b$ and b may be used as a variable of summation. To simplify the notation the variables $x_1 \dots x_n$ are replaced by the subscripts $1 \dots n$. With these modifications (6) becomes:

$$(7)\qquad A^{(n)}_{N_0 P_0} = \sum_{b_1=0}^{[n/2]} \binom{n}{2b_1} \begin{pmatrix} u^{(1)} \dots u^{(N_0)} & \overline{1 \dots n-2b_1} \\ v^{(1)} \dots v^{(N_0)} & \overline{1 \dots n-2b_1} \end{pmatrix} \cdot$$

$$\cdot \begin{pmatrix} n-2b_1+1 \dots n \\ n-2b_1+1 \dots n \end{pmatrix} [z^{(1)} \dots z^{(P_0)} \, 1 \dots n] .$$

The points $1 \dots n - 2b_1$ are now connected to the external lines. To separate the vacuum parts it is next necessary to expand the hafnian according to (3), using the external photon lines $z^{(1)}$, $z^{(P_0)}$ and those internal points $x_1 \dots x_{n-2b_1}$ that are connected to the external electron lines as the first group of terms. With this expansion (7) becomes

$$(8)\qquad A^{(n)}_{N_0 P_0} = \sum_{b_1=0}^{[n/2]} \sum_{b_2=0}^{b_1} \binom{n}{2b_1} \binom{2b_1}{2b_2} \begin{pmatrix} u^{(1)} \dots u^{(N_0)} & \overline{1 \dots n-2b_1} \\ v^{(1)} \dots v^{(N_0)} & \overline{1 \dots n-2b_1} \end{pmatrix} \begin{pmatrix} n-2b_1+1 \dots n \\ n-2b_1+1 \dots n \end{pmatrix} \cdot$$

$$\cdot [z^{(1)}, \dots z^{(P_0)}, \; 1, \dots n-2b_1, \; \overset{0}{n-2b_1+1}, \dots \overset{0}{n-2b_2}][n-2b_2+1, \dots n] .$$

The lower limit for the b_2 sum is more precisely maximum $(0, 2b_1 - (P_0+n)/2)$. However the second limit imposed by the vanishing of the hafnian if there are two many circled terms will be ignored.

In (8) the term $b_2 = b_1$ contains an obvious vacuum part. The remaining terms may or may not contain vacuum parts but all the points $1 \dots n - 2b_2$ are connected to the external lines. To discover the remaining vacuum parts it is necessary to repeat the two expansions until all terms are found to be connected to the external lines. In practice this may be done by dropping the term $b_2 = b_1$ from the sum: note that when this is done the sum on b_1 begins at 1 not at 0, the remainder is then expanded again. It is not difficult to guess and then prove by induction the following result for the repeated

2456

application of this process.

$$(9)\quad A^{(n)}_{N_0P_0}=\sum_{b_1=c}^{[n/2]}\sum_{b_2=c-1}^{b_1-1}\sum_{b_3=c-1}^{b_2}\sum_{b_4=c-2}^{b_3-1}\cdots\sum_{b_{2c-1}=1}^{b_{2c-2}}\cdot$$

$$\cdot\sum_{b_{2c}=0}^{b_{2c-1}-1}\binom{n}{2b_1}\binom{2b_1}{2b_2}\binom{2b_2}{2b_3}\cdots\binom{2b_{2c-1}}{2b_{2c}}\begin{pmatrix}u^{(1)}\ldots u^{(N_0)} & 1\ldots n-2b_1\\ v^{(1)}\ldots v^{(N_0)} & \overline{1\ldots n-2b_1}\end{pmatrix}\cdot$$

$$\cdot\ \ldots\ \begin{pmatrix}n-2b_1+1\ldots n-2b_2 & \overline{n-2b_2+1\ldots n-2b_3}\\ n-2b_1+1\ldots n-2b_2 & \overline{n-2b_2+1\ldots n-2b_3}\end{pmatrix}\ldots\cdot$$

$$\cdot\begin{pmatrix}n-2b_{2c-1}\ldots n\\ n-2b_{2c-1}\ldots n\end{pmatrix}[z^{(1)}\ldots z^{(P_0)}\ 1\ldots n-2b_1\ n-2\overset{0}{b}_1+1\ldots n-2\overset{0}{b}_2]\cdot$$

$$\cdot[n-2b_2+1\ldots n-2b_3\ n-2\overset{0}{b}_3+1\ldots n-2\overset{0}{b}_4]\cdot$$

$$\cdot[n-2b_{2c-2}+1\ldots n-2b_{2c-1}\ n-2\overset{0}{b}_{2c-1}+1\ldots n-2\overset{0}{b}_{2c}][n-2b_{2c}+1\ldots n]+$$

$$+\sum_{d=0}^{c-1}\sum_{b_1=d}^{[n/2]}\sum_{b_2=d-1}^{b_1-1}\sum_{b_3=d-1}^{b_2}\sum_{b_4=d-2}^{b_3-1}\cdots\sum_{b_{2d}=0}^{b_{2d-1}-1}\sum_{b_{2d+1}=0}^{b_{2d}}\cdot$$

$$\cdot\binom{n}{2b_1}\binom{2b_1}{2b_2}\binom{2b_2}{2b_3}\cdots\binom{2b_{2d}}{2b_{2d+1}}\begin{pmatrix}u^{(1)}\ldots u^{(N_0)} & 1\ldots n-2b_1\\ v^{(1)}\ldots v^{(N_0)} & \overline{1\ldots n-2b_1}\end{pmatrix}\cdot$$

$$\cdot\begin{pmatrix}n-2b_{2d-1}+1\ldots n-2b_{2d} & \overline{n-2b_{2d}+1\ldots n-2b_{2d-1}}\\ n-2b_{2d-1}+1\ldots n-2b_{2d} & \overline{n-2b_{2d}+1\ldots n-2b_{2d+1}}\end{pmatrix}\cdot$$

$$\cdot[z^{(1)}\ z^{(N_0)}\ 1\ n-2b_1\ n-2\overset{0}{b}_1+1\ n-2\overset{0}{b}_2]\cdot$$

$$\cdot\ \ldots[n-2b_{2d}+1\ n-2b_{2d+1}]\ V^{(2b_{2d+1})}\,.$$

If this expansion is continued until $c=[n/2]+1$ the first term will vanish and only the second will remain in which all of the vacuum pieces are explicitly exhibited. It may appear that the terms for which $b_{2s+1}-b_{2s}$ have concealed vacuum parts but because of the hafnians these terms vanish; use will be made of this to achieve a slight simplification. To bring the matrix element into the form (1) it is necessary to move the sum on b_{2d-1} to the extreme left as b_{2d+1} is the index of the vacuum part. If we call the product of binomial coefficients, determinants and hafnians under the summation (BDH) after this transposition we obtain,

$$(10)\qquad A^{(n)}_{N_0P_0}=\sum_{b_{2d+1}=0}^{[n/2]}\sum_{d=0}^{[n/2]-b_{2d+1}}\sum_{b_1=b_{2d+1}+d}^{[n/2]}\sum_{b_2=b_{2d+1}+d-1}^{b_1-1}\cdots\sum_{b_{2d}=b_{2d+1}}^{b_{2d-1}-1}(BDH)\,.$$

The binomial coefficients must be adjusted to bring out a factor $(2b^{n}_{2d-1})$.

The required identity is that

$$B = \binom{n}{2b_1}\binom{2b_1}{2b_2}\cdots\binom{2b_{2d}}{2b_{2d+1}} = \binom{n}{2b_{2d+1}}\binom{n-2b_{2d+1}}{2b_1-2b_{2d+1}}\cdots\binom{2b_{2d-1}-2b_{2d+1}}{2b_{2d}-2b_{2d+1}}.$$

After making this substitution for B it is clear that the term $b_{2d+1}=0$ is $\bar{M}_{FI}^{(n)}$ and is given by,

$$(11)\qquad \bar{M}_{FI}^{(n)} = \frac{(-1)^{p_{FI}}}{\sqrt{\sigma_s!\ldots\tau_\alpha!}}\int \mathrm{d}x_1\ldots\int \mathrm{d}x_n \sum r^{(1)}\ldots r^{(n)}\cdot$$

$$\cdot \sum_{d=0}^{[([n/2]+1)/2]} \sum_{b_1=2d-1}^{[n/2]} \sum_{b_2=2d-2}^{b_1-1} \sum_{b_3=2d-3}^{b_2-1} \sum_{b_{2d}=0}^{b_{2d-1}-1} \binom{n}{2b_1}\binom{2b_1}{2b_2}\cdots\binom{2b_{2d-1}}{2b_{2d}} DH\,.$$

Where the terms with $b_{2s-1}=b_{2s}$ have been eliminated and the exapnsion of this expression gives all diagrams without vacuum-vacuum parts.

4. – Alternative expansions and applications to other processes.

The previous expression was derived by introducing the external electron and-photon lines in a particular way. There is no particular reason for this method, it is possible for example to start at a single photon line and find all points connected to it. Since the expressions encountered in expanding the determinants and hafnians will be less symmetric if the approach is followed to some extent the inner sums in (3) and (5) can no longer be lumped into binomial coefficients this will make this work more complicated although this program may be followed to find connected diagrams.

The extraction of self energies by this process does not seem very hopeful. It is possible to find self energies attached to a particular pair of points but this is a very cumbersome method of removing all self energies. There is one class of self energies that is obvious in the present formalism. When $b_{2s}=b_{2s-1}-1$ there is a part joined by only two photon lines.

RIASSUNTO (*)

Una formula concisa per un elemento della matrice S è stata data da Caianiello in termini delle particelle reali che appaiono nel processo. Questa formula contiene in aggiunta ai contributi dei diagrammi che descrivono le interazioni mutue di tutte le particelle che interagiscono fra loro, i contributi di processi disgiunti che avvengono simultaneamente. Nella presente nota si dà un metodo per escludere pezzi sconnessi non desiderati. Come esempio si esegue la rimozione di transizioni vuoto-vuoto nella elettrodinamica quantistica.

(*) *Traduzione a cura della Redazione.*

IL NUOVO CIMENTO Vol. XVII, N. 2 16 Luglio 1960

Upper Limit for the Intrinsic Electric Dipole Moment of the Proton and the Neutrino (*).

S. Rosendorff

Department of Physics, Washington University - St. Louis, Mo.

(ricevuto il 12 Aprile 1960)

Summary. — The elastic scattering of electrons by a proton with an intrinsic electric dipole moment (e.d.m.) is calculated in first Born approximation. The cross section is quite sensitive to the e.d.m. interaction at high energies and large angles. It therefore seems likely that high energy electron-proton scattering may give valuable information of the value or upper limit of the proton e.d.m. coupling strength. Certain spin correlation effects between the recoil proton and the initial electron arising from the e.d.m. interaction are also discussed. In the last section the calculation of the ionization power of a neutrino due to its intrinsic e.d.m. is briefly outlined and compared with the experimental results of Cowan and Reines.

1. – Introduction.

It has been shown [1,2] that if space reflection (P) or time reversal (T) invariance holds, the existence of electric dipole moments (e.d.m.) is impossible. Therefore, detection of an e.d.m. would mean the non-invariance of physical laws under the P and T operations.

However, Ramsey [3] has pointed out that if magnetic monopoles exist electric dipole moments are possible without violating the invariance under the combined inversion PC, where C represents electric charge conjugation.

(*) This work was supported by the U. S. Air Force Office of Scientific Research.

(1) L. Landau: *Nucl. Phys.*, **3**, 127 (1957).

(2) T. D. Lee and C. N. Yang: BNL 443(T-91) (1957).

(3) N. F. Ramsey: *Phys. Rev.*, **109**, 225 (1958).

2159

Such possibility would imply an additional degeneracy for elementary particles, and because of the Pauli principle would change the form of the periodic table and the nuclear shell structure. It is therefore very unlikely that the electron, proton and the neutron have such a degeneracy.

In recent years upper limits for the intrinsic electric dipole moment of several of the elementary fermions have been determined by different techniques. The lowest upper limit for any e.d.m. has been determined for the neutron. SMITH, PURCELL and RAMSEY ([4]) obtained by a magnetic resonance method a value of $5 \cdot 10^{-20} e \cdot \mathrm{cm}$, where e is the charge of the electron. Very recently, BERLEY and GIDAL ([5]) have found that the e.d.m. of the muon must be less than $2 \cdot 10^{-16} e \cdot \mathrm{cm}$. This has been accomplished by deflecting an initially longitudinally polarized muon beam by a strong magnetic field and putting an upper limit on the polarization component perpendicular to the final momentum.

Upper limits for the e.d.m. of the electron have been found by various methods. FEINBERG ([6]), SALPETER ([7]) and SACHS ([8]) have obtained an upper limit of $1 \cdot 10^{-13} e \cdot \mathrm{cm}$ for the e.d.m. of the electron by calculating the effect on the Lamb shift of hydrogen-like atoms due to the hypothetical e.d.m. interaction of the electron and comparing it with known experimental results. Until now, the precession technique ([9,10]) has yielded the lowest upper limit for the e.d.m. of the electron: $3 \cdot 10^{-15} e \cdot \mathrm{cm}$. By a quite different technique, *viz.* high energy Coulomb scattering of electrons by spinless targets ([11]), an upper limit for the e.d.m. of the electron of $8 \cdot 10^{-15} e \cdot \mathrm{cm}$ has been obtained ([12]). It should by pointed out, however, that the e.d.m. of the electron may be considered momentum-transfer dependent. Therefore, as the last mentioned experiment is performed at a much higher energy, it does not necessarily yield the same information as the two other ones.

STERNHEIMER ([13]) has discussed the effects of a proton electric dipole moment on the energy levels of the hydrogen atom and obtained that the e.d.m. of the proton must be less than $1.3 \cdot 10^{-13} e \cdot \mathrm{cm}$.

In Section 2 of the present paper, we discuss in first Born approximation

---

([4]) J. H. SMITH, E. M. PURCELL and N. F. RAMSEY: *Phys. Rev.*, **108**, 120 (1957).
([5]) D. BERLEY and G. GIDAL: *Phys. Rev.* in press.
([6]) G. FEINBERG: *Phys. Rev.*, **112**, 1637 (1958).
([7]) E. E. SALPETER: *Phys. Rev.*, **112**, 1642 (1958).
([8]) M. SACHS: *Ann. Phys.*, **6**, 244 (1959).
([9]) R. L. GARWIN and L. M. LEDERMAN: *Nuovo Cimento*, **11**, 776 (1959).
([10]) D. F. NELSON, A. A. SCHUPP, R. W. PIDD and H. R. CRANE: *Phys. Rev. Lett.*, **2**, 492 (1959).
([11]) B. MARGOLIS, S. ROSENDORFF and A. SIRLIN: *Phys. Rev.*, **114**, 1530 (1959).
([12]) H. W. KENDALL and BURLESON: *Kiev Conference on High Energy Physics* (1959).
([13]) R. M. STERNHEIMER: *Phys. Rev.*, **113**, 828 (1959).

2460

the elastic scattering of electrons by a proton target with an intrinsic e.d.m. It seems likely that high energy electron-proton scattering may give valuable and independent information on the value or upper limit of the proton e.d.m. interaction. As in the electron case, the proton e.d.m. coupling strength is to be considered momentum-transfer dependent. Therefore, such a high energy experiment would shed light also on this particular point. Certain spin correlation effects between the recoil proton and the initial electron arising from the e.d.m. interaction are discussed also in this section. In Section 3 we calculate the ionization power of a neutrino with an intrinsic e.d.m. and compare it with known experimental results.

2. – The e.d.m. of the proton.

Let us consider the elastic scattering of an electron by a proton having a total magnetic moment $(1+K)e/2M$, and an e.d.m. $\lambda e/2M$. K is known to be equal to 1.79. The matrix element for the first Born approximation in momentum space may be written in the form:

$$\mathscr{M} = -4\pi i j_p^\mu(q_2, q_1)\frac{1}{q^2} j_{e\mu}(p_2, p_1)\,, \tag{1}$$

where the proton charge-current density is equal to

$$j_p^\mu(q_2, q_1) = e\overline{U}(\boldsymbol{q}_2)\left[\gamma^\mu F_1(q^2) + \frac{i}{2M}\left(KF_2(q^2) + \lambda F_3(q^2)\gamma_5\right)\sigma^{\mu\nu}q_\nu\right] U(\boldsymbol{q}_1)\,. \tag{2}$$

$U(\boldsymbol{q}_1)$ and $U(\boldsymbol{q}_2)$ are free particle spinors describing the initial and final proton states, $q_\nu = (q_2 - q_1)_\nu = -(p_2 - p_1)_\nu$ is the four-component momentum-energy transfer ([14]), and $q^2 = 4E_1^2\sin^2(\theta/2)/(1 + (2E_1/M)\sin^2(\theta/2))$, where θ is the scattering angle in the lab. system, and E_1 the initial electron energy, assuming always $E_1 \gg m_e$. The three functions $F_i(q^2)$ $(i = 1, 2, 3)$ are form factors associated with the charge, the anomalous magnetic moment, and the e.d.m. of the proton, respectively. The electron charge-current density is, as usually, given by

$$j_{e\mu}(p_2, p_1) = e\,\overline{u}(\boldsymbol{p}_2)\gamma_\mu\, u(\boldsymbol{p}_1)\,, \tag{3}$$

([14]) We have set $\hbar = c = 1$. Furthermore, we use the definitions

$$\gamma^0 = \beta, \qquad \boldsymbol{\gamma} = \beta\boldsymbol{\alpha}, \qquad \sigma^{\mu\nu} = \frac{i}{2}(\gamma^\mu\gamma^\nu - \gamma^\nu\gamma^\mu), \qquad \gamma_5 = \gamma^0\gamma^1\gamma^2\gamma^3\,.$$

where $u(\boldsymbol{p}_1)$ and $u(\boldsymbol{p}_2)$ are the appropriate initial and final free electron spinors. Eq. (1) is invariant under the C operation, but not under the P and T operations. Taking advantage of the fact that $U(\boldsymbol{q}_1)$ and $U(\boldsymbol{q}_2)$ are solutions of the free Dirac equation, eq. (2) may be reduced to:

$$(2') \qquad j^{\mu}_{p}(q_2, q_1) = e\,\overline{U}(\boldsymbol{q}_2)[\gamma^{\mu}F_1 - D^{\mu}_2 F_2 - D^{\mu}_3 F_3]U(\boldsymbol{q}_1)\,,$$

where

$$D^{\mu}_2 = \frac{K}{2M}\left((q_1+q_2)^{\mu} - 2M\gamma^{\mu}\right)\,; \qquad D^{\mu}_3 = \frac{\lambda}{2M}(q_1+q_2)^{\mu}\gamma_5\,.$$

Summing over the initial and final spin states of both particles, the differential cross-section in the lab. system is readily obtained:

$$(4) \qquad \sigma/\sigma_{\mathrm{Ro}} = 1 + (\lambda F_3)^2 (q/2M)^2 / R(q,\theta)\,.$$

σ_{Ro} is the well known «Rosenbluth scattering» cross-section by a physical proton:

$$(5) \qquad \sigma_{\mathrm{Ro}} = \frac{1}{1 + (2E_1/M)\sin^2(\theta/2)}\cdot\sigma_M R(q,\theta)\,,$$

$$(6) \qquad R(q,\theta) = F_1^2 + (q/2M)^2\left[2(F_1 + KF_2)^2 \operatorname{tg}^2\frac{\theta}{2} + (KF_2)^2\right],$$

where σ_M is the Mott scattering cross-section from a spinless point nucleus.

A priori, there is no reason why the three form factors F_i should have the same functional form. Yet, so far, no significant difference between F_1 and F_2 has been detected experimentally ([15]), and all electron-proton scattering experiments up to 550 MeV are consistent with the assumption $F_1 \approx F_2$. This however, could be a misinterpretation of the experimental data, as it is based on the *a priori* assumption of vanishing e.d.m. interaction of the proton. Nevertheless, we will, for the time being, stick to $F_1 = F_2$ even for a non-vanishing e.d.m. interaction. Later, at the discussion of possible polarization effects, it will become clear that this is no more necessary. Of course, nothing can be said about F_3. With $F_1 = F_2$, it is a relatively easy task to determine for a given value of q an upper limit to the e.d.m. term λE_3 ([16]). All one has to do is to compare the values of $\sigma/\sigma_{\mathrm{Ro}}$ at two different angles with the same value of q. As a numerical example, if $\lambda F_3/F_1 = 5$ (according to the Lamb

([15]) R. Hofstadter: *Ann. Rev. Nucl. Sci.*, **7**, 231 (1957).

([16]) See also ref. ([11]), Sect. 2 for a similar discussion about the e.d.m. interaction of the electron.

2462

shift calculation of Ref. ([13]) $\lambda < 13$) the ratio of eq. (4) at $\theta = 60°$ and $\theta = 140°$ for $q/M = 0.5$ would be 1.75. Accurate elastic electron-proton scattering experiments have already been performed ([15]) up to energies of 550 MeV and angles of 135°. As this example shows, such an experiment seems to provide a sensitive method to put an upper limit on the e.d.m. interaction. As this hypothetical interaction may be regarded q-dependent, the experiment should be performed for different values of q.

Additional information on the e.d.m. interaction in particular, and non-invariance of the electromagnetic interaction under space reflection and time reversal operations in general, could be obtained by detecting certain spin correlation effects between the recoil proton and the initial electron. In order to see that, we have to calculate the cross-section $\sigma(q, \zeta; \zeta_e, \zeta_p)$, where ζ_e describes the initial electron polarization and ζ_p the final proton polarization. This cross-section is readily obtained by standard trace technique, if use is made of the known ([17]) relativistically covariant spin projection operator:

$$P(\zeta_e) = \tfrac{1}{2}(1 + i\gamma_5 S_e) ,$$

where

$$\left| \begin{array}{l} S_e^{\mu} = \left(\dfrac{(\boldsymbol{p}_1 \cdot \boldsymbol{\zeta}_e)}{m}, \ \boldsymbol{S}_e' \right) \\ \boldsymbol{S}_e' = \boldsymbol{\zeta}_e + \dfrac{\boldsymbol{p}_1 (\boldsymbol{p}_1 \cdot \boldsymbol{\zeta}_e)}{m(E_1 + m)} \end{array} \right.$$

with an analogous operator for the proton. The result, assuming again $E_1 \gg m_e$, can be written in the form:

$$(7) \qquad \sigma(q, \theta; \zeta_e, \zeta_p) = \frac{\sigma_M}{1 + (2E_1/M) \sin^2 \theta/2} \Big[R(q, \theta) + (q/2M)^2 (\lambda F_3)^2 + \\ + (\lambda F_3)(F_1 + KF_2)(q/2M)^2 \sec^2 \frac{\theta}{2} (\boldsymbol{n}_1 \cdot \boldsymbol{\zeta}_e)(\boldsymbol{n}_1 \times \boldsymbol{n}_2 \cdot \boldsymbol{\zeta}_p) + S(q, \theta; \zeta_e, \zeta_p) \Big] ,$$

where $\boldsymbol{n}_1$ and $\boldsymbol{n}_2$ are units vectors in the direction of the initial and final electron momenta $\boldsymbol{p}_1$ and $\boldsymbol{p}_2$, and $R(q, \theta)$ is defined by eq. (6). As is obvious from eq. (7) the term proportional to λ arises from the interference between the e.d.m. interaction and the Dirac plus Pauli interaction. There is no polarization dependent λ^2 term. The function S has not been calculated explicitly, but is certainly λ-independent. Detection of the term proportional to λ in

([17]) H. A. TOLHOEK: *Rev. Mod. Phys.*, **28**, 277 (1956).

eq. (7) would imply the non-invariance of the electromagnetic interaction under P and T operations. This is obvious, as this term follows directly from the e.d.m. interaction which, as has already been pointed out, violates both P and T invariance.

More generally, any interaction Hamiltonian which violates P as well as T will in first Born approximation (*i.e.* neglecting final state interaction) give rise to terms in the cross-section with similar structure as the λ term in eq. (7), namely, terms which involve an even number of spins and an odd number of momenta. This follows immediately from a well known theorem proved by LEE and YANG [2]. Of course, nothing can be said about the energy and angular dependence of these terms in general. This is possible only, when the interaction Hamiltonian is given explicitly (*e.g.* the e.d.m. interaction). It is easy to show that terms of this kind, and only of this kind, (in first Born approximation) contribute to polarization of the recoil proton which is perpendicular to the scattering plane, provided the initial electron beam is longitudinally polarized. The simplest representative of this type of terms is $(\boldsymbol{q}\cdot\boldsymbol{\zeta}_e\times\boldsymbol{\zeta}_p)$; another one is $(\boldsymbol{p}_1\cdot\boldsymbol{\zeta}_e)(\boldsymbol{p}_1\times\boldsymbol{p}_2\cdot\boldsymbol{\zeta}_p)$ which appears in eq. (7), etc. On the other hand, terms which do not violate P and T invariance are even in both momenta and spins, like $(\boldsymbol{\zeta}_e\cdot\boldsymbol{\zeta}_p)$ or $(\boldsymbol{p}_1\times\boldsymbol{p}_2)\cdot(\boldsymbol{\zeta}_e\times\boldsymbol{\zeta}_p)$, etc. It is evident that these terms cannot contribute to perpendicular proton polarization (for initial longitudinal electron polarization). Thus, the function S in eq. (7) which includes only P and T invariant terms, has no influence whatsoever on the perpendicular polarization of the proton.

Now, if the initial electron beam is longitudinally polarized, the polarization of the recoil proton perpendicular to the scattering plane follows in an obvious way from eq. (7). It is given by the expression:

$$P_\perp = \frac{2(\lambda F_3)(F_1 + KF_2)(q/2M)^2 \operatorname{tg}(\theta/2)}{R(q,\theta) + (q/2M)^2(\lambda F_3)^2}\,. \tag{8}$$

As a numerical example, consider an initial electron energy of $E_1/M = 0.25$ and $\lambda F_3/F_1 = 1$, then for a scattering of 120°, the recoil energy of the proton would be $T_p/M = 0.07$ with a perpendicular polarization of 12% (assuming again $F_1 = F_2$). Thus, a substantial proton polarization could be expected for a relatively small value of the e.d.m. coupling strength. There is an additional transverse polarization of the proton to be expected which comes from the ordinary (P and T invariant) proton-electron interaction in higher Born approximations. However, this effect, which arises from a spin-orbit coupling, is estimate to be of the order of 0.75%. It is therefore negligibly small. The transverse polarization of the proton could be analysed by proton-proton or proton-nuclei scattering. Of course, such an experiment would involve the production of a high energy longitudinally polarized electron beam, which may

2464

be a difficult task at the present time. Finally, it should be pointed out, that the measurement of the differential cross-section (4) as a function of the scattering angle θ (for a constant value of q) plus a measurement of the polarization (8) provide a unique solution for the three unknown functions F_1, F_2, and λF_3.

3. – The e.d.m. of the neutrino.

As for the e.d.m. of the neutrino, it is most easily determined by considering the ionization power due to the interaction of the e.d.m. with the electrons. If we take into account only those electrons, whose kinetic energy W is much larger than the ionization potential of the atom, it is easy to show that, to a good approximation, momentum is conserved in the collision [18]. Therefore, the electron may be regarded a free particle, and its total energy after the collision will be $\sqrt{(\boldsymbol{p}_2 - \boldsymbol{p}_1)^2 + m^2}$. It follows, that the matrix element responsible for this interaction is given by eq. (1), provided we put there $F_1 = F_2 = 0$.

Then, after summing over the spin states of the neutrino and the electron, we obtain for the energy distribution of the secondary electrons the expression:

$$\Phi(W)\,\mathrm{d}W = 4\pi(e\lambda_\nu F_3)^2(1 - W/E)\,\mathrm{d}W/W\,, \tag{9}$$

where λ_ν is the e.d.m. of the neutrino and E its initial energy. Eq. (9) is obtained after taking the limit of vanishing neutrino mass.

Now, exactly the same expression is obtained for a magnetic dipole interaction. This has been calculated a long time ago by BETHE [19]. COWAN and REINES [20] have performed an experiment in order to determine an upper limit for the magnetic dipole of the neutrino. We can directly take over their result:

$$\lambda_\nu F_3 < 2 \cdot 10^{-20}\, e \cdot \mathrm{cm}\,.$$

---

[18] For a more thorough discussion of this problem, see H. A. BETHE: *Handb. d. Phys.*, Bd. **24** (1) (Berlin, 1933), p. 491.

[19] H. A. BETHE: *Proc. Cam. Phil. Soc.*, **31**, 108 (1935). Actually, our formula differs from Bethe's expression by a factor $m/(m+W)$. This is so, because we use a slightly different approximation in the derivation of the density of final states.

[20] C. L. COWAN and F. REINES: *Phys. Rev.*, **107**, 528 (1957).

It is perhaps worth-while mentioning that a hypothetical e.d.m. due to the weak interaction would most probably be smaller than $(10^{-23} \div 10^{-24})\, e \cdot \mathrm{cm}$.

* * *

The author is much indebted to Prof. H. PRIMAKOFF and Dr. S. TANI for many helpful discussions.

RIASSUNTO (*)

Si calcola in prima approssimazione di Born lo scattering elastico di elettroni su un protone con un momento elettrico dipolare (e.d.m.) intrinseco. La sezione trasversale è molto sensibile alle interazioni e.d.m. di alte energie ed angoli grandi. Sembra quindi verosimile che lo scattering protone-elettrone di alta energia possa dare valide informazioni sul valore o sul limite superiore della forza dell'accoppiamento e.d.m. del protone. Si discutono anche alcuni effetti di correlazione di spin fra il protone di rinculo e l'elettrone iniziale nascenti dalla interazione e.d.m. Nell'ultima sezione si delinea brevemente il calcolo del potere ionizzante del neutrino dovuto al suo e.d.m. intrinseco e si paragona ai risultati sperimentali di Cowan e Reines.

(*) *Traduzione a cura della Redazione.*

2466

(La responsabilità scientifica degli scritti inseriti in questa rubrica è completamente lasciata dalla Direzione del periodico ai singoli autori)

Search for Antineutron Annihilation Events in Nuclear Emulsions.

TSAI-CHÜ, M. MORAND, G. BOURLET, C. SIMONIN and D. SCHUNE

Laboratoire de Physique Enseignement, Faculté des Sciences - Paris

(ricevuto il 13 Aprile 1960)

Shortly after the production of antiprotons [1] by the Bevatron, antineutrons [2,3] were created by charge exchange of antiprotons in matter and detected by electronic means. However, up to now, no antineutron annihilation event has been observed in nuclear emulsions. We followed more than 250 antiproton tracks through the plates contained in a stack of K-5 emulsions exposed to the enriched antiproton beam of 740 MeV/c. About half of the antiprotons had been annihilated in flight; among them we observed seven « stops ». In two cases a small nuclear recoil was possibly present. An antiproton stop should indicate either a charge exchange of the antiproton into an antineutron or an annihilation star without any charged prongs. Antineutrons can also be created in charge exchange stars produced inside the stack or in antiproton interactions occurred outside. In the course of scanning, we happened to find a star produced by a neutral primary, with more than two minimum-ionizing tracks emerging from the star. We suspected it to be an antineutron annihilation event. A systematic search was made afterwards along the prolongation of the stops and their neighborhood and in the proximity of the charge exchange stars. As a result, four other antineutron annihilation events were found.

Fig. 1 shows a projection drawing of one of our antineutron annihilation events observed. The star has 17 prongs; it involves an associated production of K^--K^0-mesons, with the K^0 decaying as θ^0 into two π^0's immediately after the production and each π^0 in turn decaying, respectively, into a Dalitz pair and a γ-ray. In our experiment, the antiproton beam arrives at the stack from the upper side of Fig. 1 and follows a direction approximately parallel to that of prong 15. After 1.5 cm, the antiproton comes to a stop in the emulsion. This occurs at 50 μm from the glass of the second plate. It has a kinetic energy of 240 MeV, and a dip angle of $-4^\circ\ 20'$

[1] O. CHAMBERLAIN, E. SEGRÈ, C. WIEGAND and T. YPSILANTIS: *Phys. Rev.*, **100**, 947 (1955).

[2] B. CORK, G. R. LAMBERTSON, O. PICCIONI and W. A. WENZEL: *Phys. Rev.*, **104**, 1193 (1956).

[3] J. BUTTON, T. ELIOFF, E. SEGRÈ, H. M. STEINER, R. WEINGART and T. YPSILANTIS: *Phys. Rev.*, **108**, 1557 (1957).

in the direction from glass to air. The antineutron annihilation star and the stop appear in the same plate 1.95 cm apart. The probability for an accidental coincidence of the two events is less than 10^{-4}. The arrow shown in Fig. 1 represents the direction of the antineutron and the dip angle of the antineutron is estimated at $-1° 20'$. The resultant momentum of the prongs of this star shows a major unbalanced component in the direction of the antineutron. The two electron pairs of the θ^0-meson are formed by the four minimum-ionizing tracks (prongs 1, 2, 5, and 14): the space angle between the first pair is 33°; that between the second is 46°. Electrons are identified by ioni-

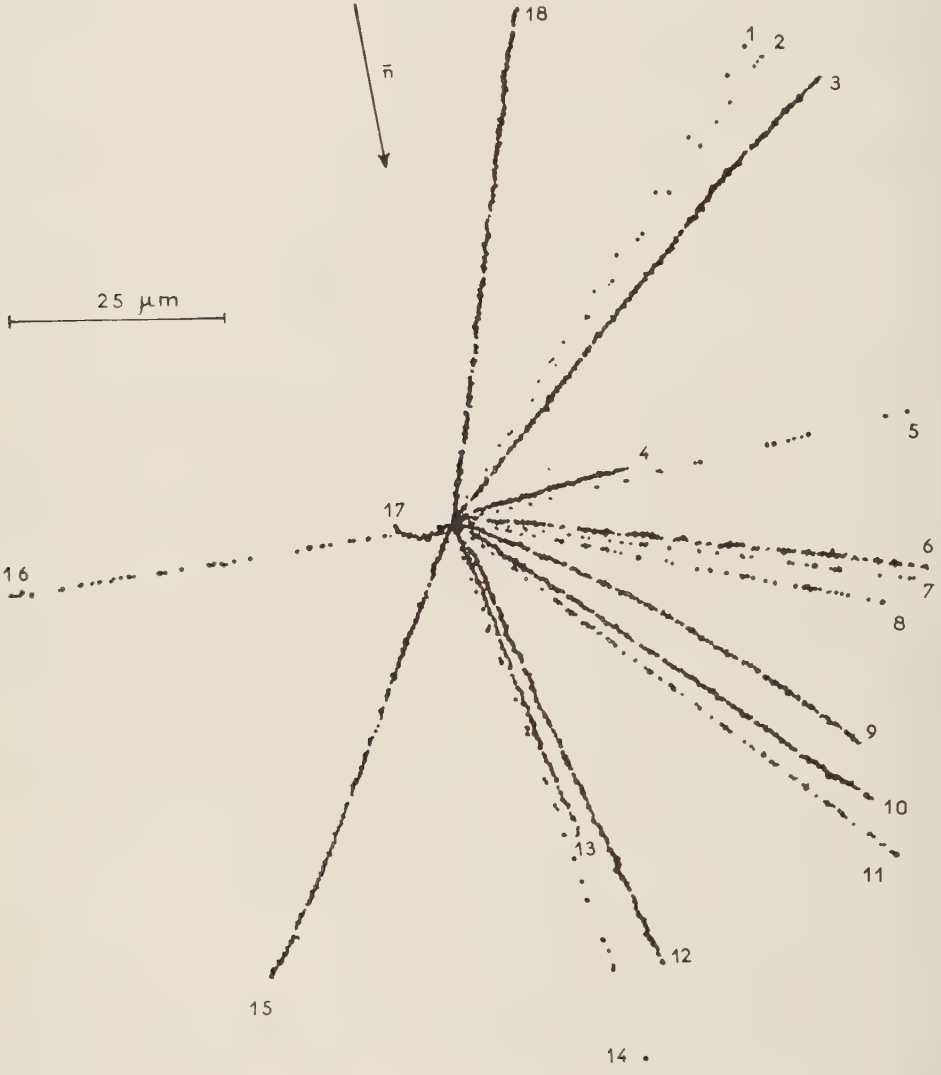

Fig. 1. – The antineutron annihilation star.

zation and multiple scattering. Distortion is considered and eliminated for steep tracks. Prong 14 is doubtless an electron, as it degenerates into a low energy electron in the middle of the emulsion. The K^--meson (prong 7) is emitted with an energy of (124 ± 11) MeV. After 1.63 cm across 13 plates, it makes an inelastic scattering involving an energy loss of 55 MeV and a deflection of 22° 30′. 1.3 mm further on, it interacts again and produces a small star containing two protons and a nuclear recoil with a total visible energy of 20 MeV. The mass of the K^--meson measured by ionization and scattering is (944 ± 90) m_e before, and (940 ± 200) m_e after, deflection. The three knock-on protons (prongs 8, 11, and 16) are identified by the increase of grain density along the trajectory. Prong 11 produces a small star of 66 MeV after 9.6 mm. After 2.45 cm, prong 16 also produces a star of two protons: one of 11 MeV is ejected nearly perpendicular to it and the other of 79 MeV at an angle of about 10°. Prong 17 is a low-energy electron. The other prongs (3, 6, 9, 10, 12, 13, 15, and 18) are all low-energy evaporation protons, except prong 4 which could be an α particle; all come to rest in the emulsion. Assuming a binding energy of 8 MeV for a proton and 2 MeV for an α particle, we have a total energy of 1.44 GeV for the whole star (Table I). The total available energy of the antineutron and the nucleon before annihilation is about 2 GeV Therefore the remaining energy, 0.6 GeV, is shared among the two γ-rays of the π^0's and the knock-on and evaporation neutrons. Through charge conservation, at least one positive pion is emitted together with the K-mesons in the annihilation of the antineutron with a neutron and at least two positive pions are emitted in an antineutron-proton annihilation The positive pions are absorbed afterwards and produce the knock-on and evaporation nucleons.

TABLE I. – *Nature, direction and energy of the prongs of the antineutron annihilation star.*

Prong no.	Nature	Dip (degree)	Energy (MeV)
1	e	— 11	90 ± 9
2	e	22	67 ± 10
3	p	— 43	8.7
4	α	8	5.3
5	e	52	80 ± 30
6	p	59	15.6
7	K^-	24	124 ± 11
8	p	33	106 ± 10
9	p	— 23	8.6
10	p	11	3.1
11	p	45	91 ± 10
12	p	— 32	4.7
13	p	9	2.0
14	e	46	73 ± 18
15	p	30	13.2
16	p	22	168 ± 10
17	e	—	—
18	p	— 31	6.4

It is very unlikely that the antineutron events mentioned in this paper could be produced by cosmic-ray neutrons. High energy protons and neutrons in cosmic rays have a sharp zenithal distribution in lower altitudes; 94% of them are contained in a cone having a half opening angle of 45° and an axis in the vertical direction. For one day's flight, the number of stars produced by fast cosmic ray neutrons outside the cone should be 0.01 instead of 5 as in our scanned volume. Furthermore, if it were a cosmic-ray event, the estimated energy for a primary neutron should be hardly over the threshold value for the production of K-mesons. Again, all the secondary prongs of the star should be collimated along the direction of the primary, instead of the observed distribution.

The four electrons of the star cannot be interpreted as the decay products

2469

from a single π^0. Their resultant momentum is $p=211$ MeV, their total energy $E=313$ MeV, the mass of the π^0 calculated from $m_0c^2 = (E^2 - p^2c^2)^{\frac{1}{2}}$ will be 230 MeV. This impossible supposition is quite evident from their wide angular separations (Fig. 1). The next alternative is to interprete them as the products from two independent π^0's. This is again excluded by the insufficient energy available from antineutron annihilation.

It is still too early to predict that complete similarities exist between antiproton and antineutron annihilation events. But, for the moment, it is interesting to point out the excess of pions of different signs. The study of antiprotons has furnished a large number of $\bar{p}p$ and $\bar{p}n$ annihilation events; while the study of antineutrons will give $\bar{n}n$ and $\bar{n}p$ annihilation events. An excess of negative pions is observed in antiproton annihilation events; this follows directly from the conservation of charge. In contrast with the antiproton annihilation events, an excess of positive pions will be present in antineutron annihilation events.

* * *

We wish to express our sincere thanks to our colleagues in Berkeley and Bristol for the exposure and preparation of the emulsions. We also want to thank Mr. R. CUNYGHAM-BROWN, Mrs. M. CALLIAUD, Mrs. L. VAN ROSSUM, and Mrs. H. Y. CHANG for technical assistance.

2470

Some Remarks about the Spectral Representation of the $K^{\pm} \to 3\pi$ Decay Amplitude.

S. Fubini

CERN - Geneva
Istituto di Fisica dell'Università - Padova

R. Stroffolini (*)

CERN - Geneva

(ricevuto il 15 Giugno 1960)

The effect of pion-pion interaction on the $K^{\pm} \to 3\pi$ spectrum has been recently investigated [1,2].

The following representation has been proposed for the decay amplitude $A^d(s_1, s_2, s_3)$:

$$A^d(s_1, s_2, s_3) = \frac{1}{\pi}\int_{4\mu^2}^{\infty} \frac{g(x)\,\mathrm{d}x}{x - s_1 - i\varepsilon} + \frac{1}{\pi}\int_{4\mu^2}^{\infty} \frac{g(x)\,\mathrm{d}x}{x - s_2 - i\varepsilon} + \frac{1}{\pi}\int_{4\mu^2}^{\infty} \frac{g(x)\,\mathrm{d}x}{x - s_3 - i\varepsilon}\,, \tag{1}$$

where

$$s_i = (K - \pi_i)^2\,,$$

(K and π_i denote the momenta of the K-particle and of the pions). [3]

From the representation (1) an integral equation has been derived which can be approximately solved by taking into account only the effect of the lowest singularities. This has enabled some information to be obtained from the K spectrum about the s-wave pion-pion interaction.

Representation (1) can be simply understood in the following manner. Let us consider the unphysical case in which the mass of the K-meson is of the same order of magnitude as the pion mass; in such a case we have to deal with the scattering process

$$\mathrm{K} + \pi \to \pi + \pi\,. \tag{2}$$

(*) On leave from: Istituto di Fisica Teorica dell'Università di Napoli.

(1) N. N. Khuri and S. B. Treiman: Princeton preprint.

(2) R. F. Sawyer and K. L. Wali: University of Wisconsin preprint.

(3) In order to simplify the notation we shall disregard here the complications due to the charge of the pions.

Perturbation theory then suggests the validity of the Mandelstam representation for the scattering amplitude A^s of the process (2)

$$(3) \qquad A^s(s_1, s_2, s_3) = \frac{1}{\pi^2}\iint \frac{\varrho(x, y)\,\mathrm{d}x\,\mathrm{d}y}{(x - s_1 - i\varepsilon)(y - s_2 - i\varepsilon)} + \\ + \frac{1}{\pi^2}\iint \frac{\varrho(x, y)\,\mathrm{d}x\,\mathrm{d}y}{(x - s_2 - i\varepsilon)(y - s_3 - i\varepsilon)} + \frac{1}{\pi^2}\iint \frac{\varrho(x, y)\,\mathrm{d}x\,\mathrm{d}y}{(x - s_3 - i\varepsilon)(y - s_1 - i\varepsilon)} .$$

It has been shown by M. CINI and one of us [4] that under very general arguments on the location of the singularities, the Mandelstam representation can be transformed into the approximate form, valid for $|s_i| < 16\mu^2$

$$(4) \qquad A^s(s_1, s_2, s_3) = \frac{1}{\pi}\int_{4\mu^2}^{\infty} \frac{g(x)\,\mathrm{d}x}{x - s_1 - i\varepsilon} + \frac{1}{\pi}\int_{4\mu^2}^{\infty} \frac{g(x)\,\mathrm{d}x}{x - s_2 - i\varepsilon} + \frac{1}{\pi}\int_{4\mu^2}^{\infty} \frac{g(x)\,\mathrm{d}x}{x - s_3 - i\varepsilon} ,$$

the spectral function $g(x)$ can be obtained by computing the imaginary part of A^s for $s_1 > 4\mu^2$. Since only the denominator of the first term can vanish, we get

$$(4') \qquad \mathrm{Im}\, A^s(s_2, s_2, s_3) = g(s_1) .$$

On the other hand, the theorem of final state interaction [5] as applied to the process (2) gives

$$(5) \qquad g(s) = A_0(s) \exp[-i\delta(s) \sin \delta(s) ,$$

where $\delta(s)$ is the s-wave pion-pion phase shift and $A_0(s)$ is the s-wave part of the amplitude A. Eq. (5) follows from the fact that the K-meson is here connected to pions only through a weak interaction.

Now it is easy to observe that the representation for the decay amplitude can be written in the form (1) by assuming that eq. (4), together with the expression (5) of $g(x)$ valid for the scattering process, can be extended also to the actual value of M_K corresponding to the decay process.

The possibility of justifying such continuation has been studied by G. BONNEVAY [6] who has investigated in detail the analytical properties of the decay amplitude in the mass of the K-meson.

We point out here that in the representation (1) for the decay process a new feature arises. All three denominators in eq. (1) can vanish simultaneously for values of s_1, s_2, s_3 in the physical region.

If we assume the validity of (1) and (5) for the decay process, then the spectral function $g(s)$ must be a complex quantity [7]. This can be easily seen in the following manner. Let us assume $g(s)$ to be real, then eq. (5) tells us that

$$\mathrm{Im}\, A_0(s) = g(s) .$$

---

[4] M. CINI and S. FUBINI: to be published in *Ann. of Phys.*

[5] S. FUBINI, Y. NAMBU and V. WATAGHIN: *Phys. Rev.*, **111**, 329 (1958), Appendix II.

[6] G. BONNEVAY: private comunication.

[7] This result has also been obtained independently by G. BONNEVAY and A. STANGHELLINI.

2472

This result is in contrast with what one would obtain for g real by taking the imaginary part of eq. (1)

$$\text{Im } A^d(s_1, s_2, s_3) = g(s_1) + g(s_2) + g(s_3) .$$

We see therefore that the representation (1) for the decay process has a completely different mathematical structure than the similar equation for scattering. In order to understand the physical meaning of the imaginary part of g let us write

$$\varrho(s) = \frac{g(s) - g^*(s)}{2i} . \tag{6}$$

Let us take the imaginary part of A^d

$$\text{Im } A^d = g(s_1) + g(s_2) + g(s_3) + \frac{1}{\pi}\left[\int_{4\mu^2}^{\infty} \frac{\varrho(x)\,\mathrm{d}x}{x - s_1 + i\varepsilon} + \int_{4\mu^2}^{\infty} \frac{\varrho(x)\,\mathrm{d}x}{x - s_2 + i\varepsilon} + \int_{4\mu^2}^{\infty} \frac{\varrho(x)\,\mathrm{d}x}{x - s_3 + i\varepsilon}\right] . \tag{7}$$

We note that the term containing $\varrho(x)$ must vanish for $M_K \to 3\mu$.

Now, using the unitarity of the S-matrix, and invariance under time reversal and under the Lorentz transformations ([5]), one obtains the following general expression for the imaginary part of the decay amplitude:

$$\text{Im } A^d(\pi_1, \pi_2, \pi_3) = \int T^+(\pi_1, \pi_2, \pi_3;\ \pi_1', \pi_2', \pi_3') A^d(\pi_1', \pi_2', \pi_3') \cdot \tag{8}$$

$$\cdot \delta(\pi_1'^2 + \mu^2)\,\delta(\pi_2'^2 + \mu^2)\,\delta(\pi_3'^2 + \mu^2)\,\theta(\pi_1')\,\theta(\pi_2')\,\theta(\pi_3') \cdot \mathrm{d}^4\pi_1'\,\mathrm{d}^4\pi_2'\,\mathrm{d}^4\pi_3'$$

where T is the transition matrix element from the state π_1, π_2, π_3 to the state π_1', π_2', π_3'. By comparing eq. (7) with eq. (8) it is possible to recognize the contributions to eq. (7) as due to the effect of correlations between 2 pions or 3 pions.

We thus split the matrix element T into a connected and a disconnected part

$$T = T_c + T_{nc} , \tag{9}$$

where

$$T_{nc} = 2\pi_1^0 \delta^3(\boldsymbol{\pi}_1 - \boldsymbol{\pi}_1')\, t(\pi_2, \pi_3;\ \pi_2', \pi_3') + 2\pi_2^0 \delta^3(\boldsymbol{\pi}_2 - \boldsymbol{\pi}_2')\, t(\pi_1, \pi_3;\ \pi_1', \pi_3') + \tag{10}$$

$$+ 2\pi_3^0 \delta^3(\boldsymbol{\pi}_3 - \boldsymbol{\pi}_3')\, t(\pi_1, \pi_2;\ \pi_1', \pi_2') ,$$

$t(\pi_i, \pi_j;\ \pi_i', \pi_j')$ is the pion-pion scattering amplitude, and $T_c\ (\pi_1, \pi_2, \pi_3;\ \pi_1', \pi_2', \pi_3')$ is the matrix element representing the sum of all those graphs in which all three pions are involved.

Let us substitute eqs. (9) and (10) into eq. (8). It is easy to verify that the contribution of the disconnected part T_{nc} (if one keeps only the pion-pion s-waves) reproduces exactly the term $\sum_i g(s_i)$ in the r.h.s. of eq. (7) where $g(s)$ is given by eq. (5).

The contribution of the connected part T_c can therefore be identified with the

term $\sum_i \int \varrho(x)\,\mathrm{d}x/(x - s_i + i\varepsilon)$, such a term, as previously stated, vanishes where M_K decreases to 3μ.

We see therefore that the imaginary part $\varrho(x)$ of the spectral function $g(x)$ is directly connected with the 3 pion transition amplitude. Thus eq. (1) might be a tool for constructing the 3 pion amplitude in terms of the pion-pion phase shifts.

* * *

We wish to thank Dr. D. AMATI, G. BONNEVAY, A. STANGHELLINI and B. VITALE for very useful comments and criticism. We are particularly grateful to Dr. G. BONNEVAY for having shown us his unpublished work; many questions have become clearer from comparison with his results.

2474

IL NUOVO CIMENTO Vol. XVII, N. 2 16 Luglio 1960

An Improved Version of an Ergodic Theorem in Quantum Mechanics.

G. M. Prosperi and A. Scotti

Istituto di Scienze Fisiche dell'Università - Milano
Istituto Nazionale di Fisica Nucleare - Sezione di Milano

(ricevuto il 21 Giugno 1960)

In this letter we intend giving an improved version of a theorem established in a previous paper (1) (this paper will be referred to in the following as A). The new version is stronger than the older one and conceptually more satisfactory.

The fundamental formula proved in A is the following:

$$\text{(A.10)} \qquad P\Big\{\bigcup_{\nu=1}^{N}[\vartheta_\nu(a,\psi_0)>\bar{\vartheta}]\Big\}<\exp\left[-\varkappa\sqrt{s_{\min}a}+\varkappa+\log\frac{SN}{\bar{\vartheta}}\right], \qquad \varkappa\simeq 0.3,$$

where $\vartheta_\nu(a,\psi_0)$ denotes the time fraction during which the quantity

$$\Delta_\nu(t,\psi_0)\equiv\frac{(u_\nu(t)-s_\nu/S)^2}{s_\nu^2/S^2},$$

(square deviation of the quantum mechanical probability of occupation of the ν^{th} cell from the microcanonical value s_ν/S) remains greater than a and P denotes the measure of the set of initial state vectors ψ_0 for which even one of the $\vartheta_\nu(a,\psi_0)$ alone is greater than $\bar{\vartheta}$.

Formula (A.10) will here be substituted by the following one, which expresses our new version of the theorem:

$$\text{(1)} \qquad P\{\vartheta(a,\psi_0)>\bar{\vartheta}\}<\exp\left[-\varkappa\sqrt{s_{\min}a}+\varkappa+\log\frac{SN}{\bar{\vartheta}}\right],$$

where now $\vartheta(a,\psi_0)$ (*) represents the time fraction during which even one of the $\Delta_\nu(t,\psi_0)$ alone is greater than a and P is the measure of the set of initial state vectors ψ_0 for which ϑ is greater than $\bar{\vartheta}$.

---

(1) G. M. Prosperi and A. Scotti: *Nuovo Cimento*, **13**, 1007 (1959).
(*) Notice that the symbol ϑ was used in the last section of paper A with another meaning.

To deduce formula (1) let us start by considering the following relation

$$P\{\bigcup_{\nu=1}^{N}[\Delta_\nu(t,\psi_0)>a]\}<\exp[-\varkappa\sqrt{s_\nu a}+\varkappa+\log SN]\,. \tag{A.6}$$

Let us, then, call Ω the hypersphere of the vectors of unit norm of the energy shell and $(0, T)$ the time interval during which the evolution of the system is considered (assumed to be fixed, and, at least in the first instance, finite).

Proceeding now in a way analogous to that followed in lemma (A.7) let $C(\overline{\psi}_0, a)$ and $D(\overline{t}, a)$ be the set of values of the time interval $(0, T)$ and the part of Ω for which at least one of the following relations is verified

$$\Delta_\nu(t,\psi_0)>a\,, \qquad (\nu=1,2,\ldots,N), \tag{2}$$

for $\psi_0=\overline{\psi}_0$ and $t=\overline{t}$ respectively.

Then by definition we have

$$\vartheta(\overline{\psi}_0,a)=\int_{C(\overline{\psi}_0,a)}\frac{\mathrm{d}t}{T}\,,\qquad P\{\bigcup_{\nu=1}^{N}[\Delta_\nu(\overline{t},\psi_0)>a]\}=\int_{D(\overline{t},a)}\frac{\mathrm{d}\sigma}{\Sigma}\,, \tag{3}$$

where $\mathrm{d}\sigma$ denotes the element of area of the spherical hypersurface Ω and Σ its total area.

By known theorems on integration we obtain

$$\int_{\Omega}\frac{\mathrm{d}\sigma}{\Sigma}\int_{C(\psi_0,a)}\frac{\mathrm{d}t}{T}=\int_{0}^{T}\frac{\mathrm{d}t}{T}\int_{D(t,a)}\frac{\mathrm{d}\sigma}{\Sigma}\,. \tag{4}$$

And thus, from (A.6)

$$\int_{\Omega}\frac{\mathrm{d}\sigma}{\Sigma}\,\vartheta(a,\psi_0)=\int_{0}^{T}\frac{\mathrm{d}t}{T}\,P\{\bigcup_{\nu=1}^{N}[\Delta_\nu(t,\psi_0)>a]\}<\exp[-\varkappa\sqrt{s_{\min}a}+\varkappa+\log SN]\,. \tag{5}$$

From which (1) follows immediately by noticing that the left hand side is clearly greater than $\overline{\vartheta}\,P\{\vartheta(a,\psi_0)>\overline{\vartheta}\}$.

2476

IL NUOVO CIMENTO Vol. XVII, N. 2 16 Luglio 1960

Remarks on Neutral Pion Photoproduction in the High Energy Region.

C. Pellegrini and G. Stoppini

Laboratori Nazionali del Comitato Nazionale per le Ricerche Nucleari - Frascati

(ricevuto il 30 Giugno1960)

J. J. Sakurai [1] proposed the measurement of the recoil proton polarization in the process

$$\gamma + p \to \pi^0 + p \,, \tag{1}$$

as a possible means of assigning the parity of the second resonance recently observed in the pion nucleon scattering and photo-production [2]. In the energy region between the first and the second resonance, namely around $E_\gamma = 600$ MeV, the polarization predicted was as high as 80% for negative parity and zero for positive parity.

The experimental results [3] show indeed a high polarization, though less than 80%, in the energy region (550÷850) MeV (Table I) and this can be taken as a support to the negative parity assignment.

We already pointed out [4] that the presence of a small s-wave amplitude can appreciably change Sakurai's predictions, so to make the interpretation of the experimental results not completely unambiguous, if the large experimental errors are also taken into account.

[1] J. J. Sakurai: *Phys. Rev. Lett.*, **1**, 258 (1958).

[2] J. W. De Wire, H. E. Jackson and R. Littauer: *Phys. Rev.*, **110**, 1208 (1958); P. C. Stein and K. C. Rogers: *Phys. Rev.*, **110**, 1209 (1958); M. Heinberg, W. M. McClelland, F. Turkot, W. M. Woodward and D. M. Zipoy: *Phys. Rev.*, **110**, 1211 (1958); F. P. Dixon and R. L. Walker: *Phys. Rev. Lett.*, **1**, 142 (1958).

[3] R. Querzoli, G. Salvini and A. Silverman: private communication, to be published. The errors given by these authors includes all the corrections. P. C. Stein: *Phys. Rev. Lett.*, **2**, 473 (1959); L. Bertanza, P. Franzini, I. Mannelli, V. Z. Peterson and G. V. Silvestrini: private communication; J. O. Maloy, J. I. Friedman, H. Kendall, A. Manfredini, V. Z. Peterson and G. Salandin: private communication. The two last are preliminary results, submitted to Rochester Conference on High Enegry Physics (1960). We thank the above mentioned authors for the communication of their data.

[4] C. Pellegrini and G. Stoppini: reported by G. Bernardini at the Kiev Conference on High Energy Physics (1959).

TABLE I. – *Polarization of the recoil protons emitted at 90° in the c.m.*

E_γ (MeV)	R. QUERZOLI, G. SALVIN and A. SILVERMAN	P. C. STEIN	L. BERTANZA *et al.*	I. O. MALOY *et al.*
550	—	0.30 ± 0.12	—	—
560	0.4 ± 0.14	—	—	—
585	—	—	—	0.35 ± 0.16
610	0.63 ± 0.27	—	—	
650	0.59 ± 0.24	—	—	—
658	—	—	—	0.50 ± 0.18
700	0.56 ± 0.11	0.59 ± 0.06	—	—
720	—	—	0.82 ± 0.29	—

In the region (700÷850) MeV preliminary results by R. QUERZOLI *et al.* seem to indicate a polarization yet equal to about 50 %.

As a matter of fact let us consider two models *a*) and *b*) for reaction (1) proposed respectively by R. R. WILSON [5] and R. F. PEIERLS [6] according to the transition matrices

$$(2) \qquad M_a = iE_1(\tfrac{1}{2})\boldsymbol{\sigma}\cdot\boldsymbol{e} - \frac{1}{kq}[M_1(\tfrac{3}{2},\tfrac{1}{2}) + M_1(\tfrac{3}{2},\tfrac{3}{2})]\{2\boldsymbol{q}(\boldsymbol{k}\times\boldsymbol{e}) - i(\boldsymbol{\sigma}\cdot\boldsymbol{k}\,\boldsymbol{q}\cdot\boldsymbol{e} - \boldsymbol{\sigma}\cdot\boldsymbol{e}\,\boldsymbol{q}\cdot\boldsymbol{k})\},$$

$$(3) \qquad M_b = iE_1(\tfrac{1}{2})\boldsymbol{\sigma}\cdot\boldsymbol{e} - \frac{1}{kq}M_1(\tfrac{3}{2},\tfrac{3}{2})\{2\boldsymbol{q}\cdot(\boldsymbol{k}\times\boldsymbol{e}) - i(\boldsymbol{\sigma}\cdot\boldsymbol{k}\boldsymbol{e}\cdot\boldsymbol{q} - \boldsymbol{\sigma}\cdot\boldsymbol{e}\,\boldsymbol{q}\cdot\boldsymbol{k})\} -$$

$$- iE_1(\tfrac{3}{2},\tfrac{1}{2})\frac{1}{q^2}\{3\boldsymbol{\sigma}\cdot\boldsymbol{q}\boldsymbol{e}\cdot\boldsymbol{q} - q^2\boldsymbol{\sigma}\cdot\boldsymbol{e}\},$$

where $E_e(J, T)$ and $M_e(J, T)$ are the amplitudes for the absorption of an electric or magnetic multipole of order 1 leading to a final state with total angular momentum J and total isotopic spin T.

$\boldsymbol{\sigma}$, $\boldsymbol{e}$, $\boldsymbol{k}$, $\boldsymbol{q}$ are respectively the spin of the proton, the polarization vector of the photon and the momenta of the photon and of the pion in the center of mass system.

In model *a*) it is assumed that the second resonance is excited through a magnetic dipole absorption leading to a state $T=\frac{1}{2}$, $J=\frac{3}{2}$, positive parity, while in model *b*) the multipole involved is supposed to be the electric dipole leading to the same state but with opposite parity.

In both models $E_1(\frac{1}{2})$ is the *s*-wave amplitude and $M_1(\frac{3}{2},\frac{3}{2})$ is the multipole giving rise to the first resonance.

Starting from (2), (3) and choosing as positive the polarization in the direction $\boldsymbol{k}\times\boldsymbol{q}$, we obtain for the polarization of protons emitted at 90° in the center of

(5) R. R. WILSON: *Phys. Rev.*, **110**, 1212 (1958).
(6) R. F. PEIERLS: *Phys. Rev. Lett.*, **1**, 174 (1958).

mass system

$$P_a = \frac{1}{A} \operatorname{Im} \{E_1^*(\tfrac{1}{2})[M_1(\tfrac{3}{2}, \tfrac{3}{2}) + M_1(\tfrac{3}{2}, \tfrac{1}{2})]\} , \tag{4}$$

$$P_b = \frac{1}{A} \operatorname{Im} \{E_1^*(\tfrac{1}{2}) M_1(\tfrac{3}{2}, \tfrac{3}{2}) + 4E_1^*(\tfrac{3}{2}, \tfrac{1}{2}) M_1(\tfrac{3}{2}, \tfrac{3}{2})\} . \tag{5}$$

A is the isotropic term of the angular distribution for process (1)

$$\frac{\mathrm{d}\sigma}{\mathrm{d}\Omega} = A + B \cos\theta + C \cos^2\theta , \qquad \cos\theta = \frac{\boldsymbol{q}\cdot\boldsymbol{k}}{qk} . \tag{6}$$

The term $E_1(\frac{1}{2})$ introduced in (2) and (3) is necessary to obtain a non zero interference term at all energies in agreement with the experimental results (Fig. 1).

Models *a*) and *b*) are not the only possible ones. Furthemore they are not able to explain facts such as the third resonance at about 950 MeV. However, we shall limit ourselves and consider only them.

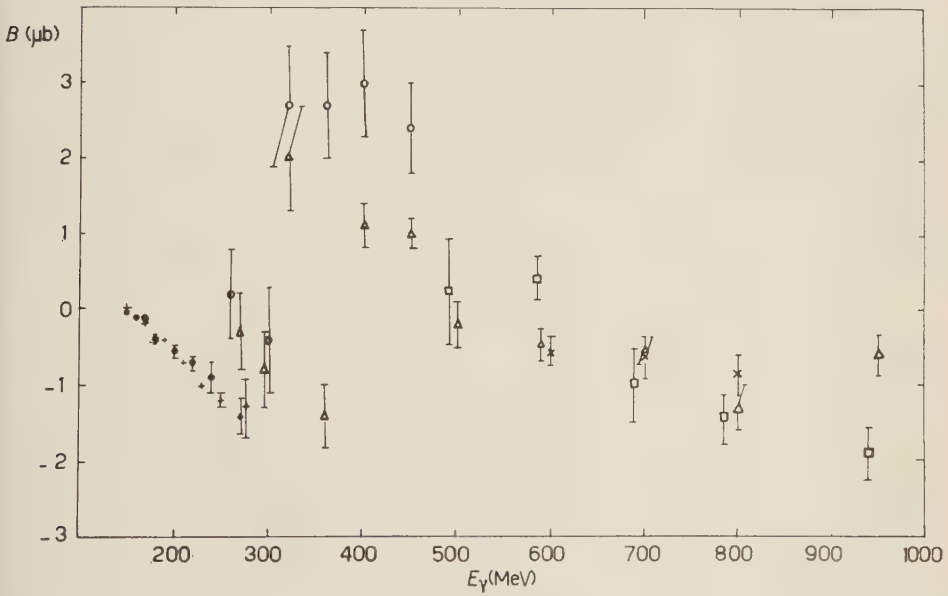

Fig. 1. – ○ W. S. McDonald, V. Z. Peterson and D. R. Corson: *Phys. Rev.*, **107**, 577 (1957); □ J. I. Vette: *Phys. Rev.*, **111**, 622 (1958); △ K. Berkelman and J. A. Waggoner: *Phys. Rev.*, **117**, 1364 (1960); x R. M. Worlock: *Phys. Rev.*, **117**, 537 (1960); G. E. Modesitt: + *Thesis*, unpublished; ● V. I. Goldansky *et al.*: *Nucl. Phys.*, **12**, 327 (1959).

We shall assume that they describe correctly the experimental situation around 600 MeV. Thus, roughly speaking, the polarization below the second resonance is given by (4) and (5), while above, it becomes necessary to explain the large polarization, by introducing in the models an amplitude corresponding to the third resonance.

An alternative model, which gives respectively to the resonances the parity $+ + -$, and explains all the polarization as due to the interference between the third and the first and second resonance has been proposed by L. MARSHALL and L. F. LANDOVITZ (7). We can have a justification for not considering this model in the fact that up to 700 MeV there is no appreciable evidence for a $\cos^4\theta$ term. This term follows from the model owing to the fact that the third resonant state is a $J=\frac{5}{2}$ one.

As was pointed out by J. O. MALOY (8) P_a can reach a maximum value of $\sim 31\%$. P_b, when $E_1(\frac{1}{2})$ is supposed to be negligible, can reach a maximum of 80%.

If it is assumed that the addition of $E_1(\frac{1}{2})$ does alter appreciably the value of P_b we see that model *b*) is in better agreement with the measured values around 600 MeV.

Anyway, due to the large experimental errors, it seems preferable to have a more stringent criterium of distinction between the two models.

In fact it is difficult to obtain quantitative predictions from (4) and (5), because, in spite of the simplification assumed it is impossible to derive from the experimental A, B and C all the complex multipole amplitudes. Actually in the energy region under consideration not even the multipoles phases are known. For this reason it seems that the experimental determination of the absolute polarization would serve more as additional experimental information useful for the extraction of the multipole amplitudes than for giving sharp answers of the kind required by Sakurai.

The sign of the P in (4) and (5) is a priori undetermined because of the arbitrariety in the sign of the multipole amplitudes.

We want to show that the sign of P_a and P_b can be determined if B is assumed to be known and that, within the limits of reasonable hypotheses, only model *b*) allows to predict the sign experimentally observed. By writing

$$E_1(\tfrac{1}{2}) = e_1 \exp[i\alpha_1], \qquad E_1(\tfrac{3}{2}, \tfrac{1}{2}) = E_1 \exp[i\delta],$$

$$M_1(\tfrac{3}{2}, \tfrac{1}{2}) = m_1 \exp[i\alpha_{13}], \qquad M_1(\tfrac{3}{2}, \tfrac{3}{2}) = m_3 \exp[i\alpha_{33}],$$

we get

a)
$$\begin{cases} P_a = \dfrac{1}{A} e_1\{m_3 \sin(\alpha_{33} - \alpha_1) + m_1 \sin(\alpha_{13} - \alpha_1)\}, \\ B_a = -2e_1\{m_3 \cos(\alpha_{33} - \alpha_1) + m_1 \cos(\alpha_{13} - \alpha_1)\}, \end{cases}$$

b)
$$\begin{cases} P_b = \dfrac{1}{A} m_3\{e_1 \sin(\alpha_{33} - \alpha_1) + 4E_1 \sin(\alpha_{33} - \delta)\}, \\ B_b = -2m_3\{e_1 \cos(\alpha_{33} - \alpha_1) + E_1 \cos(\alpha_{23} - \delta)\}. \end{cases}$$

At $E_\gamma \sim 450$ MeV, m_1 and E_1 are negligible, respectively and it results from the experiment $B > 0$. On the other hand $\cos(\alpha_{33} - \alpha_1) < 0$ (9). Then is has to be $e_1 m_3 > 0$. By choosing $m_3 > 0$ (all the results do not change if $m_3 < 0$ is assumed) we get $e_1 > 0$.

At $E_\gamma \sim 650$ MeV, *i.e.* below the second resonance, where m_3 and e_1 are negligible respectively, $B < 0$ and $\delta \leqslant 90°$, $\alpha_{13} \leqslant 90°$ so that $\cos(\alpha_{33} - \delta) < 0$, $\cos(\alpha_{13} - \alpha_1) > 0$.

(7) L. F. LANDOVITZ and L. MARSHALL: *Phys. Rev. Lett.*, **3**, 190 (1959).
(8) J. O. MALOY: private communication.
(9) B. PONTECORVO: *Proc. of the Kiev Conference on High Energy Physics* (1959).

2480

It follows $E_1 < 0$, $m_1 > 0$ and

$$P_a > 0\,, \qquad P_b < 0\,.$$

The polarization measurements give a negative value so excluding model *a*) on the ground of the above consideration.

To obtain this result we made the hypothesis that e_1, does not change sign going from low to high energy. Furthemore the *s*-wave term should be written $E_1(\frac{1}{2}) = e_1 \exp[i\alpha_1] + e_3 \exp[i\alpha_3]$. As experimentally we know that $\alpha_1 > \alpha_3$ we neglected the $T = \frac{3}{2}$ state.

In the argument only for the *s*-wave part has it been assumed that the multipole phase coincide with the corresponding scattering phase shift. The validity of this assumption has been justified by C. PELLEGRINI and L. TAU [10] on the ground of a quite resonable model.

The choice $E_1 < 0$ seems to be consistent with the observed π^0 angular distribution. In fact in model *b*)

$$A + \tfrac{5}{3}C = |E_1(\tfrac{1}{2})|^2 + 4e_1 E_1 \cos(\delta - \alpha_1)\,,$$

and at $E_\gamma \sim 700$ MeV, $C \simeq -A$ [11] so $A + (\frac{5}{3})C < 0$. Because $\cos(\delta - \alpha_1) > 0$ this means that e_1 and E_1 have opposite sign. In the model *a*) $A + \frac{5}{3}C = |E_1(\frac{1}{2})|^2 > 0$ in contradiction with the experimental result $C \simeq -A$. It is worth being noted that the addition of the $e_3 \exp[i\alpha_3]$ term to the *s*-wave amplitude might change the sign of P_a but not the sign of $A + \frac{5}{3}C$, in the model *a*). Instead the same addition could have the effect of changing the sign of $A + \frac{5}{3}C$ leaving the sign of P_b unaltered, in model *b*).

Furthermore it has to be noted that if $E_1 < 0$, $e_1 > 0$ the two terms in P_b tend to cancel each other so qualitatively explaining why the measured polarization is less than the value predicted by J. J. SAKURAI.

* * *

We wish to thank Prof. M. CINI for very helpful discussions.

[10] C. PELLEGRINI and L. TAU: to be published in *Nuovo Cimento*.

[11] K. BERKELMANN and J. A. WAGGONER: *Phys. Rev.*, **117**, 1364 (1960); R. M. WORLOCK: *Phys. Rev.*, **117**, 537 (1960); J. I. VETTE: *Phys. Rev.*, **111**, 622 (1958).

Forward Angle Photoproduction of Single Positive Pions on Hydrogen.

M. Beneventano, G. Finocchiaro, R. Finzi
L. Mezzetti, L. Paoluzzi and C. Schaerf

Istituto di Fisica dell'Università - Roma
Istituto Nazionale di Fisica Nucleare - Sezione di Roma

(ricevuto il 25 Luglio 1960)

Measurements of the differential cross section of the reaction

$$\gamma + p \rightarrow n + \pi^+ ,$$

for photon energies between (600÷÷1000) MeV have been performed by several experimenters ([1-3]). Systematic angular distributions have been given by Dixon and Walker ([2]). As these distributions are of considerable theoretical interest ([4-8]), we endeavoured to repeat the measurements and to extend them toward smaller angles. This is a preliminary report on measurements performed at angles between 10° and 90° in the center of mass system (c.m.).

The experimental arrangement is sketched in Fig. 1. The bremsstrahlung beam of the Frascati electron synchrotron, suitably collimated and cleaned from electron contamination, passed through a hydrogen target of the Illinois type ([9]) and was monitored by a Wilson type ionization chamber ([10]).

Charged particles produced in the target were momentum analyzed by a magnetic spectrometer. This consisted of two equal magnets M_1 and M_2 ([11,12]), focusing in the horizontal and defocusing in the vertical plane, and two scintillation counters S_1 and S_2.

The target, a vertical cylinder ~50 mm in diameter, was situated at the first focus of M_1. Particles of the right momentum and angle emerging from it

([1]) M. Heinberg, W. M. McClelland, F. Turkot, W. M. Woodward, R. R. Wilson and D. M. Zipoy: *Phys. Rev.*, **110**, 1211 (1958).

([2]) F. P. Dixon and R. L. Walker: *Phys. Rev. Lett.*, **1**, 142 (1958); **1**, 458 (1958); F. P. Dixon: *Ph. D. Thesis, California Institute of Technology* (1959).

([3]) F. Turkot: *Bull. Am. Phys. Soc.*, **4**, 22 (1959).

([4]) M. J. Moravcsik: *Phys. Rev.*, **104**, 1451 (1956).

([5]) R. R. Wilson: *Phys. Rev.*, **110**, 1212 (1958).

([6]) R. F. Peierls: *Phys. Rev. Lett.*, **1**, 174 (1958).

([7]) J. J. Sakurai: *Phys. Rev. Lett.*, **1**, 258 (1958).

([8]) A. M. Whetherell: *Phys. Rev.*, **115**, 1722 (1959).

([9]) Designed and constructed by the staff of the Cryogenic Laboratory at Frascati.

([10]) G. P. Murtas: *Laboratori Nazionali di Frascati*, internal note n. 18 (1959).

([11]) P. G. Sona: *Laboratori Nazionali di Frascati*, internal note n. 3 (1958).

([12]) R. Toschi; *Laboratori Nazionali di Frascati*, internal note n. 29 (1960).

were focused on counter S_2, situated at the second focus of M_2.

The counter S_1 (which was 1 mm thick in order to reduce scattering) defined the angular resolution $\Delta\theta$ of the system, while the counter S_2 defined the vertical acceptance as well as the resolution in momentum $\Delta p/p_0$. This system was designed so as to reduce the possibility that a particle scattered by the pole pieces be accepted by the counter telescope. The whole spectrometer could be rotated ([12]) about a pivot centered on the axis of the liquid hydrogen target.

The floating wire technique has been used to determine the mean momentum of the spectrometer p_0 as a function of the magnet current setting and the acceptance diagram $(\Delta p, \Delta\theta)$ for different target points.

The results have been checked with measurements on pions and electrons and can be summarized in the following parameters

$$\Delta p/p_0 = \pm\,(0.0265 \pm 0.005)$$

(for a point source),

$$\Delta\theta \quad = (3.08 \pm 0.1)^\circ,$$

$$\frac{1}{p_0}\frac{\partial p}{\partial x} = 0.0106 \text{ cm}^{-1}.$$

The solid angle has not yet been measured directly; a preliminary esti-

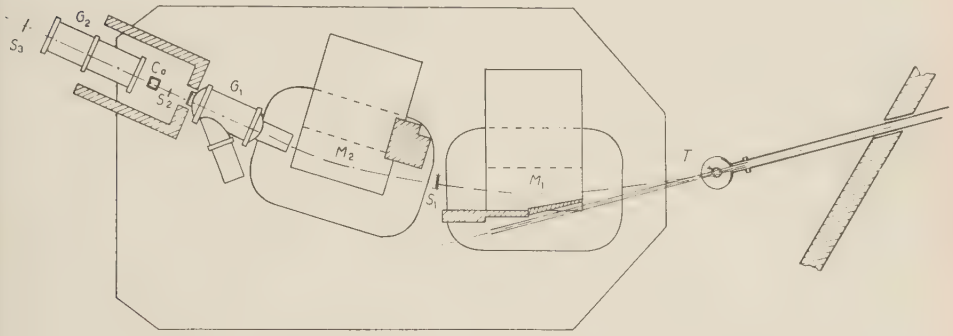

Fig. 1. – Experimental layout. The position of the spectrometer relative to the γ-ray beam is that corresponding so the smallest angle of measurement.

mate, based on the above parameters and on the calculated vertical acceptance yields the value $\Delta\Omega \sim 0.47 \cdot 10^{-3}$ sr.

The counter C_a is a water Čerenkov counter, which is sensitive to pions but not to protons in the momentum range accepted by the spectrometer. Discrimination against electrons, whose contribution is appreciable at small angles, was achieved by means of two CO_2 gas Čerenkov counters G_1 and G_2 having a threshold at a total energy $E/mc^2 \sim 15$ ([13]).

An additional scintillation counter S_3 was placed behind G_2, subtending about $\frac{2}{3}$ of the solid angle of the main telescope $S_1S_2C_a$.

A particle was identified as a pion if it caused a threefold coincidence $S_1S_2C_a\overline{G}_1$ within an effective resolving time of $2\tau = 2 \cdot 10^{-8}$ s. Fourfold coincidences of the type $S_1S_2C_aS_3\overline{G}_1\overline{G}_2$ were also registered. Accidentals for both

([13]) M. Beneventano, E. De Agostino, C. A. Galtieri, B. Rispoli and A. Serra: *Nuovo Cimento*, **12**, 156 (1959).

telescopes were continuously monitored by means of suitable delayed coincidences.

The lower intensity fourfold telescope was less sensitive to spurious events, involving low energy electrons and photons, which were the main source of trouble at the smallest angles.

Reversed field runs showed that the contribution of such spurious events to the true pion counting rates from hydrogen was always negligible except for the threefold coincidences at $\theta \leqslant 15°$ (c.m.), were it amounted to not more than 20%. The empty target background was on the average about 7%.

With this arrangement we have so far performed measurements on the angular distributions at photon energies of 600, 700, 800, 900 MeV and on the energy dependence of the cross section at the two center of mass angles $\theta = 20°$ and $\theta = 90°$. The points have been chosen with the criterion of complementing existing data ([2]).

The synchrotron was always operated at an energy between 75 and 150 MeV above the γ-ray energy concerned.

The counting rates, after subtraction of empty target background and accidentals, were converted into centre of mass differential cross sections. The three fold telescope data were used throughout in this calculation, except for the two smallest angles (10° and 15° in the centre of mass system) where we preferred to use the fourfold counting rates, because their background of spurious events was negligible. To do this, the fourfold rates were normalized to the threefold rates taking into account the measured effect of scattering and nuclear absorption in the counters.

The bremsstrahlung spectrum form used factor was that measured by DIAMBRINI *et al.* ([14]) with the same internal target but a somewhat different collimation.

No corrections have been applied for the pion decay in flight, for the muon contamination from π-μ decay, and for possible pion scatterings from the magnet pole pieces. These corrections, however, are slowly varying functions of energy and angle, and should not change appreciably the shape of the distributions. A very rough estimate gives for the highest and lowest net decay correction 10 and 6% respectively.

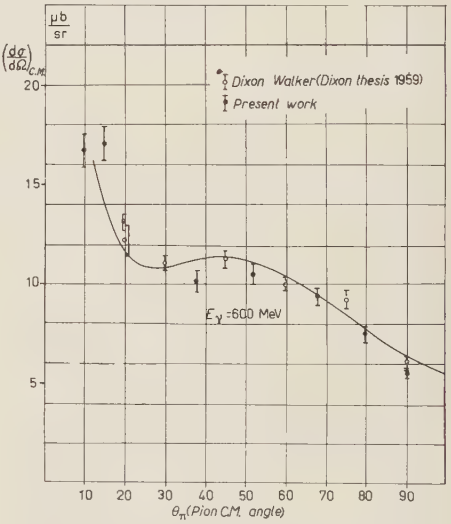

Fig. 2. – Angular distributions at fixed photon energy. The solid curves represent the least square fits calculated by DIXON and WALKER (F. DIXON: *Thesis*, 1959) following the suggestion of MORAVCSIK.

The results are given in Figs. 2, 3, 4, 5, 6; the errors indicated are purely statistical. Points calculated by averaging over experimental results obtained by DIXON and WALKER ([2]) with various arrangements are also shown in the angular distribution plots. To facilitate the comparison our points have been normalized to the best fit curves calculated by Dixon and Walker, averaging over all energies and over the angles between 20° and 90° (c.m.). The same

([14]) G. DIAMBRINI, A. S. FIGUERA, B. RISPOLI and A. SERRA: *Laboratori Nazionali di Frascati, internal note* n. 20 (1959).

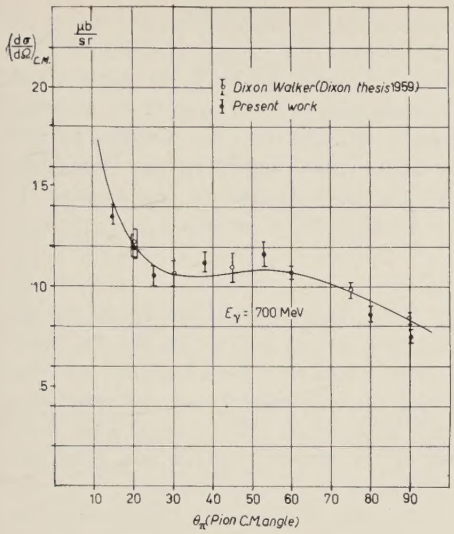

Fig. 3. – Angular distributions at fixed photon energy. The solid curves represent the least squares fits calculated by DIXON and WALKER (F. DIXON: *Thesis*, 1959) following the suggestion of MORAVCSIK.

normalization factor was used for the points in Fig. 6. The resolution in photon energy ΔE_γ is approximately ± 18 MeV (half width at half height) at the lowest energies and angles, and increases gradually with angle and energy to about ± 35 MeV at $E_\gamma = 900$ MeV, $\theta = 90°$ (c.m.).

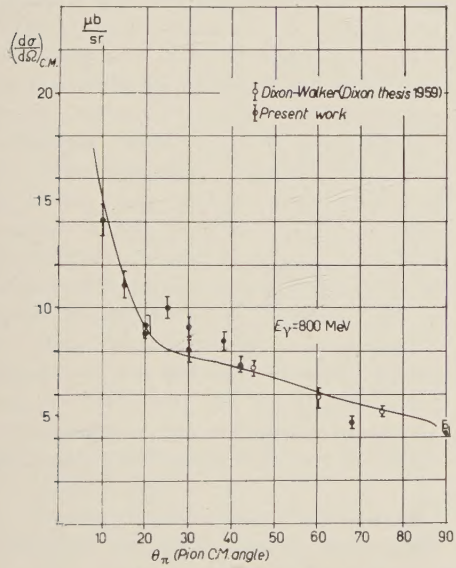

Fig. 4. – Angular distributions at fixed photon energy. The solid curves represent the least squares fits calculated by DIXON and WALKER (F. DIXON: *Thesis*, 1959) following the suggestion of MORAVCSIK.

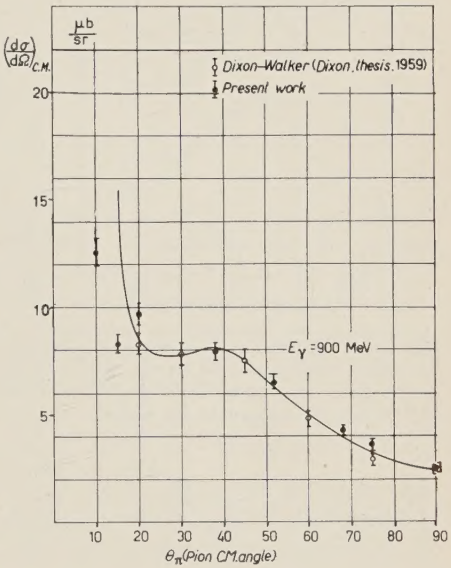

Fig. 5. – Angular distributions at fixed photon energy. The solid curves represent the least squares fits calculated by DIXON and WALKER (F. DIXON: *Thesis*, 1959) following the suggestion of MORAVCSIK.

According to the preliminary estimates of our solid angle and decay correction mentioned above, the values represented in Figs. 2, 3, 4 should be multiplied by a factor ~ 0.89 in order to get absolute cross sections; but this factor may change by as much as $\pm 15\%$ as a consequence of future better evaluations.

The analysis of the results is in progress. As regards the energy dependence at fixed center of mass angle, it is interesting to note that the maximum around 700 MeV appears to be shifted towards somewhat smaller energies than previously reported. This is not in contradiction with previous measurements,

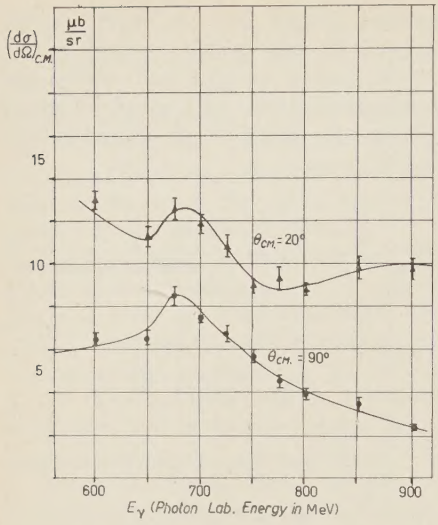

Fig. 6. – Differential cross sections as a function od photon energy at fixed centre of mass angle of the pion. The solid curves are fitted by eye to the experimental results.

but originates essentially from a narrower spacing of the experimental points. Our data seem to indicate also a somewhat steeper dependence on energy of the differential cross sections in the region around 700 MeV, an effect which has already been suggested by CORTELLESSA and REALE [15]. Further measurements with better energy resolution are however needed, in our opinion, to establish it with certainty.

* * *

Our deepest gratitude goes to the memory of our technician Mr. R. BIANCHINI, killed in a road accident while at work for this experiment; his intelligent and enthusiastic cooperation was invaluable for the preparation and good performance of the equipment.

We wish to thank all the Synchrotron staff and in particular Dr. G. GHIGO for the operation of the machine and for their help in maintaining our equipment and solving some of our technical problems.

[15] G. CORTELLESSA and A. REALE: *Nuovo Cimento*, to be published.

2982

LIBRI RICEVUTI E RECENSIONI

L. Merton – *Methods of Experimental Physics*. Vol. I: *Classical Methods*, pp. 596, Academic Press, New York, 1959, $ 12.

È questo il primo volume di una serie di sei volumi che si propone di fornire al fisico sperimentale una rappresentazione concisa dei più importanti metodi sperimentali, in modo che possa essere guidato negli argomenti in cui egli è meno esperto e trarne ispirazioni e consigli utili nel proprio lavoro. Questo fine, certo encomiabile, ci sembra che sia stato solo in parte raggiunto. Già a prima vista la suddivisione della serie in sei volumi (il secondo dovrà trattare i metodi elettronici, e gli altri quattro la fisica molecolare, atomica, nucleare e dello stato solido rispettivamente) lascia un po' perplessi. L'introduzione ci informa che con il termine « classici » si intendono le parti classiche della fisica, quali la meccanica, il calore, il suono la luce, l'elettricità ed il magnetismo. Allora c'è da chiedersi se tutto questo sia davvero solo un sesto della fisica sperimentale. Per rispondere a questa perplessità dobbiamo aspettare di vedere i volumi futuri.

Questo primo volume ci sembra assai diseguale, nel senso che in certe parti è quasi un ricettario (ad es. vengono descritti con cura i metodi per attaccare un conduttore ad un dielettrico per misurare la costante dielettrica) mentre in altre parti è di una impressionante brevità (ad es. la termometria con metodo magnetico è liquidata in due pagine) Naturalmente ci sono molte omissioni, come ci si può aspettare in un volume in fondo così piccolo che voglia trattare tanta fisica (ad es. non si parla di tecnica delle basse temperature), ma viceversa non si capisce la presenza di un lungo capitolo assai formale sui principi della termodinamica.

È nostra impressione però che il libro possa essere utile come uno studio intermedio di conoscenza dei metodi sperimentali, quando proprio non si sappia nulla sull'argomento, o anche si voglia fare una rapida ricerca di dati bibliografici di cui l'opera è abbastanza ricca. Ma ci sembra che troppo spesso manchi il consiglio dell'autore su questi metodi stessi, per cui un profano può spingers in qualche direzione senza rendersi conto delle difficoltà che incontrerà.

G. Careri

N. G. Parke III – *Guide to the Literature of Mathematics and Physics*. Dover Publications, Inc., New York, 1958, pp. xviii-436. Prezzo $ 2.64.

Questo libro costituisce un interessante tentativo di aiutare le persone, già dotate di preparazione scientifica, ad iniziare il loro aggiornamento in quei campi della matematica e della

fisica con i quali non sono in profonda consuetudine.

Per facilitare questo avvicinamento l'autore premette alla guida propriamente detta una prima parte in cui cerca di dare al lettore un'orientamento e un metodo per un proficuo studio personale. Non vengono perciò tralasciate informazioni minute per una efficiente ricerca bibliografica, accanto a chiarificazioni dei più comuni e importanti termini del linguaggio scientifico uniti a consigli sulla maniera più convenienti di apprendere direttamente dai libri quando non ci si possa valere del contatto diretto con insegnanti.

La guida propriamente detta è ordinata alfabeticamente in un centinaio di argomenti che corpono in modo alquanto completo la matematica e la fisica. Ciascuno di questi argomenti, che sono ad esempio: equazioni differenziali, teoria degli errori, fisica nucleare ecc., inizia con un breve panorama dell'autore sulle opere principali disponibili a cui segue un lungo elenco di opere raggruppate in voci, che sono ad esempio: teorie generali, applicazion tecniche, ecc., che facilitano al lettore la ricerca dei volumi che lo interessano specificatamente.

La scelta è in genere oculata anche se in qualche caso si è forse esagerato nel numero includendo opere di discutibile valore. Completa il volume un esauriente indice dei nomi unito a quello analitico assai dettagliato. Si può ritenere questa opera assai ben riuscita almeno nei limiti in cui un libro può aiutare a supplire alla mancanza di un buon insegnamento personale. Esso può risultare assai utile anche a coloro che, nella preparazione di un corso universitario, desiderano confontare il proprio procedere didattico con quello seguito da altri in libri e trattati.

A. Alberigi Quaranta

PROPRIETÀ LETTERARIA RISERVATA

Direttore responsabile: G. POLVANI

Tipografia Compositori - Bologna

Questo fascicolo è stato licenziato dai torchi il 30-VII-1960

2488